



RÉPUBLIQUE  
FRANÇAISE

*Liberté  
Égalité  
Fraternité*

**IRSN**

INSTITUT DE RADIOPROTECTION  
ET DE SÛRETÉ NUCLÉAIRE

**REPORT**

# RADIOLOGICAL CONSEQUENCES OF FALLOUT FROM ATMOSPHERIC TESTS OF NUCLEAR WEAPONS IN MAINLAND FRANCE

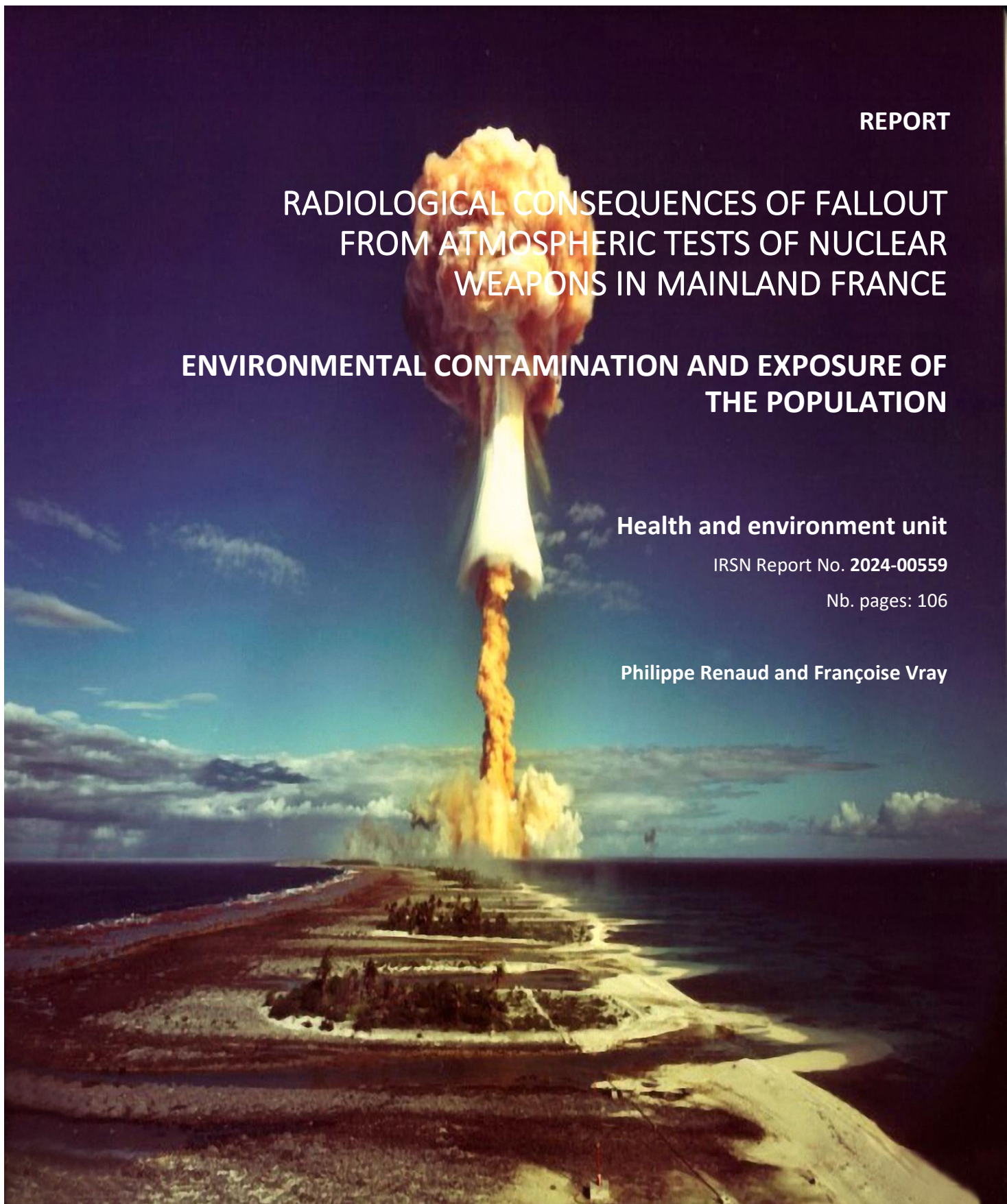
## ENVIRONMENTAL CONTAMINATION AND EXPOSURE OF THE POPULATION

**Health and environment unit**

IRSN Report No. 2024-00559

Nb. pages: 106

**Philippe Renaud and Françoise Vray**



# Radiological consequences of fallout from atmospheric tests of nuclear weapons in mainland France

## Abstract

The atmospheric tests of nuclear weapons carried out from 1945 to 1980 by the United States, the USSR, the United Kingdom, China, and France caused environmental contamination due to artificial radionuclides. This massive and worldwide addition of artificial radionuclides to the environment was greater in the northern hemisphere and more particularly between 40° and 50° northern latitude, the latitudinal band in which mainland France is located. Produced in the air during nuclear explosions, these radionuclides were dispersed in all parts of the environment, resulting in radiological exposure of the population, which continues to this day.

This exposure is a component of the radiological exposome, the subject of the CORALE project conducted at IRSN (Radiological component of the exposome, multiple exposures, risks of cancer and other chronic pathologies in the Constances cohort), in collaboration with Inserm.

In this context, the present study made it possible to reconstruct the annual records of effective doses and organ doses received by the French population from 1945 to 2020 following these nuclear tests, according to age and place of residence, for the three main exposure pathways: inhalation of radionuclides in the air, external exposure to radioactive deposits and ingestion of contaminated foodstuffs.

These dosimetric reconstructions are mainly based on the results of measurements on samples of various kinds taken from the environment, by the Central Service for Protection against Ionising Radiation (SCPRI) and the Atomic Energy Commission (CEA) from 1961 to 1978, as well as by IRSN between 2008 and 2018 (IRSN, 2022), as part of radiological monitoring programmes. Nearly 50,000 measurement results of specific activity and activity concentration of radionuclides in the air, rainwater, various types of foodstuffs, and even in the contents of meal trays from school canteens were used for this study.

The dose estimates obtained were compared with those made by UNSCEAR for the northern hemisphere, which were then used to supplement certain dosimetric records for France.

After a general presentation of nuclear tests and their radioactive fallout, this document provides, in detail, all the methodological elements used to estimate the doses for each of the exposure pathways of the population.

The dose records obtained are then discussed with regard to their changes over time, the main radionuclides that contribute to them, and their relative importance according to the organs irradiated and the age of the people exposed.

## Table of Contents

1.	Introduction .....	6
2.	Atmospheric tests of nuclear weapons.....	8
2.1.	Timeline, test power, and firing sites .....	8
2.2.	Production and dispersion of radionuclides.....	10
3.	Inventories of data available for France .....	14
4.	Activity concentration in the atmosphere .....	16
4.1.	Activity concentrations measured in air in Le Vésinet.....	16
4.2.	Activity concentrations measured in rainwater in the Paris region.....	19
4.3.	Reconstruction of complete records of activity in air in Le Vésinet.....	21
4.3.1.	Methodology.....	21
4.3.2.	Study of washout ratios.....	22
4.3.3.	Study of activity ratios of the various radionuclides .....	22
4.3.4.	Complete reconstructed records of monthly activity in air from June 1961 to July 1978 .....	25
4.3.5.	Records of annual average activities of long-lived radionuclides, 1959 to 2020 .....	26
4.3.5.1.	Case of <sup>90</sup> Sr, plutonium isotopes, and <sup>241</sup> Am.....	26
4.3.5.2.	Case of tritium and carbon-14.....	27
5.	Surface activities deposited on the ground .....	30
5.1.	Monthly dry and wet deposition estimates .....	30
5.2.	UNSCEAR vs IRSN comparison of integrated deposits.....	32
5.3.	Spatial variability of activities deposited in mainland France.....	34
6.	Specific activities and activity concentrations in the food chain .....	38
6.1.	Methods for reconstructing specific activities and activity concentrations in the food chain .....	38
6.2.	Specific activities in grasses; element of validation for deposits .....	39
6.3.	Specific activities in vegetables.....	43
6.4.	Specific activities in cereal grains.....	48
6.5.	Activity concentrations in cow's milk .....	49
6.6.	Specific activities in beef .....	52
6.7.	Case of tritium and carbon-14.....	53
6.8.	Overall assessment of food contamination.....	56
7.	Reconstruction of inhaled doses .....	58
7.1.	Methodology for calculating inhaled doses for the period of June 1961 to July 1978 .....	58

<b>7.2. Estimated effective doses by inhalation for an adult, 1961-1978; comparison with UNSCEAR estimates.....</b>	<b>59</b>
<b>7.3. Methodology for reconstructing records of effective doses by inhalation and doses to organs by age group, 1945-2020 .....</b>	<b>62</b>
<b>7.4. Estimated effective doses by inhalation, 1945-2020.....</b>	<b>63</b>
<b>8. Reconstruction of doses from external exposure to deposits .....</b>	<b>67</b>
<b>8.1. Methodology for calculating doses from external exposure to deposits for the period of June 1961 to July 1978.....</b>	<b>67</b>
<b>8.1.1. General .....</b>	<b>67</b>
<b>8.1.2. Case of an adult working outdoors.....</b>	<b>68</b>
<b>8.1.3. Case of sedentary adults and children .....</b>	<b>69</b>
<b>8.1.4. Reduction of dose rate inside buildings .....</b>	<b>69</b>
<b>8.2. Estimated external effective doses for an outdoor worker and comparison with UNSCEAR estimates.....</b>	<b>70</b>
<b>8.3. Methodology for reconstructing complete records of effective external doses, 1945-1985</b>	<b>72</b>
<b>8.4. Discussion of external dose results.....</b>	<b>73</b>
<b>8.4.1. Effective external doses for adults working outdoors.....</b>	<b>73</b>
<b>8.4.2. Effective external doses for children and sedentary adults .....</b>	<b>74</b>
<b>8.4.3. Effect of the place of residence (of the building protection factor).....</b>	<b>74</b>
<b>8.4.4. Organ-equivalent external doses.....</b>	<b>76</b>
<b>9. Reconstruction of ingested doses .....</b>	<b>77</b>
<b>9.1. Methodology for calculating ingested doses for the period of June 1961 to July 1978 .....</b>	<b>77</b>
<b>9.2. Estimated effective doses by ingestion for an adult, 1961-1978; comparison with UNSCEAR estimates.....</b>	<b>81</b>
<b>9.3. Methodology for reconstructing records of effective doses by ingestion and doses to organs by age group, 1945-2020 .....</b>	<b>82</b>
<b>9.4. Estimated effective doses by ingestion, 1945-2020 .....</b>	<b>84</b>
<b>9.5. School lunch measurement results; element of validation for ingested doses and geographical variability .....</b>	<b>87</b>
<b>10. Total doses, all exposure pathways combined.....</b>	<b>90</b>
<b>10.1. Variability by age and contribution of exposure pathways.....</b>	<b>90</b>
<b>10.2. Spatial variability.....</b>	<b>91</b>
<b>10.3. Discussion of organ doses .....</b>	<b>92</b>
<b>11. Conclusion.....</b>	<b>93</b>
<b>12. Bibliography.....</b>	<b>95</b>
<b>13. APPENDIX 1: Study of activity ratios of short-lived radionuclides. ....</b>	<b>98</b>

**14. APPENDIX 2: Model of transfer to agricultural plant and animal food products and  
adjustment of results to the available measurement data..... 100**

## 1. Introduction

The atmospheric tests of nuclear weapons carried out from 1945 to 1980 by the United States, the USSR, the United Kingdom, China, and France caused environmental contamination due to artificial radionuclides. The contribution of artificial radionuclides due to testing was massive and worldwide. Produced in the air during nuclear explosions, these radionuclides were dispersed in all parts of the environment, resulting in radiological exposure of the population, which continues to this day.

This radiological exposure is a component of the exposome, which is defined as all environmental radiological exposures to which we have been subjected since birth and which are likely to have an effect on our health (Wild CP, 2005).

The "Constances" cohort is a group of 220,000 people residing in France who agreed to participate in an epidemiological study to examine the causes of chronic diseases and, in particular, the potential causes of environmental origin (Goldberg M. et al, 2017). This cohort is monitored by Inserm's UMS11 unit. The presence of radioactive substances in our environment is one of these potential causes to be studied, and is the subject of the CORALE project (Radiological component of the exposome, multiple exposures, risks of cancer and other chronic pathologies in the Constances cohort) conducted by IRSN in collaboration with Inserm. The aim of CORALE is to reconstruct the radiation doses of environmental, medical, and occupational origin received by 80,000 participants of the Constances cohort since their birth, and then to estimate the risks of cancer and other chronic pathologies potentially related to these doses, taking into account the influence of other risk factors.

In this context, the objective of the present study is to estimate the radiation doses received by the French population from 1945 to 2020 due to the fallout from atmospheric tests of nuclear weapons, based mainly on measurement results. These results are specific activity and activity concentration of artificial radionuclides in samples of different types (air, rainwater, foodstuffs, etc.) measured by the Central Service for Protection against Ionising Radiation (SCPRI) and the Atomic Energy Commission (CEA) from 1961 to 1978, as well as by IRSN between 2008 and 2018 (IRSN, 2022), as part of radiological monitoring programmes. For certain periods during which French data are lacking, and in particular for the period from 1945 to 1961, the dose estimates made by the United Nations Scientific Committee on the Effects of Atomic Radiation (UNSCEAR) for the northern hemisphere are adapted to the characteristics of fallout on French territory.

In order to reconstruct the individual dosimetric history, since birth, of each of the 80,000 people of the "Constances" cohort for whom the residential history is available, the doses must be estimated by year, age group, and municipality. The fallout from nuclear tests greatly varied from one year to another, were not uniform throughout the country, and the doses received also depend on the age of the person at the time of exposure. This will provide an estimate of the doses received by each of these people during their life in their successive places of residence.

Also, in addition to the effective doses that account for the overall exposure of people at the whole body level, the connection with the occurrence of diseases initiating in a particular organ, requires absorbed or even equivalent doses of the organs. First, to cover the most common diseases (notably, cancers), the organs selected are: the lungs, colon, prostate, breasts, thyroid, and brain.

After a general presentation of nuclear tests and their radioactive fallout, this document provides, in detail, all the methodological elements used to estimate the doses for each of the exposure pathways

of the people in the study: inhalation of radionuclides in the air, external exposure to radioactive deposits, and ingestion of contaminated food.

The dose records for each exposure pathway are then discussed with regard to their changes over time, the main radionuclides that contribute to them, and their relative importance according to organs and age of the individuals.

## 2. Atmospheric tests of nuclear weapons

### 2.1. Timeline, test power, and firing sites

From 1945 to 1980, five nations conducted 543 atmospheric aerial tests of nuclear weapons (UNSCEAR, 2000).

Most of the power, expressed in Megatons of Trinitrotoluene equivalent (Mt of TNT), was released from 1954 to 1958, especially in 1961 and 1962 (Figure 1). Between these two periods, a moratorium was observed by the United States, the USSR and the United Kingdom from the beginning of 1959 until the autumn of 1961, during which time France carried out its first four tests in Algeria (13 February 1960 to 25 April 1961). In the autumn of 1961, the USSR unilaterally broke the 1959 moratorium. The American response followed in 1962. The powers of the devices were extremely variable, from less than one ton up to the record Soviet explosion of 50 Mt on October 30, 1961 in New Zealand (the Tsar Bomb). The Partial Nuclear Test Ban Treaty, signed in August 1963, marked the end of American, Soviet and English atmospheric tests. The French and Chinese atmospheric firings, which continued until 1974 (September 14th) and 1980 (October 16th), respectively, represent only 2.3% and 4.7% of the total estimated power of 440 Mt. Two thirds of this total power, or 289 Mt, was released in 25 Soviet and American explosions greater than 4 Mt. The main characteristics of all nuclear tests (test country and site, power, altitude, and test device, distribution between the stratosphere and the troposphere) are provided in Annex C of the 2000 UNSCEAR report (UNSCEAR, 2000).

From the early 1960s, underground tests gradually replaced aerial explosions. These tests did not result in sufficient atmospheric contamination to concern mainland France.

The sites of the aerial tests were spread across the globe, although most of the explosions occurred in the northern hemisphere (Figure 2). The explosions were carried out at different altitudes, from the surface of the ground or on barges at sea, to the upper atmosphere (rocket), as well as from towers ranging from a few metres to more than a hundred metres high, balloons located at a few hundred metres, and devices dropped from aircraft.

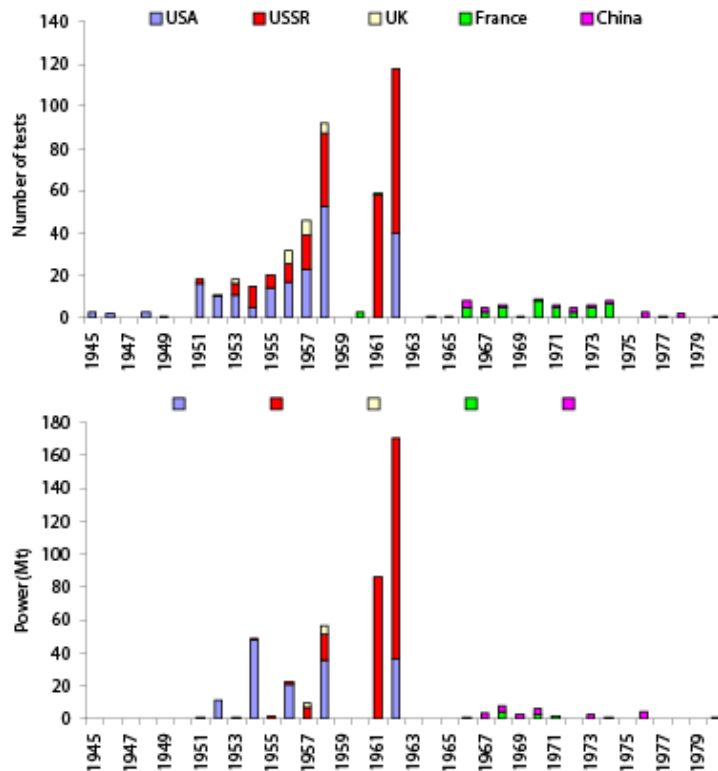


Figure 1: Number of atmospheric tests and power released per year and per country

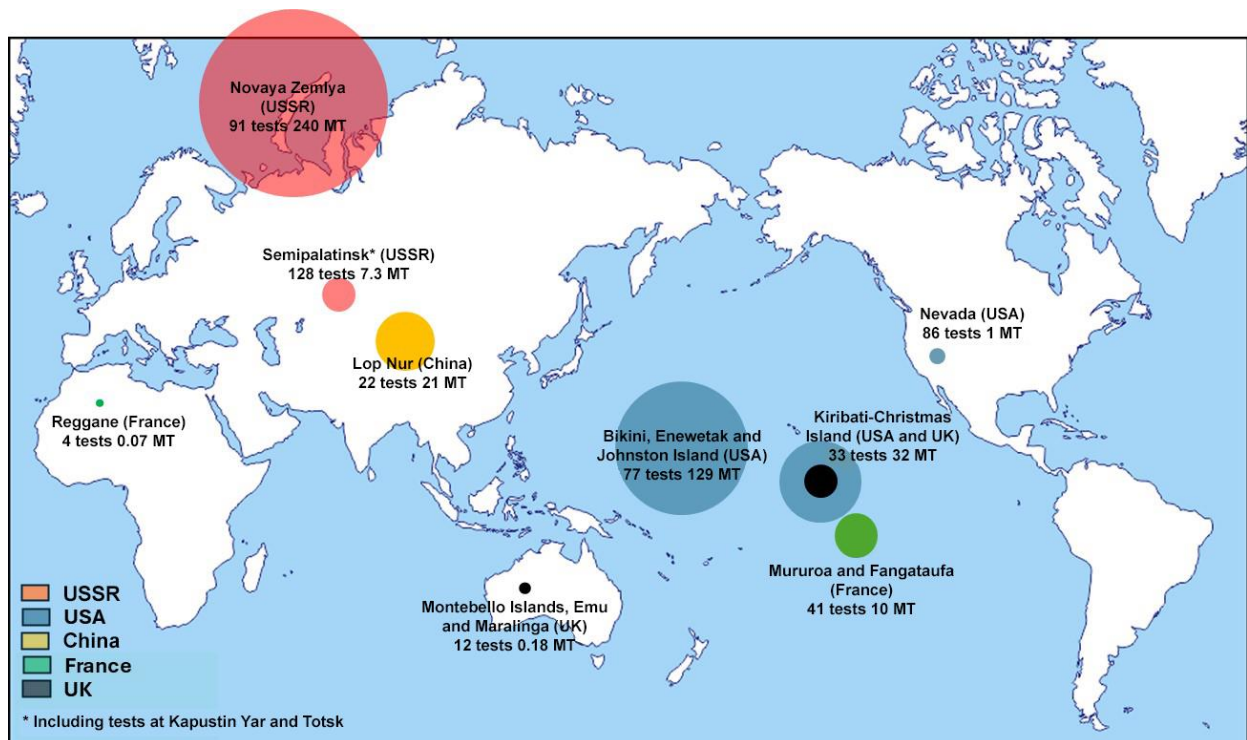


Figure 2: Location of main atmospheric test sites for nuclear weapons. The sizes of the disks are proportional to the cumulative powers.

## 2.2. Production and dispersion of radionuclides

A nuclear explosion generates dozens of primary fission products (directly from the breaking of uranium or plutonium nuclei) and secondary fission products (produced by radioactive decay of the previous products) as well as activation products (when a stable nucleus becomes radioactive by capturing a neutron emitted by the nuclear reaction). Of these radionuclides, only 21 have a sufficiently long radioactive half-life, sufficiently abundant production and radiotoxicity to contribute significantly to the exposure of populations.

Table 1 shows these radionuclides. Some of them disintegrate by producing a radionuclide with a very short half-life whose activity in the environment can be considered equal ("at equilibrium") to that of the "parent" radionuclide. The corresponding pairs are indicated in the table, but only the radioactive half-life of the "parent", which determines the evolution of activity for both, is mentioned. In this report, the radionuclide will most often be represented by its symbol accompanied by a "+" sign to recall the existence of a "radionuclide-daughter in equilibrium". Plutoniums 239 and 240 can most often not be differentiated using the most common method for measuring their activities in the environment, namely alpha spectrometry); this is why it is the sum of the activities of the two isotopes that is indicated using the symbol  $^{239+240}\text{Pu}$ . It should also be noted that americium-241 was not directly emitted during the explosions; it results from the radioactive decay of plutonium-241. Finally, in Table 1, radionuclides are classified by increasing radioactive half-life; those with a half-life greater than 12 years (starting from tritium), are still present in the environment today in measurable quantities.

Table 1 – List of main radionuclides emitted during atmospheric tests of nuclear weapons and having contributed to the exposure of the populations.

Radionuclide	Symbol	Radioactive half-life*	Radionuclide	Symbol	Radioactive half-life*
Iodine-131	$^{131}\text{I}$	8.0 days	Antimony-Tellurium-125	$^{125}\text{Sb+}$	2.8 years
Barium-Lanthanum-140	$^{140}\text{Ba+}$	13 days	Tritium	$^3\text{H}$	≈ 12 years
Cerium-141	$^{141}\text{Ce}$	33 days	Plutonium-241	$^{241}\text{Pu}$	≈ 14 years
Ruthenium-Rhodium-103	$^{103}\text{Ru+}$	39 days	Strontium-Yttrium-90	$^{90}\text{Sr+}$	≈ 29 years
Strontium-89	$^{89}\text{Sr}$	51 days	Caesium-Barium-137	$^{137}\text{Cs+}$	≈ 30 years
Yttrium-91	$^{91}\text{Y}$	59 days	Plutonium-238	$^{238}\text{Pu}$	≈ 88 years
Zirconium-Niobium-95	$^{95}\text{Zr+}$	64 days	Americium-241**	$^{241}\text{Am}$	≈ 433 years
Cerium-Praseodymium-144	$^{144}\text{Ce+}$	280 days	Carbon-14	$^{14}\text{C}$	≈ 5,600 years
Manganese-54	$^{54}\text{Mn}$	310 days	Plutonium-240	$^{239+240}\text{Pu}$	≈ 6,600 years
Ruthenium-Rhodium-106	$^{106}\text{Ru+}$	1.0 year	Plutonium-239	$^{239+240}\text{Pu}$	≈ 24,000 years
Iron-55	$^{55}\text{Fe}$	2.7 years			

\*The radioactive half-lives indicated are those of the first radionuclide ("parent")

\*\*Americium-241 was not directly emitted during the explosions; it results from the radioactive decay of plutonium-241

Radionuclides emitted into the atmosphere during a nuclear explosion attach to airborne particles of widely varying sizes, ranging from less than one-hundredth of a micrometre (<0.01 μm) to more than

10  $\mu\text{m}$ . The dispersion of these particles in the air then constitutes the radioactive "plume" that will cause three types of fallout on the ground (see Figure 3).

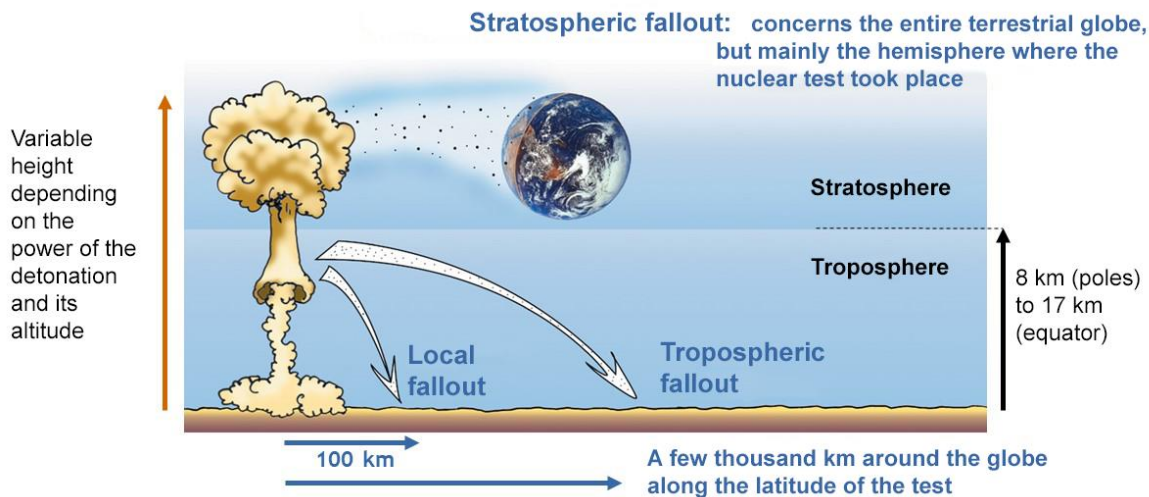


**Figure 3: The various types of fallout from radionuclides emitted during atmospheric tests of nuclear weapons**

The largest particles deposit fairly quickly, mainly by gravity, over a distance of around a few hundred kilometres downwind of the explosion site, forming the local fallout. Depending on the height and power of the explosion, the radioactive "plume" rises higher or lower and is distributed between the troposphere (the lower layer of the atmosphere between the ground and 9 to 17 km at the poles and up to 24 km at the equator), and the stratosphere above.

Above a few hundred metres in height, tropospheric plumes are carried eastward by the general circulation of air masses (western flows), in both the northern and southern hemispheres. These plumes travel around the globe, remaining mainly around the emission latitude, and form tropospheric fallout within a few weeks (two to three orbits of the globe). As an illustration, Figure 4 shows the propagation of the tropospheric plume for the Chinese test on October 16, 1980, which arrived in France after one week, on October 23. Thus, all the radionuclides mentioned in Table 1, including those with the shortest half-life ( $^{131}\text{I}$  and  $^{140}\text{Ba}^+$ ), are present in tropospheric fallout. In addition, the latitude of mainland France was particularly affected by tropospheric fallout due to the fact that several test sites were located at nearby latitudes (the American site of Nevada, the Soviet sites of Semipalatinsk and Kapustin Yar, and the Chinese test site of Lop Nur).



**Figure 4: Progress of the tropospheric plume following the Chinese test on October 16, 1980**

The stratospheric fraction of plumes is redistributed by the large circulation currents of air masses constituted by polar convective cells, Ferrel cells at mid-latitudes and Hadley cells over the tropics (see Figure 5). Hadley cells tend to bring air masses from lower latitudes to those between 40° and 50°. Similarly, Ferrel cells also tend to feed latitudes between 40° and 50° with air masses from higher latitudes. As a result, the latitudinal strip where mainland France is located, already particularly affected by tropospheric fallout, has also been affected by the stratospheric fallout from nuclear tests. Figure 5 illustrates this fact by the distribution of radioactive deposits, which are indeed greater in this latitudinal band.

This redistribution of stratospheric plumes took place over several years. UNSCEAR estimated the average residence time of radionuclides carried to the stratosphere before falling back to ground level at two years. During this time, the elements with short half-lives have disappeared. Stratospheric fallout therefore comprises only long-lived elements and elements with intermediate half-lives whose activity has decayed.

Finally, it should be noted that exchanges at the stratospheric level are low (about 25%) between the two hemispheres. As a result, the southern hemisphere, where the number and power of tests were less important, was much less affected by the fallout from nuclear tests than the northern hemisphere.

Taking all these factors into consideration, the latitudinal band that includes mainland France, alone, received nearly 18% of the total fallout from all nuclear tests.

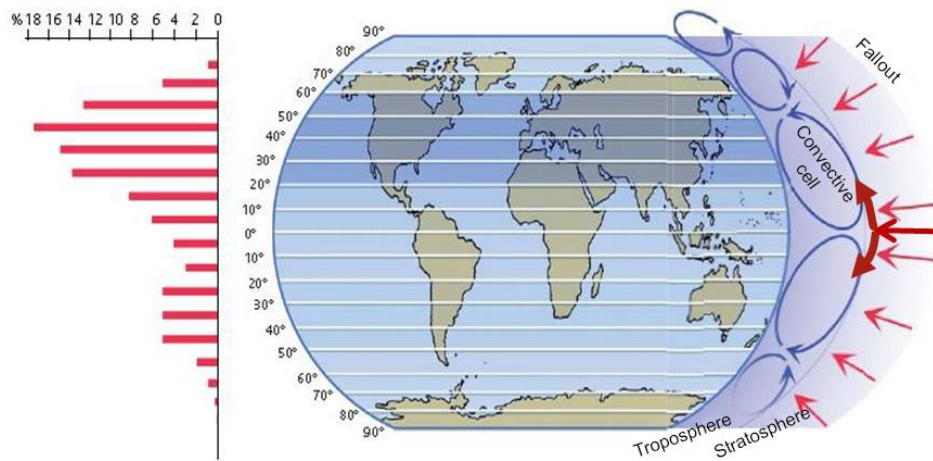


Figure 5: Distribution of stratospheric fallout according to latitude (established from strontium-90 measurements)

### 3. Inventories of data available for France

Radiological monitoring of the environment in France was gradually implemented during the 1960s by the Central Service for Protection against Ionising Radiation (SCPRI), under the supervision of the Ministry of Public Health. The objective was to characterise the fallout from nuclear weapons testing in mainland France and overseas (Guadeloupe, Martinique, Reunion and Guyana), as well as the influence of radioactive discharges from the first "nuclear" research and industrial sites in France that were established in the 1960s.

Radiological monitoring of the environment in French Polynesia, particularly during the period of French nuclear testing, was carried out by the Atomic Energy Commission (CEA), which also performed analyses in mainland France on foodstuffs originating in various regions.

SCPRI analyses of  $^{90}\text{Sr}+$  and  $^{137}\text{Cs}+$  in rainwater collected monthly and the calculation of rainfall deposits from precipitation amounts also measured monthly, began in April 1961 at four stations (Chailly en Bière, Cléville, Vioménil, and Sauveterre). Analyses of other radionuclides ( $^{140}\text{Ba}+$ ,  $^{95}\text{Zr}+$ ,  $^{103}\text{Ru}+$  and  $^{131}\text{I}$ ) in aerosols began in January 1962. The number of measuring or sampling stations, types of samples taken, types of analyses, and the radionuclides measured gradually increased throughout the 1960s and 1970s.

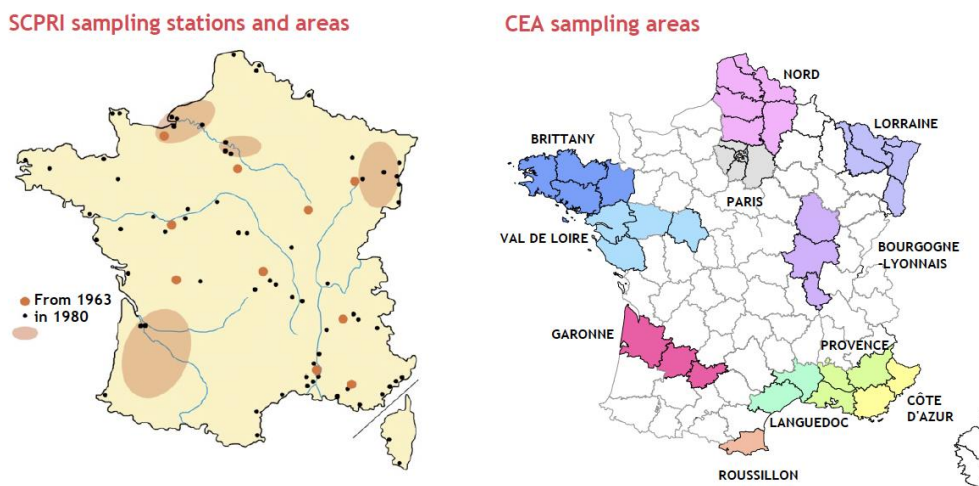


Figure 6: Stations or regions of origin of measurement results from the SCPRI and CEA

The data used for this study is taken from the monthly bulletins published by the SCPRI (1961-1980) and the quarterly bulletins of the Interministerial Sub-Committee on Health Protection (1961-1965), subsequently renamed CEA/DPS (Department of Health Protection; 1965-1978). These are mainly the SCPRI results for the Paris region, as well as some specific results from other stations or regions for the study of spatial variability. Table II shows the number of data used per radionuclide and the type of environmental samples.

While monitoring of food chain contamination by the SCPRI and the CEA was continuous throughout the period studied, the evolution of environmental contamination, the specific behaviour of radionuclides with regard to the food products studied, as well as the evolution of measurement techniques for each radionuclide, induce heterogeneities in the series of data available: some links in the food chain are particularly well informed for many radionuclides, while only a few scattered data are available for others.

The data cited in this table is for the whole of France (except for air and rainwater, compartments for which the significant number of data points were limited to the Paris Region only). These disparities mean that spatial variability should not be approached systematically; it will be studied when the measurement results allow. The regional variability of deposits will then be used as a reference.

It is worth mentioning the limits of certain sets of measurement results, in particular the inaccuracy of the sampling dates for CEA/DPS data (only the month is known) and the sampling locations (only the region is identified). These inaccuracies will contribute to unexplained variability in the measured specific activities and activity concentrations. Moreover, the specific activities of the grass in relation to the weight of ash and the fresh / ash weight ratios are not always known for the SCPRI data. The average value of this ratio was estimated to be 45.

Table II: Number of measurement results relating to French territory available for the study of contamination in the food chain between 1961 and 1978.

	<sup>90</sup> Sr	<sup>137</sup> Cs+	<sup>95</sup> Zr+	<sup>103</sup> Ru+	<sup>144</sup> Ce+	<sup>131</sup> I	<sup>106</sup> Ru+	<sup>141</sup> Ce	<sup>89</sup> Sr	<sup>140</sup> Ba+	<sup>54</sup> Mn
Air and rainwater	1440	1080	840	600	200	60	380	75		140	35
Grass	2460	1890	2030	605	570	150	120	250	285	175	
Grains	310	320									
Leafy vegetables	3050	1980	430	90	230		130	130			
Root vegetables	1255	520	30	6	20		9	9			
Fruit vegetables + fruit	430	520	55	20	40		5	30	15		
Milk	11000	9000				810			70	9	
Meat		310									
School lunches	820	735									
Total	20765	16355	3385	1321	1060	1020	644	494	370	324	35

The data originating mainly from the SCPRI is in grey; the other data mainly comes from the DPS.

In addition to the data for years 1961-1978, there are the results of measurements for long-lived radionuclides (<sup>137</sup>Cs, <sup>90</sup>Sr, <sup>238</sup>Pu, <sup>239+240</sup>Pu, <sup>241</sup>Pu and <sup>241</sup>Am) on atmospheric aerosol filters carried out by IRSN (IPSN before 2004) and by the Germany metrology institute, Physikalisch-Technische Bundesanstalt (H, Vershofen). From 1950 to 2020, records of <sup>3</sup>H contents in rainwater and <sup>14</sup>C in vegetation, taken from international literature and from measurements carried out by IRSN, were used in this study to reconstruct the specific activities and activity concentrations of these two radionuclides in the air and in foodstuffs.

Finally, for the period 2008-2018, this study also uses dose estimates based on the results from various kinds of measurements acquired by IRSN during this decade (IRSN, 2022).

## 4. Activity concentration in the atmosphere

### 4.1. Activity concentrations measured in air in Le Vésinet

Figure 7 shows the monthly activity concentrations of eight radionuclides with a half-life greater than one month, measured in atmospheric aerosols by the SCPRI between June 1961 and December 1980. Prior to 1961, the monitoring system of the SCPRI was not yet fully operational and after 1980, the levels of activity in the air were too low to be measured by this system (below the detection limits<sup>1</sup>). The activity concentrations of <sup>239+240</sup>Pu measured in Germany between 1969 and 1973 (Wershofen), which can be considered as representative of the activities of these two radionuclides in France, are also presented.

For six of these radionuclides, the completeness of the records is satisfactory, or very satisfactory: measurement results are thus available for 25% of the 238 months from June 1961 to December 1980 for <sup>144</sup>Ce+, 40% to 50% of the months for <sup>103</sup>Ru, <sup>106</sup>Ru and <sup>137</sup>Cs, and 70% for <sup>95</sup>Zr+ and <sup>90</sup>Sr+. For <sup>137</sup>Cs+ and <sup>90</sup>Sr+, the absence of data relates mainly to the period from January 1961 to March 1964, during which monitoring was still being set up. For rutheniums and <sup>95</sup>Zr+, the shortages relate to the periods between the Chinese tests when their activity in air was too low to be measured. Finally, in the case of <sup>144</sup>Ce+, the absence of data relates mainly to a long period from 1965 to 1974 when it was seemingly not measured.

The graph in Figure 7 shows that it was between the end of 1961 and 1963 that the fallout from atmospheric tests of nuclear weapons on mainland France was the greatest due to the numerous tests carried out by the Soviet Union and the United States<sup>2</sup> in the northern hemisphere. These high activity concentrations followed much lower activities during the period of the moratorium from 1958 to 1961, prior to implementation of the SCPRI's monitoring system. After the Partial Test Ban Treaty of June 1963, which became effective in October, the atmosphere was fairly quickly purified due to the radioactive decay, dispersion and deposit of aerosols on the ground. From 1964 onwards, Figure 7 shows peaks one to two orders of magnitude lower than the levels reached in 1961-1963. For these radionuclides with half-lives ranging from one month to thirty years, these seasonal peaks, which cover the summer periods (from May to October), correspond to incursions into the troposphere of stratospheric contamination due to Chinese tests<sup>3</sup>. We can see the simultaneous nature of these peaks for all radionuclides including <sup>239+240</sup>Pu measured in the air in Germany. For these radionuclides with a half-life greater than one month, the seasonal stratospheric inputs masked the very short (less than one month) tropospheric bursts following each of the Chinese nuclear tests, and which will be presented below through the activities of radionuclides with shorter half-lives, such as <sup>131</sup>I and <sup>140</sup>Ba+.

---

<sup>1</sup> The detection limit (DL) is the lowest activity that can be quantified in a sample. If the activity of the sample is lower, the metrologist declares that it is below this value (<DL). The detection limit depends on the performance of the metrological tools used.

<sup>2</sup> The French nuclear tests in the Sahara, of very low power and at a lower latitude, probably contributed very little to the activity concentrations measured in mainland France.

<sup>3</sup> These stratospheric incursions are well known for <sup>7</sup>Be and were observed for <sup>137</sup>Cs until the 1990s

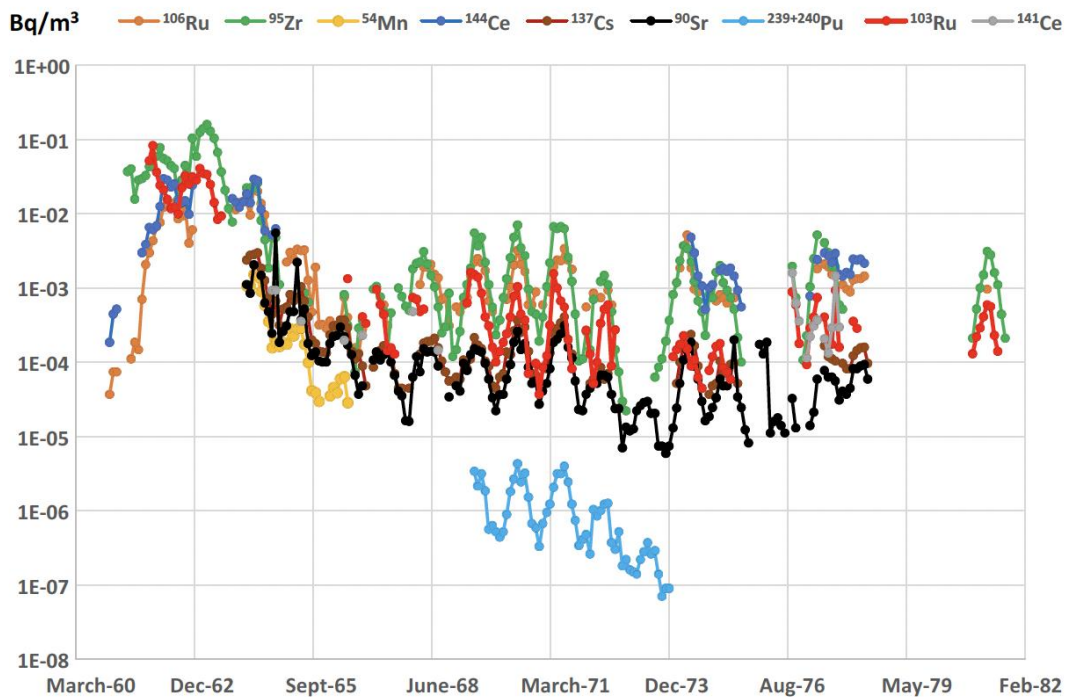


**Figure 7: Records of the monthly activity concentrations of the nine main radionuclides with a half-life greater than one month, measured in the air in Le Vésinet (Paris region) and in Germany (for  $^{239+240}\text{Pu}$ ) between 1961 and 1980 ( $\text{Bq}/\text{m}^3$ )**

In addition to the preceding radionuclides,  $^{54}\text{Mn}$ ,  $^{131}\text{I}$ ,  $^{140}\text{Ba}+$  and  $^{141}\text{Ce}$  have also been measured occasionally ( $^{54}\text{Mn}$  and  $^{141}\text{Ce}$ ) or very sporadically in the air in France ( $^{131}\text{I}$  and  $^{140}\text{Ba}+$ ).

Between 1964 and 1978, the activity concentrations of  $^{131}\text{I}$  and  $^{140}\text{Ba}+$ , short-lived (8 to 13 days respectively), were measurable only in the month following some of the Chinese tests, the dates of which are indicated in Figure 8, when the burst of tropospheric contamination reached France between 10 and 20 days after the explosion (orange and blue circles in Figure 8). Therefore, 11 of the 22 Chinese atmospheric tests carried out between October 1964 and March 1978 led to a puff of  $^{131}\text{I}$  and/or  $^{140}\text{Ba}+$  measured in the air in France. Unlike the radionuclides shown in Figure 7, the radioactive half-lives of these two radionuclides are too short for them to have accumulated in the stratosphere and given rise to stratospheric incursions.

Between 1 September and 4 November 1961, the Soviet Union carried out 28 nuclear tests at the Semipalatinsk site<sup>4</sup> in present-day Kazakhstan and 4 at the Kapustin Yar site in Russia (east of Volgograd). Like the Chinese site of Lop Nur, these two test sites are located at latitudes close to those of mainland France. The activities of  $^{131}\text{I}$  and  $^{140}\text{Ba}+$  released during the explosions led to activity concentrations measured in France during these three months which exceeded  $0.01 \text{ Bq}/\text{m}^3$  and reached  $0.15 \text{ Bq}/\text{m}^3$  of  $^{131}\text{I}$  in November 1961. Between August and November 1962, the USSR carried out 41 tests at the same Semipalatinsk site, and 4 additional tests were carried out by the United States on the Nevada Test Site, causing activity concentrations in the air in France of the same order of magnitude.

<sup>4</sup> The 62 nuclear tests carried out by the USSR at the Novaya Zemlya site in 1961 and 1962 probably contributed very little to the activities measured in France because of the high latitude of the site. The same applies to the 36 explosions carried out by the United States in the Pacific at tropical and equatorial latitudes.

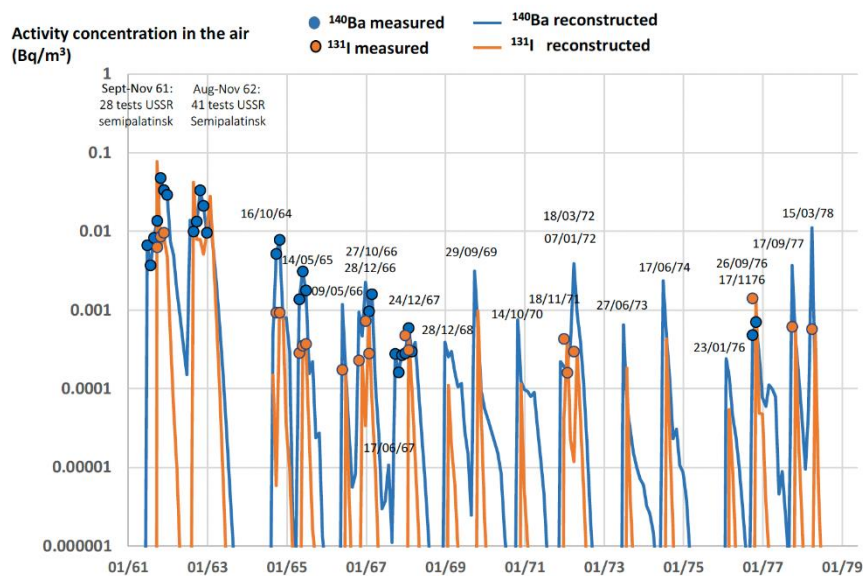


**Figure 8: Activity concentrations of  $^{131}\text{I}$  and  $^{140}\text{Ba}+$  measured monthly in the air in Le Vésinet (rounds) and reconstructed from measurements of  $^{95}\text{Zr}+$ , accounting for radioactive decay ( $\text{Bq}/\text{m}^3$ ).**

Apart from the passage of these bursts, the activity concentrations of  $^{131}\text{I}$  and  $^{140}\text{Ba}+$  were almost always below the detection limits<sup>5</sup>; they were reconstructed from the activities of  $^{95}\text{Zr}+$  taking into account radioactive decay from the date of the test (see Appendix I). We will see later that some  $^{131}\text{I}$  bursts not detected in the air were detected in other components of the environment such as rainwater, pastures, or bovine thyroids<sup>6</sup>.

In its 2000 report, UNSCEAR provides only the activity concentrations of  $^{90}\text{Sr}+$  in air (measured and calculated). The graph on the left in Figure 9 shows the remarkable correspondence between the annual averages measured in the mid-latitudes of the northern hemisphere reported by UNSCEAR, and the annual averages of the monthly measurements carried out by the SCPRI in Le Vésinet between 1961 and 1977. This correspondence is explained by the fact that France is between  $40^\circ$  and  $50^\circ$  northern latitude, so in the mid-latitude range of the northern hemisphere, and that the total fallout (stratospheric and tropospheric) was homogeneous over this latitude range (no difference related to longitude has been reported in the bibliography concerning stratospheric fallout).

In order to have values for the years before 1957, UNSCEAR proposes activity concentration values calculated from a model. The graph on the right in Figure 9 compares the average annual activity concentrations measured and calculated by UNSCEAR.

<sup>5</sup> The detection limit (DL) is the lowest activity that can be quantified in a sample. Below this value, the metrologist declares that the activity is lower than the limit value ( $< \text{DL}$ ). The detection limit depends on the performance of the metrological tools used.

<sup>6</sup> The thyroid gland concentrates iodine incorporated in the body.  $^{131}\text{I}$  analyses in bovine thyroids were regularly carried out by the SCPRI in the absence of measurement results in cow's milk, where the  $^{131}\text{I}$  concentration was usually too low to be measured.

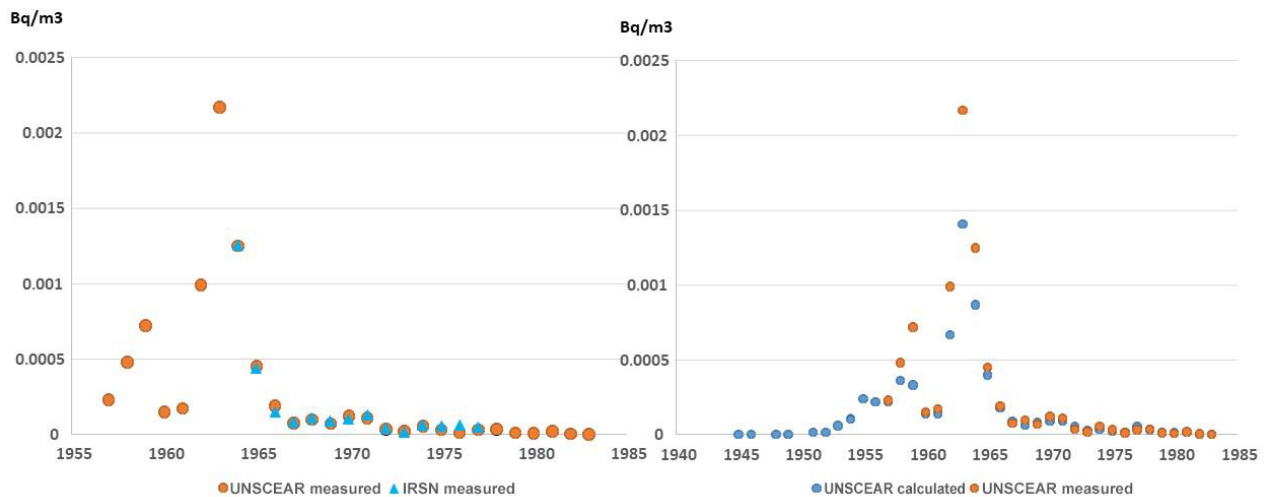
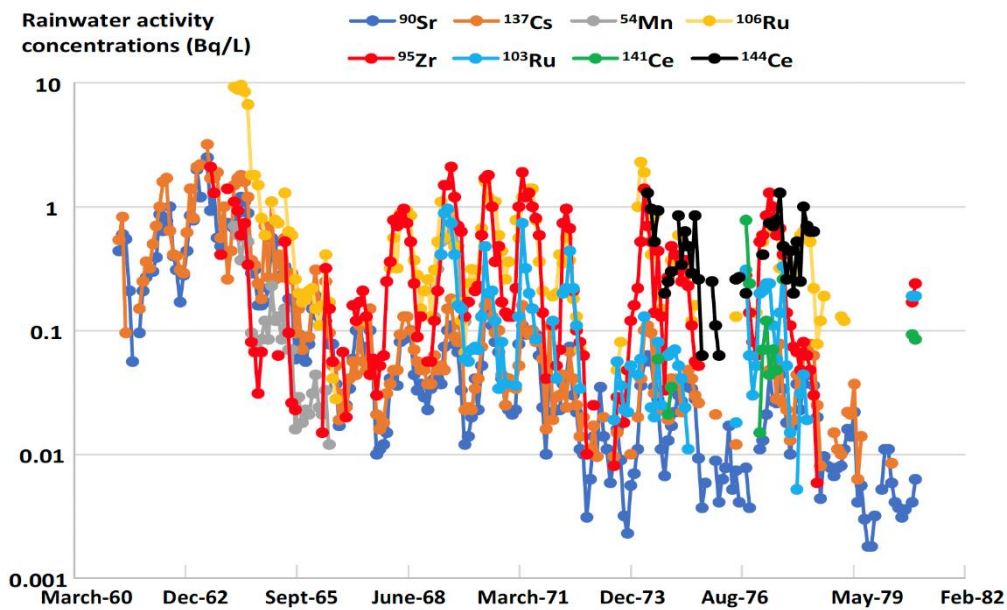


**Figure 9: Comparison of the activity concentrations of  $^{90}\text{Sr}+$  measured in the mid-latitudes of the northern hemisphere and reported by UNSCEAR (UNSCEAR 2000) to those measured at Le Vésinet (left graph in  $\text{Bq}/\text{m}^3$ ); comparison between the activity concentrations of  $^{90}\text{Sr}+$  calculated and measured by UNSCEAR (right graph in  $\text{Bq}/\text{m}^3$ ).**

## 4.2. Activity concentrations measured in rainwater in the Paris region

Figure 10 shows the activity concentrations of eight radionuclides with a half-life greater than one month, measured in rainwater collected in Fontenay-aux-Roses and then in Le Vésinet by the SCPRI. It shows changes similar to those of the activity concentrations in air, which they originate from (see Figure 7 in section 4.1). In particular, we find the highest activities during the years 1961 to 1963, and then the peaks related to incursions of stratospheric contamination into the troposphere. The completeness of records is better than those for air, with 50 to 60% of months over the period for  $^{106}\text{Ru}+$  and  $^{95}\text{Zr}+$ , nearly 80% for  $^{137}\text{Cs}+$  and up to 95% for  $^{90}\text{Sr}+$ . These records will therefore supplement those for air based on the study of washout coefficients (section 4.3.2).

Unfortunately, there are no measurement results for  $^{131}\text{I}$  in rainwater. But the measurements of  $^{140}\text{Ba}+$ , which has similar activity levels measured in air and a comparable radioactive half-life, can be used to reconstruct them. As was the case in air, the activities of  $^{140}\text{Ba}$  in rainwater were only measurable in the months following some of the Chinese nuclear tests. Figure 11 shows these activity concentrations and the dates of the corresponding Chinese tests. It is noted that the atmospheric contamination of three Chinese tests, which had not been detected in the air, was detected in rainwater (tests of October 1970, June 1974 and October 1980).



Top Figure 10: "Rainwater activity concentrations"

Figure 10: Records of activity concentrations for eight radionuclides with a half-life greater than one month measured in rainwater collected in Fontenay-aux-Roses and Le Vésinet from 1961 to 1980 (Bq/)

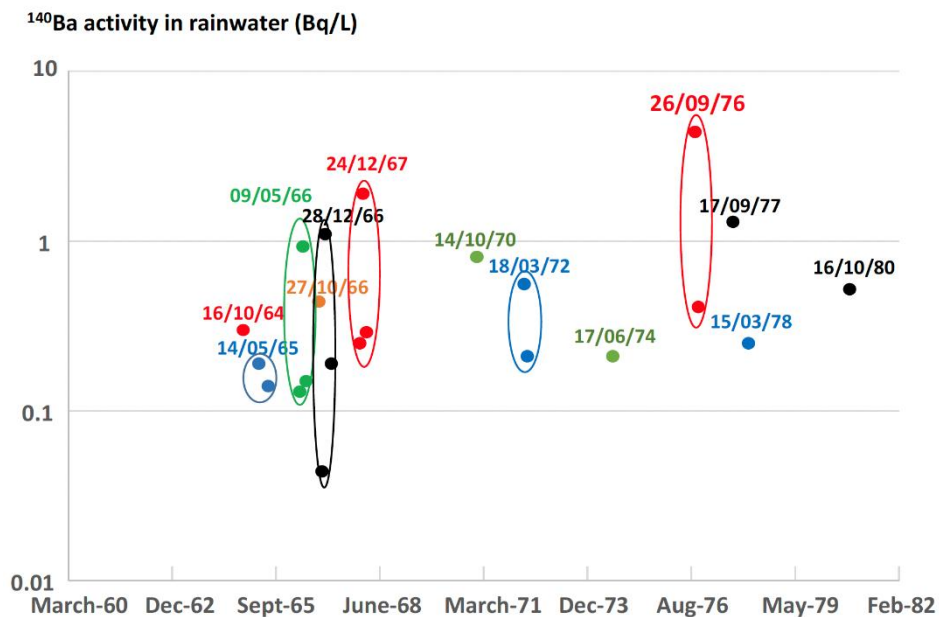


Figure 11: Activity concentrations of  $^{140}\text{Ba}+$  measured by the SCPRI in rainwater collected in Fontenay-aux-Roses and Le Vésinet between 1961 and 1980 (Bq/L) and dates of the corresponding Chinese nuclear tests

## 4.3. Reconstruction of complete records of activity in air in Le Vésinet

### 4.3.1. Methodology

Activity concentrations in the air are at the origin of activity concentrations and specific activities of all the other components of the environment: rainwater, activities deposited at ground level which have resulted in contamination of all living organisms and foodstuffs. The most complete reconstruction possible of activity records in the air is therefore decisive for all assessments of environmental activities and the exposure of the populations they have induced.

The records of activities measured in the air presented in Figure 7 were first completed using the activities measured in rainwater using the study of the relationship between the activities measured in these two media: the study of the washout ratio expressed in Bq/L of rainwater per Bq/m<sup>3</sup> of air.

The study of activity ratios of the different radionuclides measured was then used to fill in the remaining gaps.

Finally, records of radionuclides of interest not measured in France were reconstructed using activity ratios from UNSCEAR; these were the <sup>89</sup>Sr, <sup>91</sup>Y, <sup>125</sup>Sb+, <sup>241</sup>Am records and those of plutonium isotopes.

This reconstruction of activity concentrations in air covers the period from May 1961 to July 1978. The activities in air then decreased due to radioactive decay and deposition of particles on the ground. In practice, beyond 1985, only sufficiently long-lived radionuclides remain in the air: <sup>90</sup>Sr+, <sup>137</sup>Cs+, <sup>238</sup>Pu, <sup>239+240</sup>Pu, <sup>241</sup>Pu and <sup>241</sup>Am. The activity concentrations in air of these radionuclides have been measured over various periods in France and Germany since 1959. The use of isotopic activity ratios and the consideration of radioactive decay half-lives (or radioactive growing half-life in the case of <sup>241</sup>Am), allow for reconstruction of complete records of annual average activity concentrations in the air from 1959 to 2020.

Finally, tritium and carbon-14 are monitored on a global scale, which means there are complete records of their activities in the air from 1950 to the present day.

### 4.3.2. Study of washout ratios

The measurements taken by the SCPRI are used to calculate a washout ratio expressed in Bq/L of rainwater per Bq/m<sup>3</sup> of air. This ratio represents the overall loading<sup>7</sup> of water droplets with radioactive aerosols. The mean values of this ratio are fairly close for the nine radionuclides studied ranging from 353±271 m<sup>3</sup>/L to 609±298 m<sup>3</sup>/L (Table III). The average value of this ratio, all radionuclides combined, from the 595 calculated values is 502±243 m<sup>3</sup>/L. This result confirms the assumption usually made in models, that the processes concerned are mainly physical (related to the intensity of the rain, the size of the droplets, the size of the aerosols and the duration of the rain) and independent of the nature and chemistry of the radionuclide fixed to the aerosol. This value aligns with the estimate of De Bortoli (1974), obtained from similar data in Italy from 1963 to 1971: an average of 690 m<sup>3</sup>/L over a range from 120 to 760 m<sup>3</sup>/L, or that evaluated for stable isotopes of air pollutants<sup>8</sup>: from 170 to 900 m<sup>3</sup>/L for Cd and Pb (Peckar 1996) and from 200 to 700 m<sup>3</sup>/L for Cu, Ni, Co, Al (Chester et al. 1997). Given the annual precipitation in Le Vésinet, this value of 500±243 corresponds to a washout coefficient of 10<sup>-4</sup> s<sup>-1</sup>, which aligns with the values usually used in atmospheric transfer models (Renaud, 2021).

This average value of 502 m<sup>3</sup>/L was used to reconstruct the missing activity concentrations in the air from those measured in rainwater.

**Table III: Statistical indicators of washout ratio values**

	<sup>90</sup> Sr	<sup>137</sup> Cs	<sup>54</sup> Mn	<sup>106</sup> Ru	<sup>95</sup> Zr	<sup>140</sup> Ba	<sup>103</sup> Ru	<sup>141</sup> Ce	<sup>144</sup> Ce
Average	609	556	541	448	353	452	520	369	289
Standard deviation	298	291	248	246	271	385	433	247	122
Min	29	147	165	100	30	38	56	119	89
Max	2342	2226	1316	1486	2304	938	2162	889	528
Nbr of values	160	116	27	90	110	7	63	8	14

### 4.3.3. Study of activity ratios of the various radionuclides

For radionuclides other than <sup>90</sup>Sr, the UNSCEAR report from 2000 does not provide activity concentrations in air, but only total deposited activities (PBq) over the entire northern hemisphere. These values, however, make it possible to calculate activity ratios of the different radionuclides.

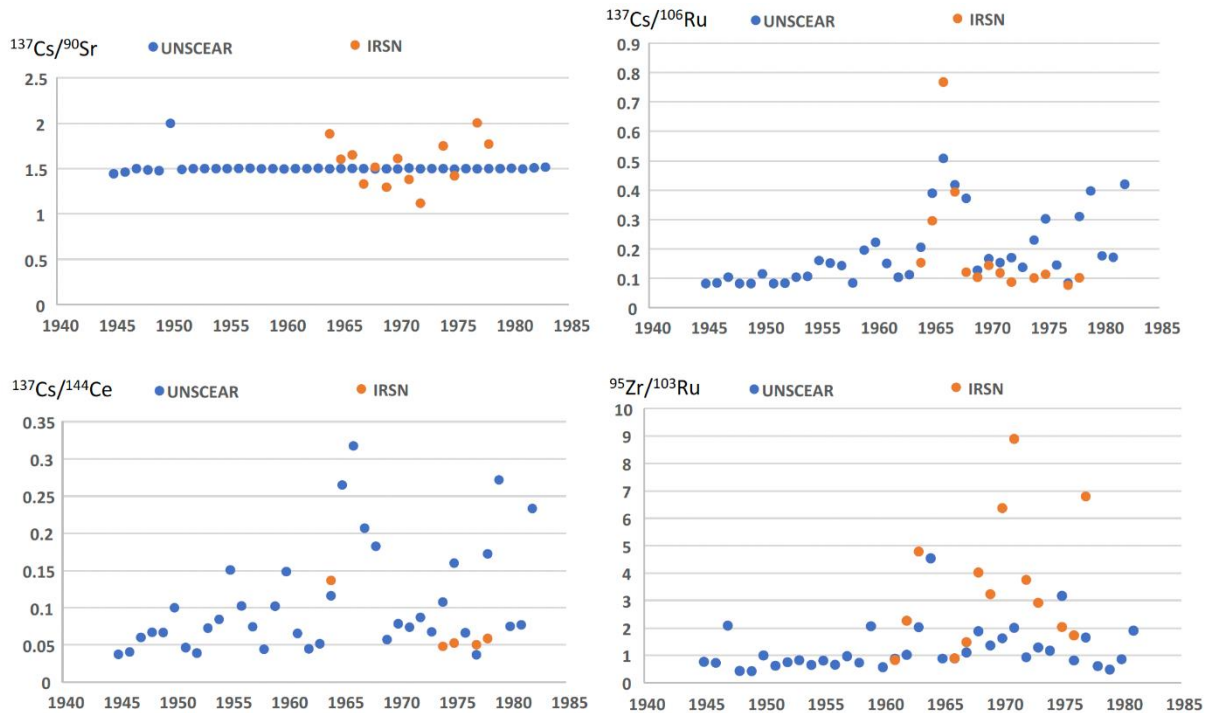
The study of these activity ratios meets two objectives. On the one hand, activity ratios calculated from activity concentrations measured by the SCPRI are compared with those deduced from total deposited activities provided by UNSCEAR; on the other hand, activity ratios can be used to reconstruct the complete records of activity concentrations in air of the main radionuclides at the origin of the population's exposures to fallout from nuclear weapons tests.

<sup>7</sup> Two processes contribute to this loading: the inclusion of particles during the formation of the droplet on the one hand (rainout), and the washing of air during the droplet's fall on the other hand (washout)

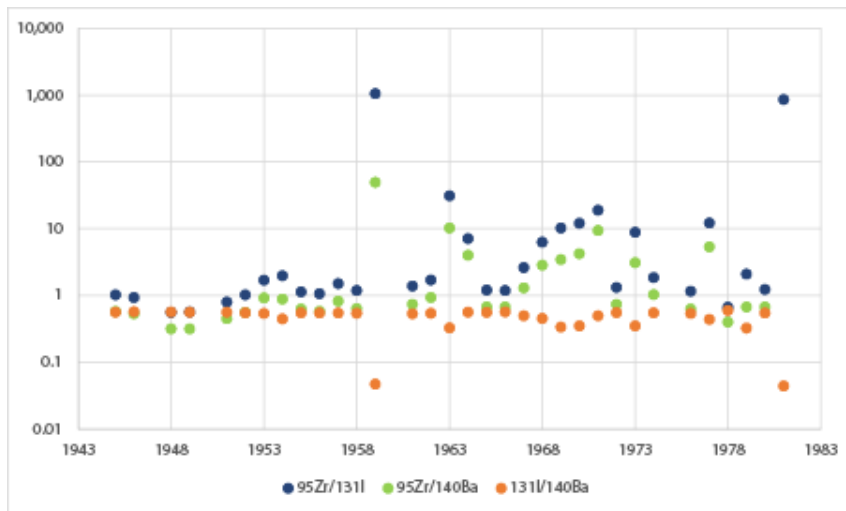
<sup>8</sup> In this case it is ng/L per ng/m<sup>3</sup>.

Figure 12 compares the average annual activity ratios  $^{137}\text{Cs}+/\text{}^{90}\text{Sr}+$ ,  $^{137}\text{Cs}+/\text{}^{106}\text{Ru}+$ ,  $^{137}\text{Cs}+/\text{}^{144}\text{Ce}+$ , and  $^{95}\text{Zr}+/\text{}^{103}\text{Ru}+$  from UNSCEAR and those calculated from measurement results in France. Figure 13 shows the annual activity ratios  $^{95}\text{Zr}+/\text{}^{131}\text{I}$ ,  $^{95}\text{Zr}+/\text{}^{140}\text{Ba}+$ , and  $^{131}\text{I}/\text{}^{140}\text{Ba}+$  from UNSCEAR.

For both UNSCEAR and IRSN, the  $^{137}\text{Cs}+/\text{}^{90}\text{Sr}+$  ratio is the least fluctuating (Figure 12) with an average, nearly identical value of 1.5 over the entire period (Table IV). This is explained by very similar radioactive half-lives and similar relative contributions for the two radionuclides between stratospheric and tropospheric fallout. The ratios  $^{137}\text{Cs}+/\text{}^{106}\text{Ru}+$  and  $^{137}\text{Cs}+/\text{}^{144}\text{Ce}+$  are more variable, particularly because of the differences in radioactive half-lives (around one year for  $^{106}\text{Ru}$  and  $^{144}\text{Ce}$  compared to thirty years for  $^{137}\text{Cs}+$ ): due to its longer half-life,  $^{137}\text{Cs}+$  accumulates in the atmosphere (especially in the stratosphere), gradually increasing activity ratios over the years. After 1963, injections of  $^{106}\text{Ru}+$  and  $^{144}\text{Ce}+$  into the atmosphere become more occasional, resulting in more fluctuating activity ratios for  $^{137}\text{Cs}+/\text{}^{106}\text{Ru}+$  and  $^{137}\text{Cs}+/\text{}^{144}\text{Ce}+$ , above a baseline that is around 0.1 for  $^{137}\text{Cs}+/\text{}^{106}\text{Ru}+$  and 0.05 for  $^{137}\text{Cs}+/\text{}^{144}\text{Ce}+$ . The difference in radioactive half-lives between  $^{95}\text{Zr}+$  (64 days) and  $^{103}\text{Ru}+$  (39 days) similarly explains the change in the annual activity ratios of these two radionuclides.



**Figure 12: Compared evolution of activity ratios  $^{137}\text{Cs}+/\text{}^{90}\text{Sr}+$ ,  $^{137}\text{Cs}+/\text{}^{106}\text{Ru}+$ ,  $^{137}\text{Cs}+/\text{}^{144}\text{Ce}+$ , and  $^{95}\text{Zr}+/\text{}^{103}\text{Ru}+$  from UNSCEAR and those calculated by IRSN, based on measurements taken in France by the SCPRI**



**Figure 13: Evolution of activity ratios  $^{95}\text{Zr}+/\text{}^{131}\text{I}$ ,  $^{95}\text{Zr}+/\text{}^{140}\text{Ba}+$ , and  $\text{}^{131}\text{I}/\text{}^{140}\text{Ba}+$  from UNSCEAR**

Figure 13, based on UNSCEAR data, shows that differences in radioactive half-lives also explain variations in activity ratios  $^{95}\text{Zr}+/\text{}^{131}\text{I}$ ,  $^{95}\text{Zr}+/\text{}^{140}\text{Ba}+$ . Until 1958, these activity ratios were around 1 for  $^{95}\text{Zr}+/\text{}^{131}\text{I}$  and 0.5 for  $^{95}\text{Zr}+/\text{}^{140}\text{Ba}+$ . In 1959, due to the absence of nuclear testing and therefore of injection of  $\text{}^{131}\text{I}$  and  $\text{}^{140}\text{Ba}+$ , as well as the persistence in the air of  $^{95}\text{Zr}+$  from the 1958 explosions, the activity ratios  $^{95}\text{Zr}+/\text{}^{131}\text{I}$  and  $^{95}\text{Zr}+/\text{}^{140}\text{Ba}+$  were very high (up to 1000 for the  $^{95}\text{Zr}+/\text{}^{131}\text{I}$  ratio) while the ratio  $\text{}^{131}\text{I}/\text{}^{140}\text{Ba}+$  was, inversely, very low. In 1961 and 1962, the numerous injections due to Soviet testing brought the activity ratios  $^{95}\text{Zr}+/\text{}^{131}\text{I}$  and  $^{95}\text{Zr}+/\text{}^{140}\text{Ba}+$  to around 1 and 0.5, respectively. During the 1970s, intermittent injections of  $\text{}^{131}\text{I}$  and  $\text{}^{140}\text{Ba}+$  caused these ratios to fluctuate. However, the activity ratio  $\text{}^{131}\text{I}/\text{}^{140}\text{Ba}+$  varied little due to the short and similar radioactive half-lives of these two radionuclides (8 and 13 days respectively), which do not allow for accumulation.

Table IV compares the average activity ratios over the entire period of 1961-1980. It shows the overall alignment between the activity ratios from UNSCEAR and those calculated by IRSN based on activities measured in France by SCPRI. The value of the ratio  $\text{}^{137}\text{Cs}/\text{}^{239+240}\text{Pu}$  was calculated by IRSN from the plutonium activities measured monthly in Germany between 1969 and 1973. The value of this ratio mentioned on the "UNSCEAR" line was calculated based on the activity ratio  $\text{}^{239+240}\text{Pu}/\text{}^{90}\text{Sr}$  of 0.018, provided in the 1982 UNSCEAR report, and the  $\text{}^{137}\text{Cs}/\text{}^{90}\text{Sr}$  ratio value of 1.5.

The activity ratios specific to certain nuclear tests were the subject of studies (Vray F. and Renaud P. 2004 and Appendix I) for Soviet tests in the 1960s and (Morin M., 2022) for Chinese tests. As before, the concordances or discrepancies between the activity ratios from these references and those indicated in Table IV are mainly explained by the radioactive half-lives of the radionuclides concerned.

Table IV: Annual average activity ratios of main radionuclides from the fallout of atmospheric tests of nuclear weapons in the air in France

	$^{137}\text{Cs}/^{90}\text{Sr}$	$^{95}\text{Zr}/^{90}\text{Sr}$	$^{137}\text{Cs}/^{106}\text{Ru}$	$^{137}\text{Cs}/^{144}\text{Ce}$	$^{137}\text{Cs}/^{239+240}\text{Pu}$	$^{106}\text{Ru}/^{144}\text{Ce}$	$^{106}\text{Ru}/^{64}\text{Mn}$
UNSCEAR	1.50	24	0.23	0.12	84	0.50	12
IRSN Air	1.56	20	0.20	0.07	97	0.67	14
IRSN rain	1.46	10	0.56	0.05	-	0.8*	8.4*
	$^{106}\text{Ru}/^{125}\text{Sb}$	$^{106}\text{Ru}/^{65}\text{Fe}$	$^{95}\text{Zr}/^{140}\text{Ba}$	$^{95}\text{Zr}/^{103}\text{Ru}$	$^{95}\text{Zr}/^{91}\text{Y}$	$^{95}\text{Zr}/^{90}\text{Sr}$	$^{95}\text{Zr}/^{131}\text{I}$
UNSCEAR	11	11.5	1.5**	1.5	1.3	1.8	5.6**
IRSN Air	-	-	2.6*	3.6	-	-	2.7*
IRSN rain	11*	-	0.8*	5	-	-	-
	$^{131}\text{I}/^{140}\text{Ba}$	$^{241}\text{Pu}/^{239+240}\text{Pu}$	$^{238}\text{Pu}/^{239+240}\text{Pu}$	$^{241}\text{Am}/^{239+240}\text{Pu}$			
UNSCEAR	0.50**	13***	0.025***	0.025***			
IRSN Air	0.39*	-	-	-			
IRSN rain	-	-	-	-			

\*based on a very limited number of monthly ratios (it is not possible to determine average annual ratios)

\*\*the annual activity ratios for the years 1959, 1960, 1964, and 1975 have not been taken into account in this value (no tests, resulting in a distorted ratio)

\*\*\* values from the 1982 UNSCEAR report

These are the activity ratios estimated by IRSN on the basis of activity concentrations measured in the air, and, failing that, those proposed by UNSCEAR, which were used to complete the records of activities in the air (already completed using measurements on rainwater). The activity ratios of radionuclides with similar radioactive half-lives were selected as a priority.

#### 4.3.4. Complete reconstructed records of monthly activity in air from June 1961 to July 1978

Figure 14 shows the reconstructed activity concentrations in air for the 16 main radionuclides with a half-life greater than one month (excluding  $^3\text{H}$  and  $^{14}\text{C}$ ) that contributed to exposure of the population.

These records are used to reconstruct the specific activities and activity concentrations in the other components of the environment in the following paragraphs. The records relating to  $^{131}\text{I}$  and  $^{140}\text{Ba}$  are presented in Figure 8.

The measurements taken on filters from stations other than Le Vésinet (Cléville, Méaudre, Sauveterre, Vioménil, etc.) show that the activities in the air were fairly homogeneous throughout mainland France. This can be explained by the homogenisation of radioactive plumes during their west-east journey of several thousand kilometres (around 20,000 km separate the Chinese sites of Lop Nur and the Soviet sites of Semipalatinsk from France) and the small size of the French territory in relation to such distances.

All the radioactive elements mentioned were present in the air exclusively in the form of aerosols, with the exception of iodine, some of which was emitted during the explosions and remained in gaseous form. This gaseous fraction has not been measured in air and the activity concentrations of  $^{131}\text{I}$  presented above represent only a fraction of the activities of this radionuclide actually present in air. Observations made after the Chernobyl and Fukushima accidents show that the activity concentration

of iodine gas is two to three times greater than the particulate activity concentration. There is no data on this proportion in the fallout from nuclear weapons tests. By default, a proportion of 50% was used; the activity concentrations of  $^{131}\text{I}$  measured in aerosols were therefore doubled.

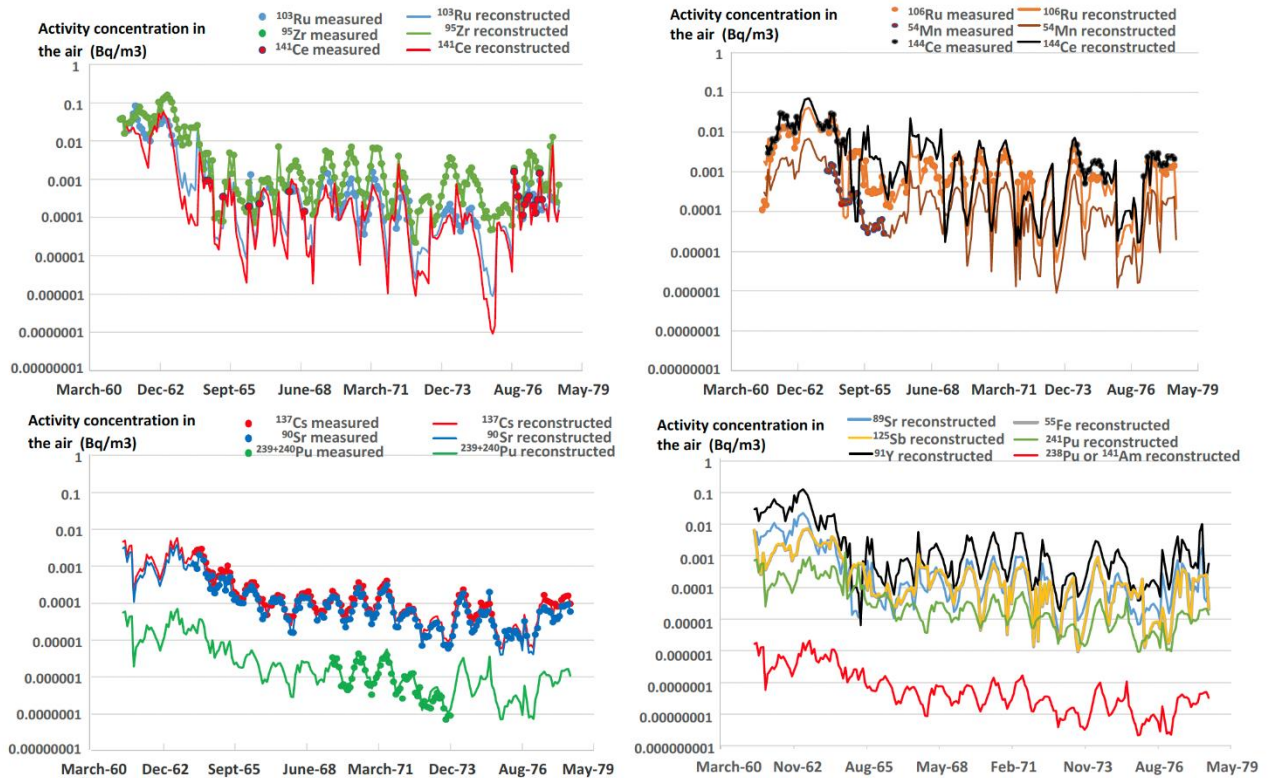


**Figure 14: Complete records of the monthly activity concentrations of the main radionuclides resulting from the fallout of nuclear tests in the air in mainland France between 1961 and 1978 (Bq/m<sup>3</sup>).**

### 4.3.5. Records of annual average activities of long-lived radionuclides, 1959 to 2020

#### 4.3.5.1. Case of $^{90}\text{Sr}$ , plutonium isotopes, and $^{241}\text{Am}$

Caesium-137 has been measured in the air in France since 1959 and the use of increasingly efficient sampling and analysis methods allow measurement to be continued today. However, since May 1986, its presence in the air in France has mainly resulted from the fallout of the Chernobyl accident. The activity concentrations of  $^{238}\text{Pu}$  and  $^{239+240}\text{Pu}$  have been measured in the air in Germany since January 1986; those of  $^{90}\text{Sr}$  since January 1990, and the results can be considered as representative of the situation in mainland France (similar latitudes with respect to stratospheric and tropospheric fallout). Finally, these radionuclides have been measured quarterly in France since 2012. Based on this data, records of annual average activities of these radionuclides can be reconstructed for the period 1959 to 2020 using reliably and accurately known isotopic activity ratios (see section 4.3.3 and Table II). Therefore, even if the activity concentrations of  $^{238}\text{Pu}$  have been measured in Germany and France, given the metrological uncertainties associated with the very low levels of activity of this radionuclide,

the values deduced from measurements of  $^{239+240}\text{Pu}$  using a  $^{238}\text{Pu}/^{239+240}\text{Pu}$  activity ratio of 0.03 are preferred.

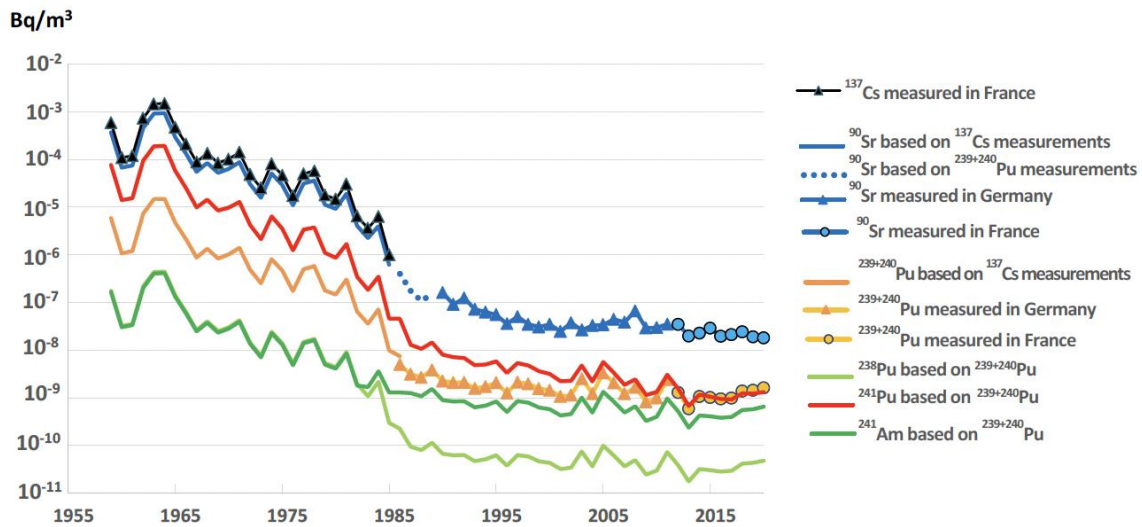


**Figure 15: Average annual activity concentrations in air of  $^{137}\text{Cs}$ ,  $^{90}\text{Sr}$ ,  $^{241}\text{Am}$ , and plutonium isotopes from 1959 to 2020**

Figure 15 shows that after the last Chinese test in 1980, the activity concentrations decreased significantly during the 1980s by purification of the atmospheric compartment linked to aerosol deposition. From the early 1990s, resuspension phenomena (wind turbines and combustion of organic matter) partially compensated for the deposition phenomena, leading to a much slower decrease in activity concentrations. The activities of  $^{241}\text{Pu}$  (red curve), initially 13 times higher than those of  $^{239+240}\text{Pu}$ , decreased more rapidly than activities of other radionuclides due to its 14-year radioactive half-life, reaching a level lower than that of  $^{239+240}\text{Pu}$  in 2020 (orange curve). On the other hand, for  $^{241}\text{Am}$  (dark green curve), purification of the atmospheric compartment was limited due to its production through the disintegration of  $^{241}\text{Pu}$  present in soil and resuspended in air; since the late 1990s, the ratio of  $^{241}\text{Am}/^{239+240}\text{Pu}$  is 0.4 (IRSN, 2022).

#### 4.3.5.2. Case of tritium and carbon-14

Carbon-14 and tritium are naturally produced, continuously, in the upper layers of the atmosphere due to the action of cosmic rays;  $1.54 \times 10^{15}$  Bq of  $^{14}\text{C}$  and  $7.2 \times 10^{16}$  Bq of tritium are thus produced annually.

Nuclear tests injected into the atmosphere  $2.1 \times 10^{17}$  Bq of  $^{14}\text{C}$ , the equivalent of 140 years of annual cosmogenic production of this radionuclide, and  $2.4 \times 10^{20}$  Bq of tritium, or 3,300 years of annual cosmogenic production of this radionuclide.

Although carbon-14 and tritium are incorporated into the living environment during photosynthesis before following the cycles of organic matter and water (for tritium), the reservoir of these radionuclides remains the air, in which they are mainly found in the form of water vapour (HTO) or gas (mainly carbon dioxide,  $^{14}\text{CO}_2$ ). So, unlike the other radionuclides emitted by nuclear tests, which are present in particulate form in the air and have been deposited on the soil, carbon-14 and tritium are

still present in the air in large amounts and in a fairly homogeneous state, on the scale of the globe for  $^{14}\text{C}$  and the northern hemisphere for  $^3\text{H}$ <sup>9</sup>.

The activity concentration of tritium in rainwater, which is fairly representative of tritium in atmospheric water vapour, is regularly measured at different points around the world. In this study, we will take the annual average of the monthly measurements taken in Ottawa, Canada since 1953, Thonon-les-Bains, France since 1963 and Opme, France by IRSN since 2015. From these measured activities, an average activity concentration of 0.4 Bq/L<sup>10</sup>, corresponding to the cosmogenic background, was subtracted in order to estimate the activity concentration added by the nuclear tests. The activity concentration of tritium in air can then be deduced from these values by considering an average content of 10 ml of water vapour per cubic metre of air. So, for a tritium activity of 1 Bq/L of atmospheric water vapour the corresponding activity concentration in air is 0.01 Bq/m<sup>3</sup>. Figure 16 shows the evolution in the average annual activity concentration of tritium in air for the northern hemisphere since 1953. Before the nuclear tests, this activity concentration was constant and between 0.001 and 0.006 Bq/m<sup>3</sup> as a result of a balance between cosmogenic production and elimination by radioactive decay (half-life of 12.3 years). The nuclear tests caused this activity concentration of tritium in the air to increase beyond 3 Bq/m<sup>3</sup> as an annual average in 1964 (higher values were measured monthly or weekly). Since then, this activity concentration has been decreasing due to the radioactive decay and dilution of tritium in ocean waters; it was slightly lower than 0.01 Bq/m<sup>3</sup> in 2020.

The carbon-14 content in the environment is also monitored on a global scale. The measurements carried out as part of this monitoring are those of the activity of  $^{14}\text{C}$  per unit of carbon mass (Bq/kg of C.; see section 6.7). The activity concentration of  $^{14}\text{C}$  in air, expressed in Bq/m<sup>3</sup>, can be deduced from these measurements by estimating the mass of carbon in the air using the CO<sub>2</sub> content of the air (in ppm). The blue curve in Figure 16 shows the evolution in the average annual activity concentration of  $^{14}\text{C}$  in air from 1950 to 2020. After an increase, due to nuclear tests, from 0.035 Bq/m<sup>3</sup> of air in the early 1950s to 0.07 Bq/m<sup>3</sup> in 1964, followed by a decrease over about 15 years due to the homogenisation on a global scale of  $^{14}\text{C}$  injected mainly in the northern hemisphere, the activity concentration of  $^{14}\text{C}$  in the air stabilised around 0.05 Bq/m<sup>3</sup> in the late 1970s. This consistency over several decades is explained by the fact that  $^{14}\text{C}$  can only be eliminated very slowly by radioactive decay (half-life of 5,630 years), with the other losses (sediment trapping, in particular) also being very low. In order to estimate the activity added by the fallout from nuclear weapons tests, an activity of 226 Bq/kg of C. corresponding to the cosmogenic level prior to tests, was subtracted from the measured values.

---

<sup>9</sup> Due to a much larger ocean water mass in the southern hemisphere, the tritium content of the air is lower. It is influenced (particularly *via* sea spray) by the content in marine waters, which are little affected by the fallout from nuclear tests due to their high dilution capacity.

<sup>10</sup> The tritium activity prior to nuclear tests was between 0.2 and 0.6 Bq/L; an intermediate value of 0.4 Bq/L was selected in this study.

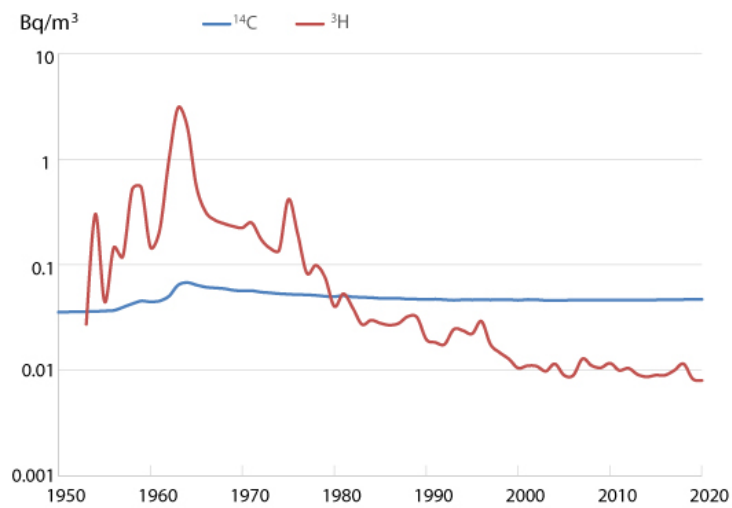


**Figure 10: Average annual activity concentrations of tritium and carbon-14 in air from 1950 to 2020 ( $\text{Bq/m}^3$ )**

## 5. Surface activities deposited on the ground

### 5.1. Monthly dry and wet deposition estimates

During the entire period of nuclear tests (1945-1980) as well as a few years beyond that for radionuclides with a radioactive half-life greater than one year, contaminated air masses induced radioactive deposits at ground level ( $\text{Bq}/\text{m}^2$ ). These deposits occurred both in dry weather and during precipitation.

The monthly dry deposition ( $\text{Bq}/\text{m}^2/\text{month}$ ) can be estimated from the monthly activity concentrations in atmospheric aerosols ( $\text{Bq}/\text{m}^3$ ) using a dry deposition velocity of  $5 \times 10^{-3} \text{ m/s}$  ( $\text{Bq}/\text{m}^2/\text{month} = \text{Bq}/\text{m}^3 \times \text{m/s} \times 2.54 \times 10^6 \text{ s/month}$ ) (Renaud Ph., 2020).

Monthly rainfall deposits ( $\text{Bq}/\text{m}^2/\text{month}$ ) were estimated by SCPRI using activities measured monthly in rainwater and precipitation amounts also measured monthly by Météo-France on the same stations ( $1 \text{ mm/month} = 1 \text{ L}/\text{m}^2/\text{month}$ ). Figure 17 shows the monthly activities deposited for the six radionuclides most regularly measured in rainwater in the Paris region (Fontenay-aux-Roses and Le Vésinet). The changes in these deposited activities are to be directly correlated with the activity concentrations in the air and in rainwater (figures 1 and 4). In particular, we find the summer incursions of stratospheric contamination for these radionuclides with a half-life greater than one month. For  $^{140}\text{Ba}$  and  $^{131}\text{I}$ , the measurement results are, as in the case of air, very sporadic and limited to the month following each of the Chinese tests.

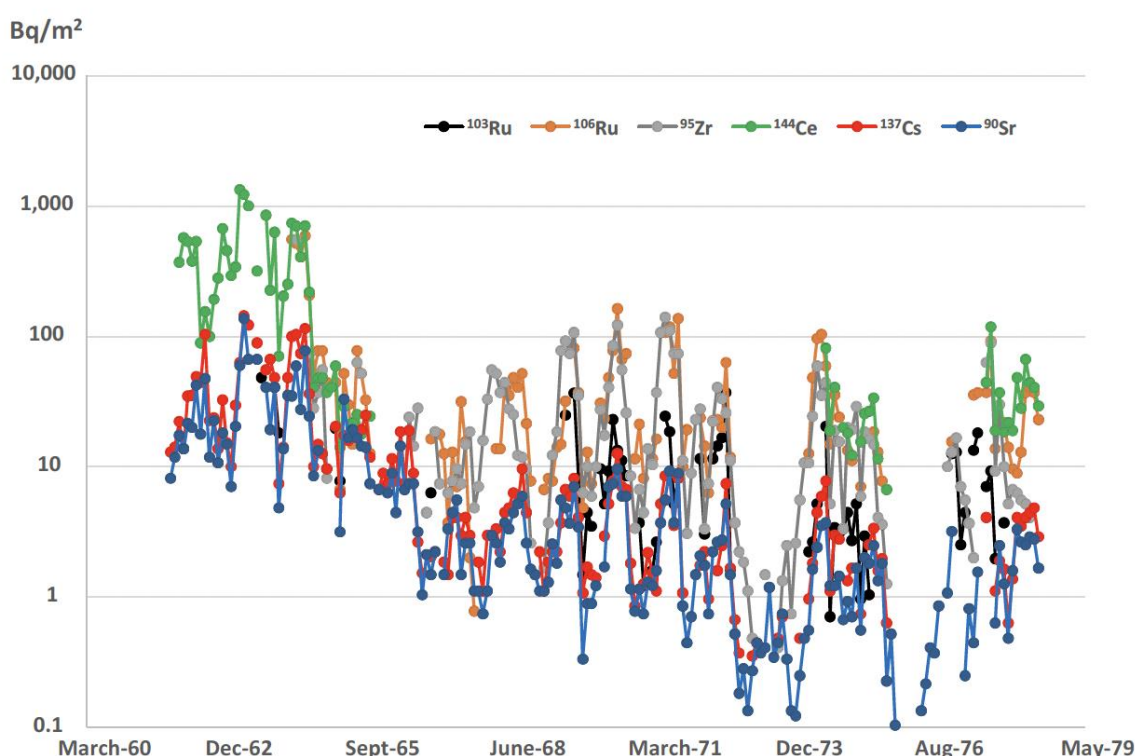
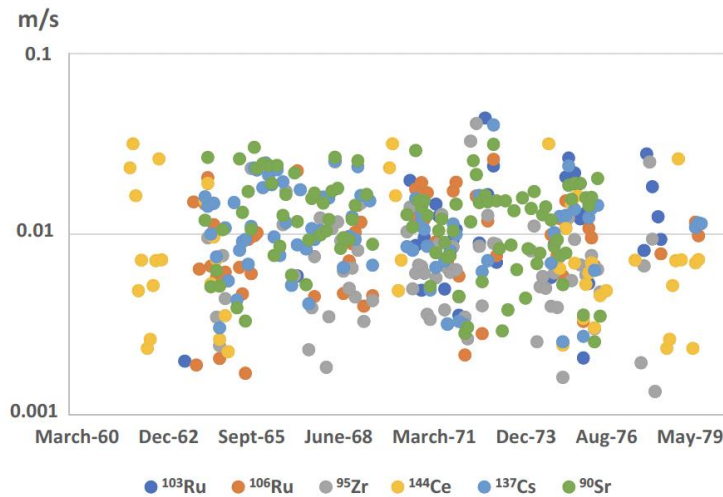


Figure 17: Surface activities deposited monthly for the six radionuclides most regularly measured in rainwater by SCPRI from 1961 to 1978 ( $\text{Bq}/\text{m}^2/\text{month}$ )

From March 1964, concomitant collection of monthly results for measurements of activity concentrations in the air ( $\text{Bq}/\text{m}^3$ ) and in rainwater ( $\text{Bq}/\text{L}$ ), make it possible to calculate fairly regularly the ratio of the activities deposited monthly during rainfall ( $\text{Bq}/\text{m}^2/\text{month}$ ) to the activities in the air ( $\text{Bq}/\text{m}^3$ ). This ratio corresponds to a rainfall deposition velocity expressed in  $\text{m}/\text{month}$ , which, converted into  $\text{m}/\text{s}$ , is then comparable to the dry deposition velocity mentioned above.



**Figure 18: Wet deposition velocities (m/s) estimated at Le Vésinet**

Figure 18 shows the deposition velocities thus calculated for the Paris region (Fontenay-aux-Roses, Le Vésinet, and Paris) where the data is most plentiful; Table V shows the values of the corresponding statistical indicators (averages, standard deviations, minimums, maximums, and number of values) calculated to compare with the 238 months covered by the period June 1961-December 1980.

**Table V: Wet deposition velocities (m/s) at Le Vésinet**

	$^{103}\text{Ru}$	$^{106}\text{Ru}$	$^{95}\text{Zr}$	$^{144}\text{Ce}$	$^{137}\text{Cs}$	$^{90}\text{Sr}$
Average	0.012	0.010	0.008	0.010	0.012	0.013
Std dev	0.009	0.006	0.007	0.009	0.007	0.007
Min	0.002	0.002	0.001	0.002	0.003	0.003
Max	0.044	0.026	0.041	0.032	0.040	0.031
Nbr of values	37	58	81	48	80	105

The averages of the deposition velocities calculated for the various radionuclides are very close, ranging from 0.008 to 0.013  $\text{m}/\text{s}$ . The minimum deposition velocities (0.002 to 0.003  $\text{m}/\text{s}$ ), close to the dry deposition velocity used in this study (0.005  $\text{m}/\text{s}$ ), correspond to months with very low precipitation; the maximum values (around 0.04  $\text{m}/\text{s}$ ) correspond to months with high precipitation. The average of the 409 deposition velocities calculated for the six radionuclides shown in Table V is  $0.011 \pm 0.007 \text{ m/s}$ . This value is twice the value used for dry deposition (0.005  $\text{m}/\text{s}$ ). It indicates that in the Paris region, precipitation induced wet deposition that was twice as high, on average, as dry deposition.

This is confirmed by Table VI, which directly indicates the ratios of wet to dry deposits. The averages of this ratio for the various radionuclides are between 1.7 and 2.5. The minimum values of 0.4 correspond to very dry months and the maximums (five to six) correspond to very wet months. The average of the 532 monthly "wet/dry" deposition ratios obtained for the Paris region, all radionuclides combined, is  $2.1 \pm 1.2$ .

Table VI: "Wet/dry" deposition ratio (dimensionless)

	<sup>103</sup> Ru	<sup>106</sup> Ru	<sup>95</sup> Zr	<sup>144</sup> Ce	<sup>140</sup> Ba	<sup>137</sup> Cs	<sup>90</sup> Sr
Average	2.2	1.9	1.7	1.7	2.2	2.3	2.5
Std dev	1.3	1.1	1.0	1.1	1.2	1.1	1.3
Min	0.4	0.4	0.4	0.5	0.8	0.5	0.4
Max	5.6	5.2	5.1	5.3	3.6	5.1	6.4
Nbr of values	50	74	108	42	4	107	147

The deposition velocities calculated are therefore directly related to the monthly precipitation amounts for the location in question.

## 5.2. UNSCEAR vs IRSN comparison of integrated deposits

In its 2000 report, UNSCEAR provides the annual trends in integrated deposition for various radionuclides (cumulative deposition density), for the northern hemisphere, weighted according to population numbers. This is the accumulation of surface activities (Bq/m<sup>2</sup>) deposited up to the year in question, taking into account radioactive decay. Weighting according to population numbers tends to give more weight to the temperate latitudes, which are the most populated and which include mainland France.

These integrated surface activities can also be calculated using the previously estimated monthly deposited surface activities from French data, in order to compare them with those estimated by UNSCEAR.

Figures 19 and 20 show this comparison for the main radionuclides and Table VII provides the statistical elements.

While the activity concentrations of <sup>90</sup>Sr in the air estimated by UNSCEAR for the mid-latitudes of the northern hemisphere were very close to those measured in France (see chapter 4.1 and figure 9), the cumulative surface activities of this radionuclide, estimated for France, are 1.7 times higher than those estimated by UNSCEAR. The same applies to <sup>137</sup>Cs, whose cumulative surface activities in France are also, on average, 1.7 times higher than those estimated by UNSCEAR. This deviation is related to precipitation, which, as indicated above, determines wet deposition. France, under oceanic influence, would therefore receive rainfall around twice that of the mid-latitudes in the northern hemisphere.

For shorter-lived radionuclides, this difference is greater, between 3.1 and 3.8. Greater activities in the air could be responsible for the increase in this deviation, by a factor of 1.7 to a factor of 3.1, or even 3.8. Indeed, the tropospheric component of the fallout of short-lived radionuclides is much greater than that of <sup>90</sup>Sr and <sup>137</sup>Cs. However, France is, as indicated above, in the same latitudinal range as the Semipalatinsk, Lop Nur and Nevada test sites. It is therefore likely that the activity in the air during tropospheric bursts were higher on the French mainland than the average in the northern hemisphere.

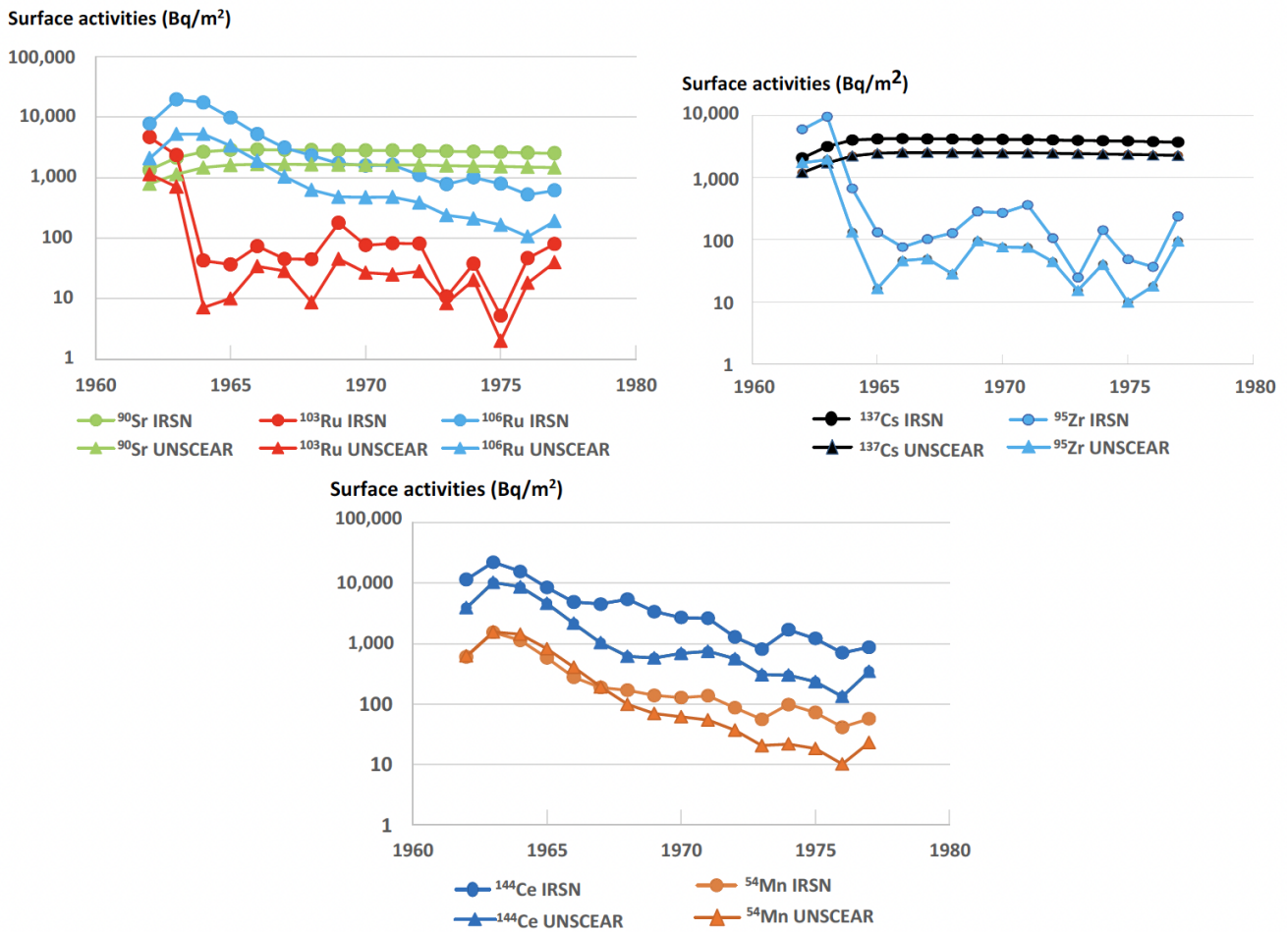


Figure 19: Comparison of integrated surface activities estimated by IRSN for mainland France and by UNSCEAR for the northern hemisphere, weighted by population (Bq/m<sup>2</sup>)

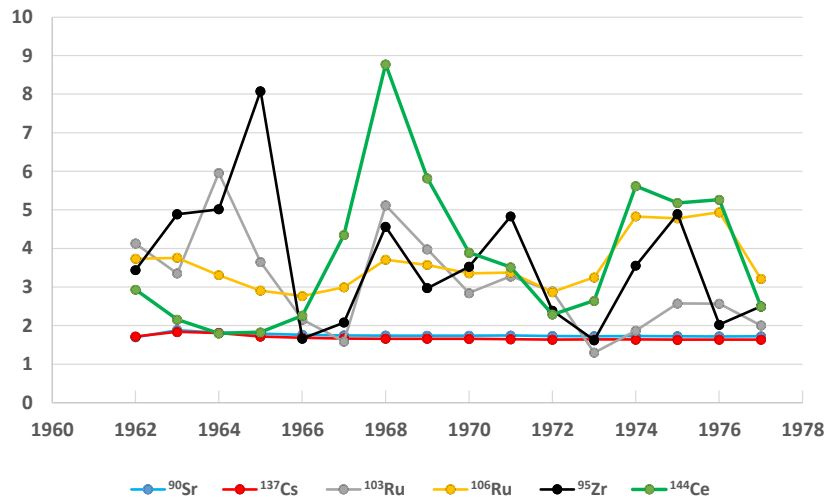


Figure 20: Evolution of the ratio of integrated surface activities estimated for mainland France by IRSN to those estimated by UNSCEAR for the northern hemisphere, weighted by population

**Table VII: Averages and standard deviations of the IRSN/UNSCEAR annual integrated surface activities ratio**

	<sup>90</sup> Sr	<sup>137</sup> Cs	<sup>103</sup> Ru	<sup>106</sup> Ru	<sup>95</sup> Zr	<sup>144</sup> Ce
<b>Average</b>	1.7	1.7	3.1	3.6	3.6	3.8
<b>Std dev</b>	0.05	0.06	1.3	0.7	1.7	1.9

### 5.3. Spatial variability of activities deposited in mainland France

Several approaches are possible when it comes to spatial variability of deposits at the scale of mainland France. The concordance of the results from these different approaches is studied below. The consequences of spatial variability of deposition on the variability of specific activities and activity concentrations in the food chain will then be studied in chapter 6; and the consequences on spatial variability of ingested doses will be studied in section 9.5 to demonstrate consistency of the whole.

Since the activity concentrations in the air, and therefore dry deposits, can be considered homogeneous at the scale of mainland France, the spatial variability of deposits results only from the variability of wet deposits linked to the amount of precipitation.

The first approach to spatial variability of deposits is based on the study of variability of the wet deposition velocity as a function of the average annual levels of precipitation. In France, average annual rainfall levels are essentially between 600 mm/year and 1,600 mm/year, even if certain areas of the territory may experience lower (400 mm/year in the lower Rhône Valley, for example) or higher levels of rainfall (more than 2,000 mm/year in the Cevennes).

Among the sites where deposition velocities can be estimated using measurements taken by the SCPRI, we have Le Vésinet where the average annual precipitation is representative of the lowest observed in France (around 700 mm/year), and Vioménil in the Vosges with significantly higher levels of average annual precipitation (around 1,200 mm/year). Figure 21 shows the wet deposition velocities (m/s) calculated for Vioménil using the surface activities deposited monthly during rainfall (Bq/m<sup>2</sup>/month) and the activity concentrations in the air (Bq/m<sup>3</sup>); Table VIII provides the statistical parameters.

**Table VIII: Wet deposition velocities (m/s) at Vioménil (to be compared with those mentioned in Table III)**

	<sup>137</sup> Cs	<sup>90</sup> Sr	<sup>106</sup> Ru	<sup>95</sup> Zr	<sup>103</sup> Ru
Average	0.019	0.020	0.017	0.015	0.020
Std dev	0.008	0.012	0.009	0.009	0.013
Min	0.005	0.003	0.005	0.002	0.003
Max	0.049	0.067	0.046	0.058	0.061
Number	93	67	45	99	46

As in the case of Le Vésinet, the deposition velocity does not vary significantly by radionuclide. On the other hand, the average values calculated for Vioménil indicated in Table VIII are 1.5 to 1.8 times higher than those calculated for Le Vésinet, shown in Table V. The average of the 350 values calculated for Vioménil is 0.018±0.01 m/s to be compared with that of 0.011±0.007 m/s for Vésinet. According to this approach, wet deposits at Vioménil are 1.7 times higher than those at Le Vésinet.

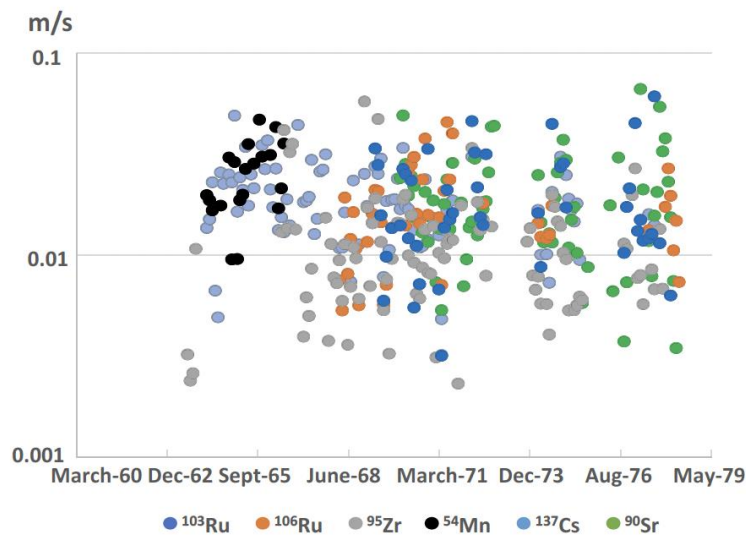


**Figure 21: Wet deposition velocities (m/s) calculated for Vioménil (to be compared with those mentioned in figure 18)**

The second approach to studying spatial variability of deposition consists of calculating the total surface activities deposited over a given time period. Figure 22 shows the activities of  $^{90}\text{Sr}$ ,  $^{137}\text{Cs}$  and  $^{95}\text{Zr}$  deposited between January 1967 and December 1972 at three sampling stations: Le Vésinet (700 mm/year), Vioménil in the Vosges (1,200 mm/year) and Méaudre in the Isère at an altitude of more than 1,000 m (1,500 mm/year). These deposited activities are directly derived from measurements taken in rainwater and the time period was selected due to the completeness of records. This figure confirms that the activities deposited increase with rainfall at the same proportion as the deposition velocities. The activities deposited at Vioménil from 1967 to 1972 are 1.7 times higher on average than those deposited at Le Vésinet over the same period (from 1.6 times higher for  $^{95}\text{Zr}$  to 1.8 times higher for  $^{137}\text{Cs}$ ). This average ratio is strictly identical to that of the deposition velocities calculated previously between the two municipalities.

Finally, the third approach to studying the spatial variability of radioactive deposits following fallout from atmospheric tests of nuclear weapons is based on completely different data. Relationships between activities deposited following nuclear tests and average annual precipitation have been established in various countries, including France, on the basis of activity measurements of  $^{239+240}\text{Pu}$  and  $^{137}\text{Cs}$  persisting in soils (Bunzl & Krack, 1988; Hölgge & Filgas, 1995; Mitchell et al., 1990; LeRoux et al., 2002). The specific activities measured in soil samples taken by coring, at depths sufficient to contain most of the activities initially deposited, allowed reconstruction of the corresponding surface activities. By comparing these surface activities to the average annual precipitation levels provided by Météo-France, a "rainfall-deposit" relationship is obtained. In the case of France, this relationship has made it possible to prepare the map presented in Figure 23. By applying the "rainfall-deposit" ratios established by the various authors, it is possible to calculate the ratio of results obtained for Vioménil to those for Le Vésinet. The values of this ratio, which are presented in Table IX, show that the values calculated according to the various relationships are consistent with those obtained according to the other approaches presented above (deposition velocity ratios and deposited activities ratios from 1967 to 1972).

Because it allows total coverage of the territory, the IRSN relationship for  $^{137}\text{Cs}$  is used to account for the spatial variability of surface activities deposited during fallout from atmospheric tests of nuclear weapons.

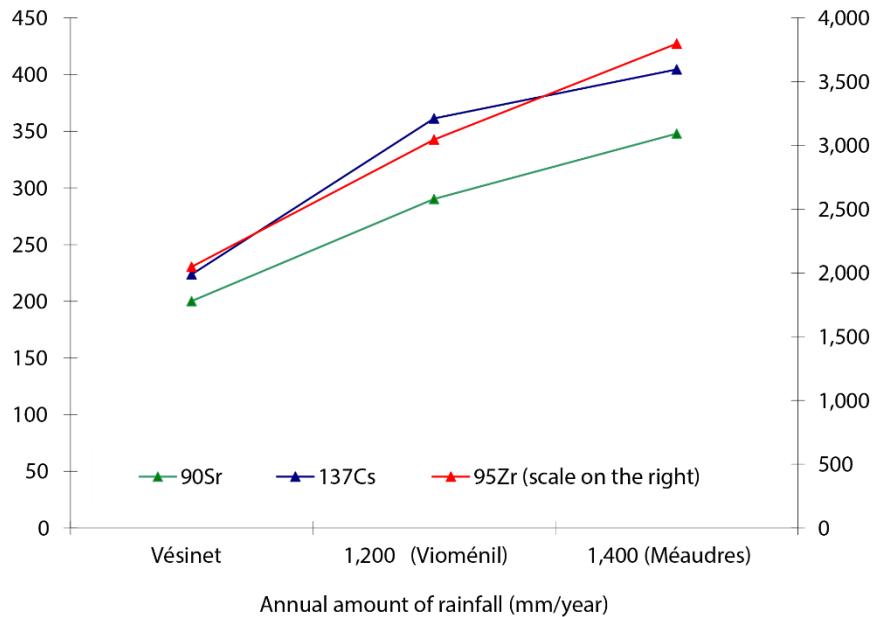


**Figure 22: Deposited surface activities from 1967 to 1972 in three municipalities receiving average annual precipitation representative of the range of rainfall in mainland France (Bq/m<sup>2</sup>)**

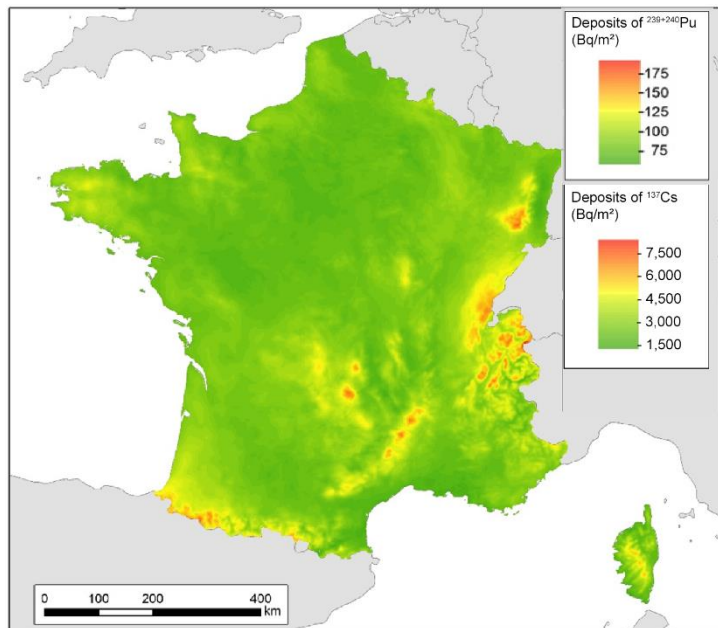


**Figure 23: Mapping of deposited surface activities following fallout from atmospheric tests of nuclear weapons (Bq/m<sup>2</sup>)**

Table IX: Ratio of deposited activities after the fallout from nuclear tests in Vioménil and Le Vésinet according to various "rainfall-deposit" relationships

	$^{137}\text{Cs}$	$^{239+240}\text{Pu}$
Mitchell et al. (1990)	1.6	1.7
Bunzl & Krack (1988)	1.6	-
Hölgge & Filgas (1995)	-	1.7
Pourcelot et al. (2021)	1.9	1.5

## 6. Specific activities and activity concentrations in the food chain

### 6.1. Methods for reconstructing specific activities and activity concentrations in the food chain

As for activity concentrations in the atmosphere and deposited surface activities, the reconstruction of specific activities and activity concentrations in the food chain is first based on measurement results. These results were taken from the monthly bulletins published by the SCPRI (1961-1980) and the quarterly bulletins of the Interministerial Sub-Committee on Health Protection (1961-1965), subsequently renamed CEA/DPS (1965-1978).

While monitoring of food chain contamination by these two organisations was continuous throughout the period studied, the evolution of environmental contamination, the specific behaviour of radionuclides with regard to the food products studied, as well as the evolution of measurement techniques, led to heterogeneities in the completeness of data records available: some links in the food chain are particularly well documented for the main radionuclides, while only a few scattered data are available for others.

As stated above for atmospheric activities, it is necessary to fill in the gaps. To do this, we use radionuclide transfer modelling. Due to the relatively continuous nature of activity contributions related to atmospheric activities from fallout of nuclear testing, the transfer equations chosen are those used to assess the impact of chronic discharges from nuclear facilities, and are the same for most operational models that calculate the impact of chronic discharges, in particular the IRSN CONDOR model (Thomassin, 2008).

It is then a question of determining the values of these parameters that allow the best possible approximation between the results of the model and the available measurement results, while remaining within the range of values commonly recommended by the bibliography on transfer of radionuclides into the environment. The suitability of a set of parameter values for the available data has been quantified by the ratio of the calculated to measured specific activities and activity concentrations, which must remain close to one; records of this ratio demonstrate its variability and verify the absence of temporal drifts.

In the absence of measurement results or if they are insufficient, the missing parameter values were searched for in the bibliography. These are mainly the default values of the models CONDOR (Thomassin, 2008), ECOSYS (Müller and Proehl, 1993) or FARMLAND (Brown & Simmonds, 1995). In all cases, the set of parameters used is reconstructed using these values, considered as references. The values used for the parameters are presented in Appendix II. The average ratio of calculated / measured values resulting from these choices can be found in Appendix III.

Finally, it is worth mentioning the inaccuracies of the sampling dates for CEA/DPS data (only the month is known) and the sampling locations (only the region is identified). These inaccuracies contribute to the unexplained variability in measured specific activities and activity concentrations.

## 6.2. Specific activities in grasses; element of validation for deposits

During all fallout periods due to atmospheric tests of nuclear weapons, grasses intercepted radioactive deposits. For sufficiently long-lived radionuclides, in particular  $^{137}\text{Cs}$  and  $^{90}\text{Sr}$ , a significant portion of their contamination resulted from the root absorption of activities accumulated in the soil.

Several radionuclides were measured more or less frequently by the SCPRI in grasses taken from eight stations throughout France. Figures 24a, 24b, and 24c present these measurement results. The records relating to  $^{95}\text{Zr}$ ,  $^{137}\text{Cs}$ , and  $^{90}\text{Sr}$  are fairly complete, including for samples from the Paris region alone, which is why graphs containing only the results of this region are also presented. On the other hand,  $^{89}\text{Sr}$ ,  $^{106}\text{Ru}$ ,  $^{103}\text{Ru}$ ,  $^{141}\text{Ce}$ ,  $^{144}\text{Ce}$ ,  $^{140}\text{Ba}$ , and  $^{131}\text{I}$  were measured only occasionally, either by choice or because the specific activities were not high enough to be detectable by measurement. For these radionuclides, the graphs show all data available for all sites.

The records for  $^{95}\text{Zr}$  specific activities in grasses are particularly illustrative of the interception of radioactive deposits by the leaves of vegetation, mainly due to the half-life of this radionuclide: long enough to accumulate in the stratosphere but short enough that, given its low root uptake, its accumulation in the soil hardly contributes to the activities measured. Mirroring the records of deposits, these records also reveal the "peaks" related to seasonal stratospheric incursions into the troposphere following Chinese tests. The results of the model are generally aligned with the measurement results since the average of the 538 "calculated/measured" ratios is 1.54. On the other hand, the values of this ratio are very scattered around this average with a standard deviation of 3.51. This dispersion mainly results from the very high variability of activities measured due to the heterogeneity of deposits and the potentially very different characteristics of the samples taken throughout a region (foliar type and mass of the grasses, in particular).

In the case of  $^{137}\text{Cs}$ , and especially  $^{90}\text{Sr}$ , the activity peaks corresponding to stratospheric incursions into the air at low altitude are almost no longer visible: the significant contribution of root uptake keeps the specific activities of the grasses at a level similar to those observed at the peaks during which foliar interception predominates. This "smoothing" is even more pronounced for  $^{90}\text{Sr}$  than for  $^{137}\text{Cs}$  due to a more intense root uptake. For these two radionuclides, the concordance of the model results and the measurement results is even better when using averages of the "calculated/measured" ratio equal to 1.1 and 1.05 respectively, and standard deviations of 0.92 and 0.5 respectively. Finally, for these two radionuclides, we can see that the spatial variability of the specific activities measured in the grasses may be different from those expected because of the spatial variability of the deposits. This results from the significance of root uptake and its inherent variability depending on the characteristics of the soil. The specific activities of  $^{90}\text{Sr}$  measured in Anglade are the highest out of all the sampling stations, most likely due to a soil that is conducive to particularly significant root uptake of this radionuclide.

As with air and rainwater, and due to short radioactive half-lives, the specific activities of  $^{131}\text{I}$  and  $^{140}\text{Ba}$  were only measurable in the grasses in the weeks following each of the nuclear tests. For these two radionuclides, the "calculated/measured" ratio is less than 1: 0.23 and 0.51 respectively. This results from the fact that the measurements are occasional, linked to the sampling date, and most often correspond to the highest points of the "peaks" of fallout (the activities of the other samples being too low to be measured), while the calculation results (models) are monthly values.

For all the radionuclides, the specific activities measured in grasses are generally in line with those expected due to deposits. The fact that the values of the parameters derived from this "calculated/measured" adjustment (see Appendix II) are close to those used generically in the models (and sometimes even equal), is an additional element that validates deposits. For the 1,810 measurement results on samples from the Paris region, the average "calculated/measured" ratio is 1.27.

Similarly, the spatial variability of the activities measured in grasses is consistent with that of deposits. For example, the ratio of activities of  $^{95}\text{Zr}$  measured in the grass samples taken at Vioménil to those taken at Cléville (where precipitation is slightly higher than that at Le Vésinet) is 1.4; the value of this ratio when comparing Vioménil and Le Vésinet for deposits of this same radionuclide was 1.6 (see section 5.3). It should be noted, however, that for the two long-lived radionuclides ( $^{137}\text{Cs}$  and  $^{90}\text{Sr}$ ), the specific activities measured show greater inter-regional variability than expected due to deposits. It reaches a factor of about five for  $^{90}\text{Sr}$ , particularly between the Paris Region and the "Anglade" location in the municipality of Saint-Laurent-de-Céris in Charente. This is most likely due to root uptake, which means that the nature of the soil or farming practices can cause significant spatial variability.

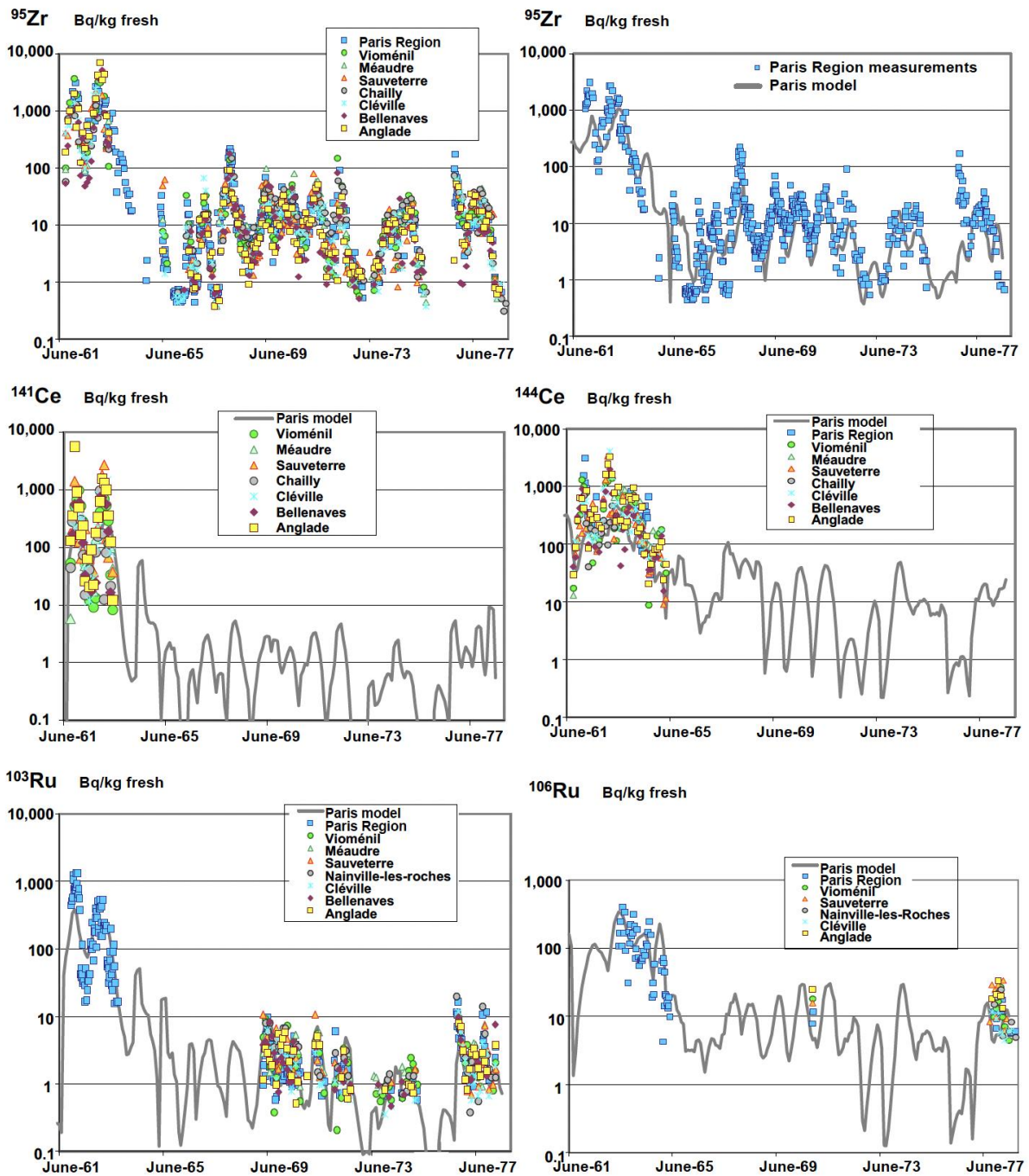


Figure 24a: Changes in specific activities of  $^{95}\text{Zr}$ ,  $^{141}\text{Ce}$ ,  $^{144}\text{Ce}$ ,  $^{103}\text{Ru}$ , and  $^{106}\text{Ru}$  measured in grasses sampled in the Paris region from March 1961 to July 1978 and results of the model for Paris (Bq/kg fresh)

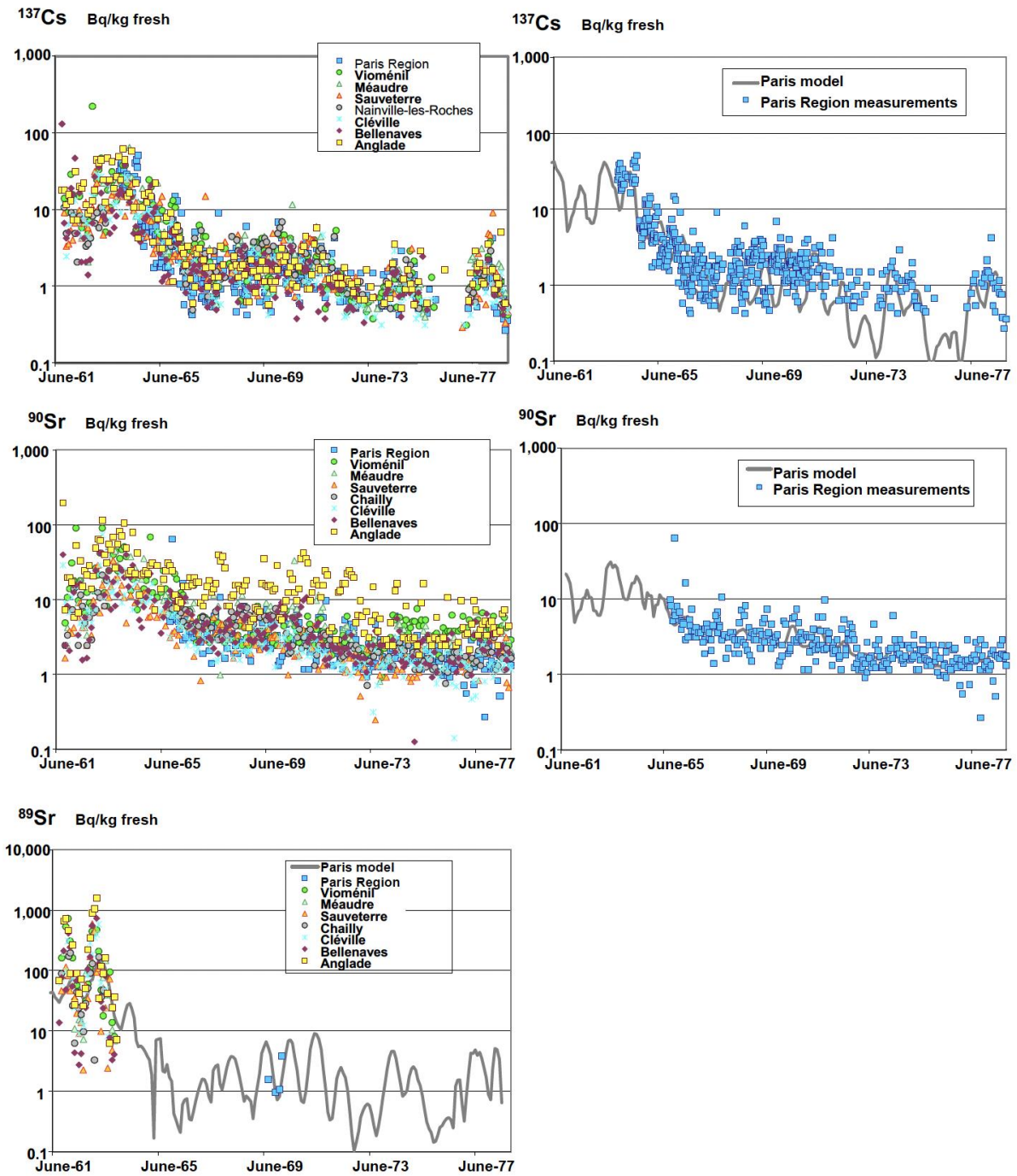
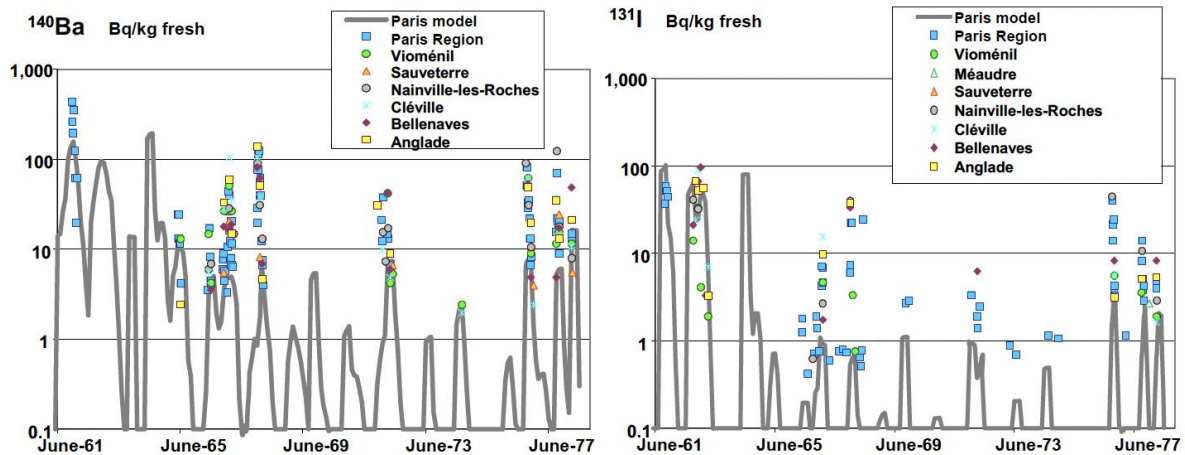


Figure 24b: Changes in specific activities of  $^{137}\text{Cs}$ ,  $^{90}\text{Sr}$ , and  $^{89}\text{Sr}$  measured in grasses sampled in the Paris region from March 1961 to July 1978 and results of the model for Paris (Bq/kg fresh)



**Figure 24c: Changes in specific activities of  $^{140}\text{Ba}$  and  $^{131}\text{I}$  measured in grasses sampled in the Paris region from March 1961 to July 1978 and results of the model for Paris (Bq/kg fresh)**

### 6.3. Specific activities in vegetables

The specific activities of  $^{90}\text{Sr}$  and  $^{137}\text{Cs}$  in vegetables began to be measured in the early 1960s. Analyses of these two radionuclides provided fairly complete records for several sampling areas and were used to adjust the model in a satisfactory way (see Appendix III). On the other hand, analyses of shorter-lived radionuclides began only in 1972 ( $^{95}\text{Zr}$ ,  $^{106}\text{Ru}$ , and  $^{144}\text{Ce}$ ) or at the end of 1976 ( $^{103}\text{Ru}$  and  $^{141}\text{Ce}$ ), and have provided few results that only make it possible to judge alignment with the model in terms of orders of magnitude.

Most of the available results are shown in Figures 25a, 25b, and 25c. These figures show a very significant variability in the specific activities measured for the various categories of vegetables; a variability that is most often spread over two and sometimes three orders of magnitude. Several causes explain this very significant variability.

First of all, the word "vegetables" includes a widely diverse selection of plant species and varieties, and there is also great diversity in which organs are consumed for each plant, causing significant variability in the transfer of radionuclides. To reduce this diversity, vegetables have been grouped together according to a "radioecological" perspective. We consider three main categories: leafy vegetables (lettuces, spinach, cabbages, etc.), root vegetables (potatoes, carrots, turnips, etc.) and fruit vegetables (tomatoes, peppers, peas, courgettes, etc.) with which fruit has also been associated (apples, peaches, apricots). These groupings are used in most operational radioecology models and are justified by the mechanisms involved in plant contamination. However, they remain very rough categories in terms of the parameters affecting transfer of contamination such as foliar mass, growth time, etc. In each category, species as different as lettuce and leeks (leafy vegetables), apples and beans (fruit vegetables and fruit), or beets and radishes (root vegetables) are grouped together. Apart from the fact that modelling in radioecology is most often limited to these categories, the number of measurement results available does not make it possible to go further into the differentiation of types of vegetables.

In addition, for most measurement results, only the sampling region and the month are indicated. Whereas, for a given date, the deposits within a region such as Provence or Languedoc may double from one location to the next. Also, given the change in deposits from one month to the next and the

kinetics of radionuclides decay in vegetables (around a few days), not knowing the precise date of sampling (most often only the month of sampling is known) generates uncertainty of up to a factor of 10. This very significant variability completely masks the temporal changes related to deposits.

Adjustment of the model to the measurement results, which is based on the average of the "calculated/measured" monthly ratios over the entire period, significantly reduces variability relative to the individual measurement results. Beyond a "calculated/measured" ratio close to one, the quality of this adjustment is also based on the number of measurements available.

In the case of leafy vegetables, the average "calculated/measured" ratios between 0.9 and 1.5 (see Appendix III) are quite satisfactory given the number of measurements and despite significant dispersion around these averages (standard deviations ranging from 0.5 to 3.8). The adjustment of the model to the measurements for  $^{90}\text{Sr}$  (average "calculated/measured" ratio of 1.1 and standard deviation of 0.5) is particularly satisfactory. This is due, in particular, to the significance of root uptake for this radionuclide, which "smooths" the variability related to foliar interception of deposits. However, it is difficult to put forward an explanation for the high value of the average "calculated/measured" ratio of  $^{106}\text{Ru}$  (2.54).

For root vegetables and fruit vegetables, the number of measurement results of  $^{90}\text{Sr}$  and  $^{137}\text{Cs}$  available also allows for proper adjustment of the model. The average "calculated/measured" ratios range from 1.05 to 1.1 for  $^{90}\text{Sr}$  and from 1.02 to 1.60 for  $^{137}\text{Cs}$ .

For the other radionuclides, the very limited number of measurement results for fruit vegetables and root vegetables only allows us to compare the orders of magnitude of the calculated and measured specific activities. It therefore appears that for root vegetables, the "calculated/measured" ratios are low for  $^{106}\text{Ru}$ ,  $^{95}\text{Zr}$ , and  $^{144}\text{Ce}$  (from 0.4 to 0.5) and very low for  $^{103}\text{Ru}$  and  $^{141}\text{Ce}$  (0.1 and 0.2). While it should be remembered that there is little confidence in these values given the very limited number of measurement results, we can see that the specific activities of these radionuclides measured in root vegetables are of the same level as those measured in leafy vegetables (between 0.1 and 10 Bq/kg fresh). This does not align with our knowledge on transfers. In fact, these radionuclides are known for their very low root uptake and their very low mobility in plants. Transfer from the leaves that intercepted the deposits to the roots is therefore theoretically limited and should not result in specific activities as high as those of the leaves. The explanation could be insufficient washing of the samples and the presence of soil particles during analysis, whose specific activities are much higher than those of the plants.

With the exception of these activities of short-lived radionuclides measured in root vegetables, which seem abnormally high, the activities measured in vegetables are in line with those expected due to monthly deposits and the accumulation of these deposits in soils: our knowledge on transfers explains the results. For all 6,650 vegetable measurement results, the average "calculated/measured" ratio is 1.30, which would reflect a moderate overestimation of the model.

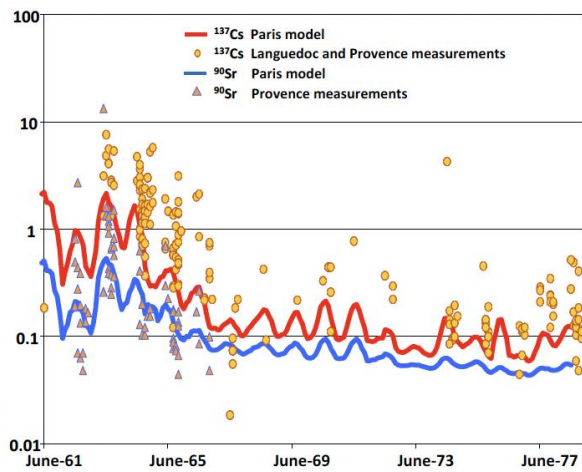
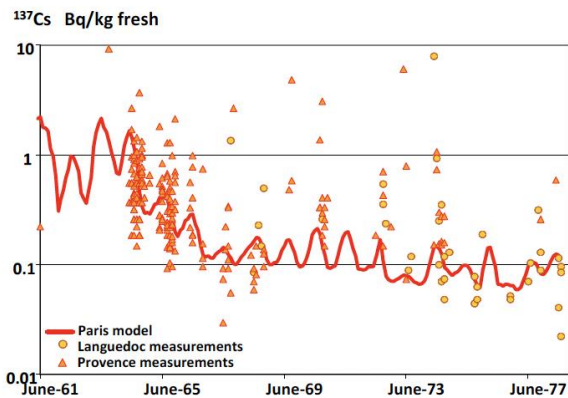
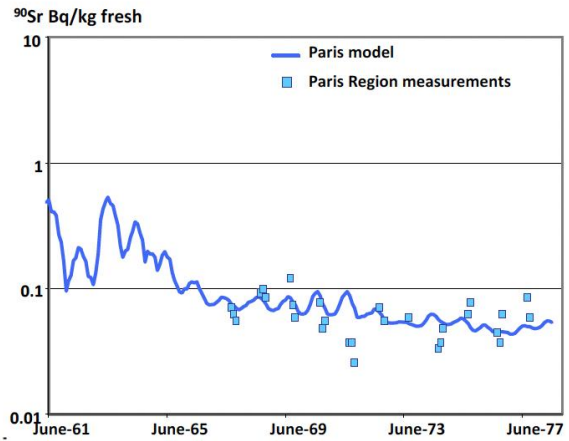
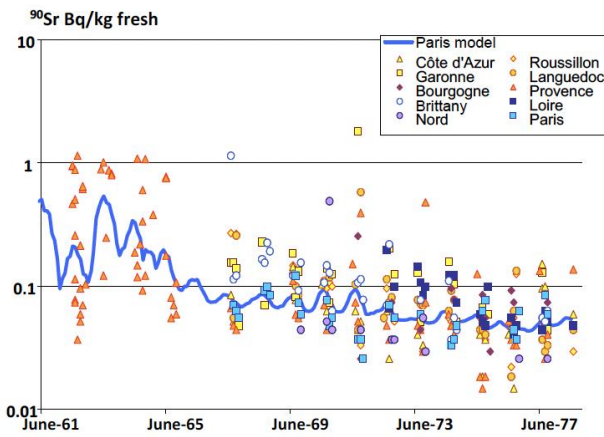
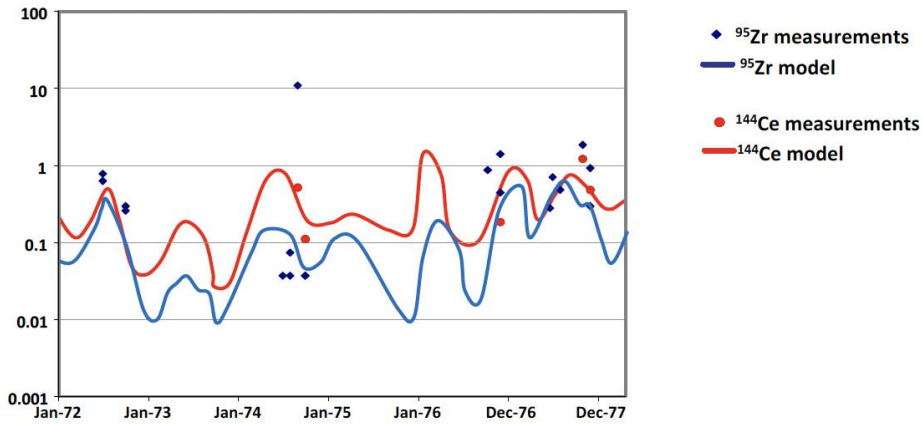
With regard to spatial variability, we can see that the intra-regional variability of the activities measured can be significantly greater than the inter-regional variability related to that of the deposits. A more or less intense root uptake, linked to the characteristics of the soil or to farming practices, may therefore have a significant impact on the specific activities of  $^{90}\text{Sr}$  in vegetables.

Radiological consequences of fallout from atmospheric tests of nuclear weapons in mainland France -  
 Environmental contamination and exposure of the population  
 IRSN Report no. 2024-00559



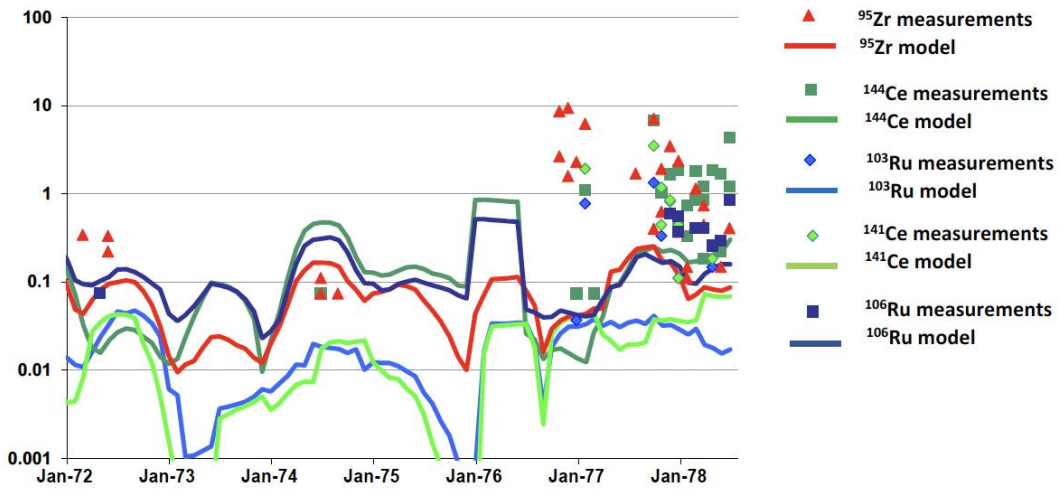
**Fruit Vegetables**

Bq/kg fresh

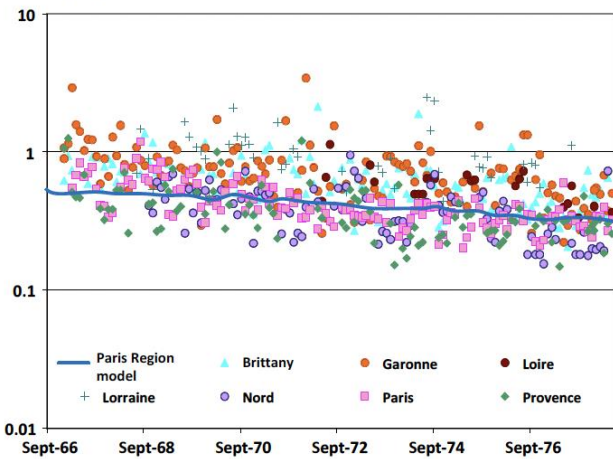


**Root vegetables**

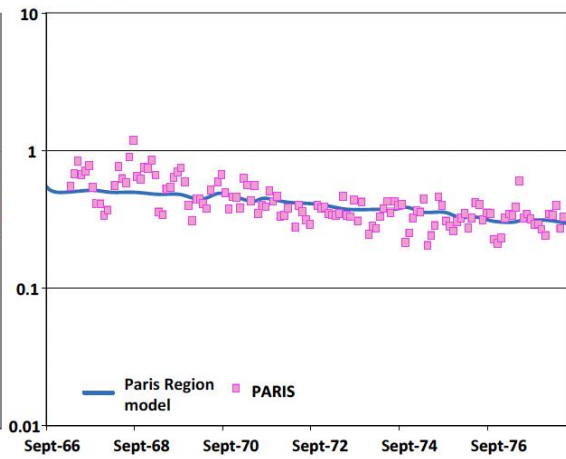
Bq/kg fresh



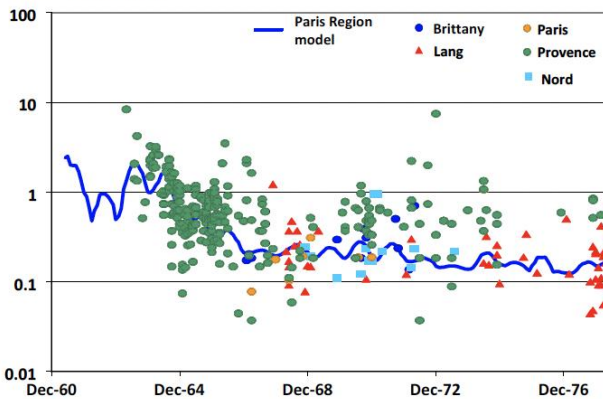
<sup>90</sup>Sr Bq/kg fresh



<sup>90</sup>Sr Bq/kg fresh



<sup>137</sup>Cs Bq/kg fresh



## 6.4. Specific activities in cereal grains

In France, among the cereal grains grown, wheat plays a major role because of its predominance in the average diet (bread, pasta). The other cereal grains are either intended for livestock feed or, like rice, are of very minor significance when it comes to human consumption or production. In addition, there are fewer differences from a radioecological point of view, between two species of cereal than between two types of leafy vegetables, for example. For the purpose of dosimetric evaluation, the assumption that the contamination of wheat is representative of the contamination of all cereal grains may be used.

The wheat grain consists of an endosperm from which most flour is produced, a germ and its bran coat (the germ and coat can be mixed to produce bran and whole wheat). In its bran coat, the endosperm does not directly receive radioactive deposits and its contamination results solely from translocation (transfer from the leaf to the seed). In addition, translocation to the endosperm is lower than to the bran coat. It follows that the specific activity of the endosperms, and therefore of flour, is lower than that of the whole wheat grain.

Samples of whole wheat grains, collected in large grain cooperatives in seven major "agroclimatic regions" (see map in Figure 26) have been measured by SCPRI since 1969; flour samples have also been collected from the same centres, as well as in other (administrative) regions or departments since 1964.

For wheat grains and flours, the radionuclides measured are limited to  $^{90}\text{Sr}$  and  $^{137}\text{Cs}$ . The lack of results for  $^{131}\text{I}$  is due from its very short radioactive half-life, which leads to its disappearance within three months. However, this is approximately the time necessary for agricultural cooperatives to assemble harvests and proceed with commercialisation. The SCPRI measurements were carried out on these assembled and homogenised harvests in large collection centres; therefore,  $^{131}\text{I}$  could no longer be detected, nor could it be present in the cereal products intended for human consumption. With regard to the other short-lived radionuclides (rutheniums, ceriums, barium, etc.), it is mainly their very low transfer from the leaves that intercepted the radioactive deposits to the grain, which explains why their specific activities were too low to be measured. In addition, the absence of accumulation in soils due to their short radioactive half-lives means their root uptake is negligible.

The specific activities measured in flour are around 3.5 times lower than those measured in whole wheat. The bran coat of the grain therefore concentrates most of the radionuclides.

For whole grains and flours, these specific activities are homogeneous regardless of the origin of the samples, both for  $^{90}\text{Sr}$  and for  $^{137}\text{Cs}$ ; a homogeneity that contrasts with the great variability previously observed for vegetables. The inter-regional variations in specific activities are indeed low: around a factor of three at most for  $^{137}\text{Cs}$  and for  $^{90}\text{Sr}$ . This is due to the assembling of local production in large agricultural cooperatives, which conditions not only the results of measures used here, but also incorporation by humans since cereal products are distributed with the same homogeneity, if not greater, as that of the measurements taken by the SCPRI. Farming practices, and in particular the use of fertilizers, also contribute to the standardisation of soil characteristics with regard to root uptake.

Finally, we note a very satisfactory adjustment of the results of the model to the measurement results. The average "calculated/measured" ratios are 1.1 and 1.0, respectively, for  $^{137}\text{Cs}$  and  $^{90}\text{Sr}$  with standard deviations of 0.5 and 0.3, which are moderate compared to those previously calculated for vegetables. The specific activities of  $^{90}\text{Sr}$  and  $^{137}\text{Cs}$  measured in wheat are entirely consistent with those that could

be expected from monthly deposits (for foliar uptake) and cumulative deposits in soils (for root uptake).

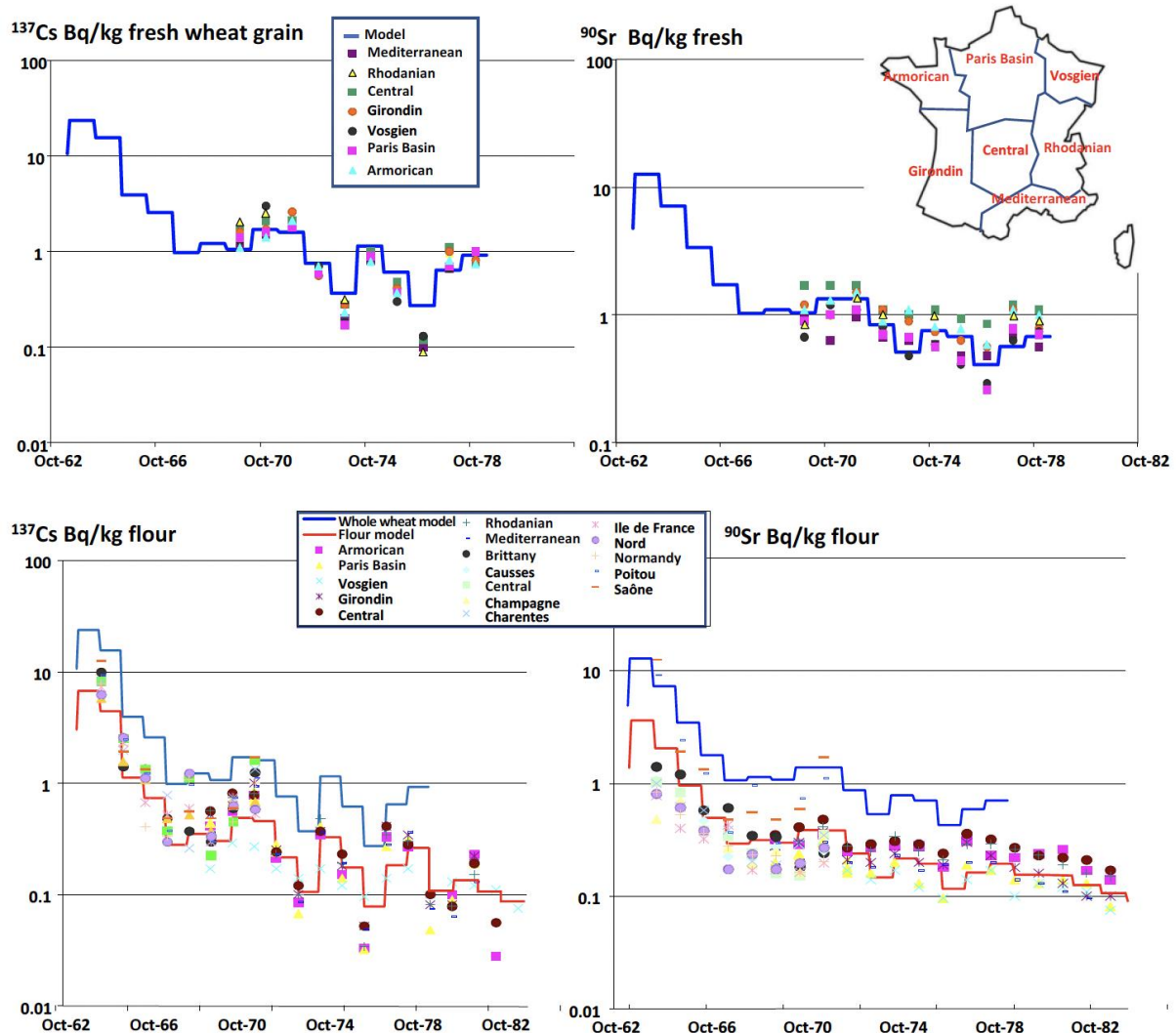


Figure 26: Specific activities of  $^{137}\text{Cs}$  and  $^{90}\text{Sr}$  in samples of whole wheat grain taken from large collection centres within expansive "agroclimatic regions" (Bq/kg fresh)

## 6.5. Activity concentrations in cow's milk

Samples of cow's milk collected at eight stations throughout mainland France have been analysed by the SCPRI since 1961. The choice to limit analyses to cow's milk alone is justified by its clear predominance in human consumption of milk and dairy products (with regard to goat's or sheep's milk).

Only five radionuclides were measured in milk:  $^{137}\text{Cs}$ ,  $^{131}\text{I}$ ,  $^{140}\text{Ba}$ ,  $^{89}\text{Sr}$  and  $^{90}\text{Sr}$  (see Figure 27). The lack of measurement results for the other radionuclides can be explained by the very low transfer to mammary glands of the activities incorporated by animals. For the same activity incorporated daily by a cow, the transfer to milk of ruthenium is around 30 times lower than that of caesium or iodine; transfer of cerium is around 100 times lower and that of plutonium, much less present in the fallout to begin with, is around 1,000 times lower. The activity concentrations of radionuclides other than those measured are therefore negligible.

The many measurement results of  $^{137}\text{Cs}$  and  $^{90}\text{Sr}$  available (see Figure 27) allow proper adjustment of the model, and they highlight a marked spatial variability. The averages of the "measured/calculated" ratios for the Paris region are 1.06 and 1.07 for  $^{137}\text{Cs}$  and  $^{90}\text{Sr}$ , respectively, and present moderate dispersion (0.4 for the two radionuclides). The values of the transfer factor to milk for these radionuclides, selected on the basis of the activity concentrations measured to complete the records, are well-aligned with the values recommended in the models. The activities measured are therefore in line with expectations. The spatial variability is illustrated by Figure 28, which compares the activity concentrations measured on samples from the Paris region and those from Anglade (municipality of Saint-Laurent-de-Céris). For both radionuclides, the activity concentrations for Anglade are nearly five times higher than those for the Paris region. This can be partially explained by the deviation among deposits (a factor of 1.5); the rest (more than a factor of 3) can be explained by the characteristics of the soils (in particular for  $^{90}\text{Sr}$  whose activities in grasses sampled at Anglade were already noticeably high; see Figure 24b) or by animal feeding practices. Unfortunately, the data available does not allow for the latter causes of spatial variability to be modelled.

As seen previously, due to its short radioactive half-life,  $^{131}\text{I}$  was measurable only within a very short time after each nuclear explosion and this analysis was very restrictive from a logistical point of view. The data available for this radionuclide in cow's milk is therefore very poorly distributed over time (only 19 separate sampling dates, covering 7 of the 18 years covered by the study). To overcome this difficulty and report on  $^{131}\text{I}$  activity levels, measurements were carried out on bovine thyroids (316 data points). As a necessary element for the functioning of the thyroid, most of the incorporated iodine is transferred to this gland, which concentrates it: during the fallout from nuclear testing, the specific activity of  $^{131}\text{I}$  in bovine thyroids was 500 times higher than the activity concentration of milk (Beninson *et al.*, 1972). The activity concentrations of  $^{131}\text{I}$  in cow's milk presented in Figure 27 were thus deduced from those measured in bovine thyroids. Using this biological indicator, the activity peaks corresponding to most of the Chinese explosions could be quantified. As in the case of grass, part of the variability of the measured activities is related to the short half-life of the radionuclide with regard to the monthly time step of the study. While overall, at the scale of France, the regional variability of radionuclide deposits due to aerial testing can be considered proportional to the regional variability of average annual rainfall, this finding cannot be considered accurate in the case of iodine, where the deposits are proportional to the amount of rainfall locally in the few weeks following each test, which are much more variable than the average annual rainfall.

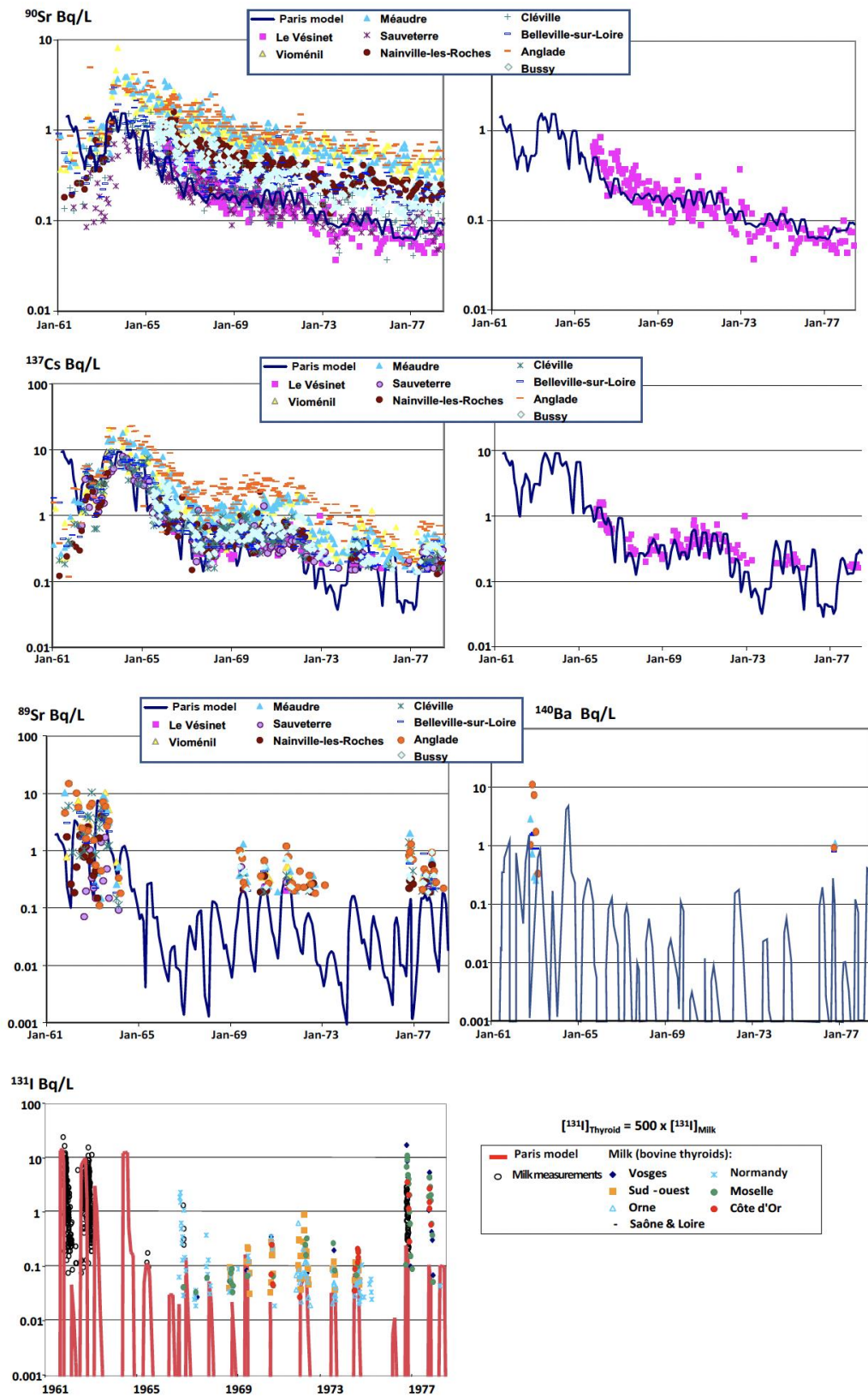
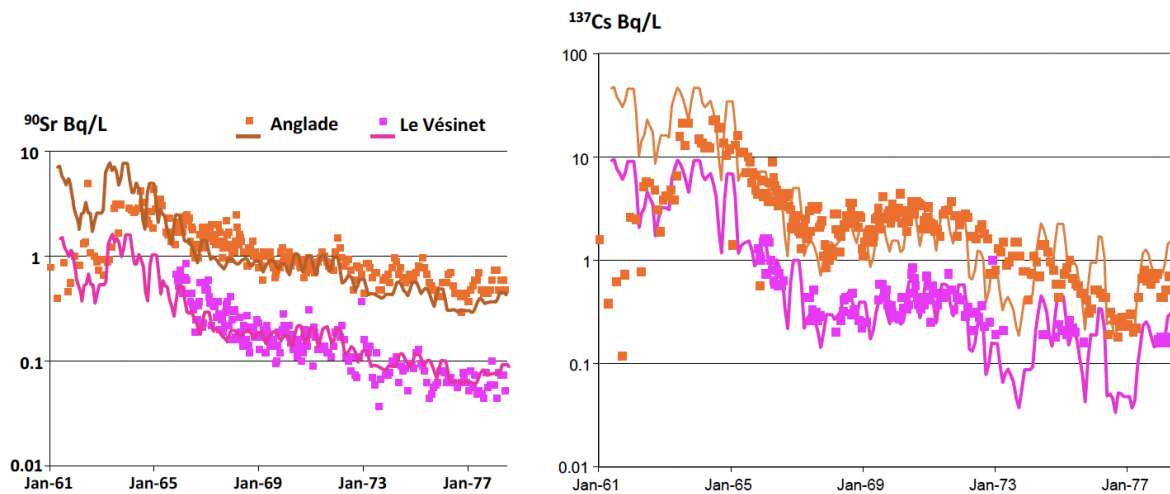


Figure 27: Activity concentrations of  $^{137}\text{Cs}$ ,  $^{131}\text{I}$ ,  $^{140}\text{Ba}$ ,  $^{89}\text{Sr}$  and  $^{90}\text{Sr}$  in cow's milk, measured and calculated by the adjusted model (Bq/L)



**Figure 28: Comparison of the activity concentrations of  $^{137}\text{Cs}$  and  $^{90}\text{Sr}$  in cow's milk from the Paris region (Le Vésinet) and Anglade (Saint-Laurent-de-Céris) (Bq/L).**

## 6.6. Specific activities in beef

Of all the radionuclides present in the fallout from atmospheric tests of nuclear weapons and incorporated by animals, caesium, a chemical analogue of potassium, is by far the most transferred to muscles and therefore to meat: 30 to 50 times more than iodine, ruthenium, cerium or antimony, 100 times more than strontium, and 1,000 times more than plutonium. This explains why only  $^{137}\text{Cs}$  could be measured in the beef samples analysed by the CEA/DPS from 1966 to 1971.

Over this period, there are enough results to adjust the model for the Paris region and account for the spatial variability of the measured specific activities (See Figure 29). Adjustment provides, for the Paris region, a "calculated/measured" ratio of 0.96 derived from 138 measurement results with a standard deviation of 0.65.

On the basis of the quantity of fodder consumed, adjusted for the measurement results of  $^{137}\text{Cs}$ , the records of specific activities of other radionuclides in beef were reconstructed using the specific transfer factors recommended in the CONDOR model.

As with milk, there is spatial variability likely related to soil characteristics and animal feeding practices, added to the spatial variability of deposits. The variability per site also seems to be greater than that observed for cow's milk. This can be explained by the fact that the meat samples generally come from a single animal and that, in addition to spatial variability, there is likely to be individual variability which does not appear for milk. The production of a herd is assembled for the entire farm, or even for an entire cooperative before sampling.

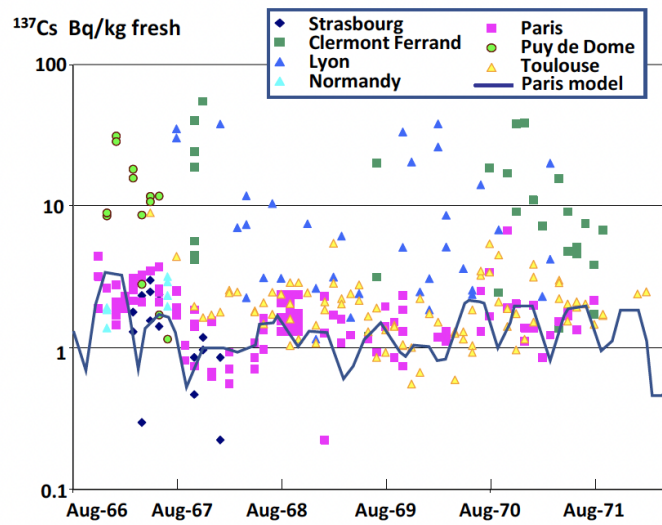


Figure 29:  $^{137}\text{Cs}$  activities in beef (Bq/kg fresh)

## 6.7. Case of tritium and carbon-14

Like stable carbon-12, carbon-14 present in the air in the form of  $\text{CO}_2$  is absorbed by plants during photosynthesis. It is then transferred to animals through ingestion of foodstuffs. Since carbon-14 is hardly differentiated from carbon-12, neither by photosynthesis nor by the metabolism of animals, the proportion of carbon-14 in total carbon, which is expressed by the activity of carbon-14 per unit of carbon mass, remains equal throughout the food chain, especially in foodstuffs. Since 1950, this activity has been measured in plants taken from different parts of the world; it is very homogeneous (Roussel-Debet, 2007). Since 1994, IRSN has also carried out this monitoring using plant samples collected in areas exempt from the influence of a nuclear facility (IRSN, 2021).

Figure 30 shows that in the early 1950s, the activity of carbon-14 per unit of carbon mass was 226 Bq/kg of C. This activity resulted from the balance between the production of natural cosmogenic carbon-14 and the losses related to the trapping of this radionuclide in carbonates, especially oceanic carbonates (the effect of radioactive decay for this radionuclide with a 5,600-year half life is negligible on our time scale). This activity rapidly increased in the 1950s, reaching around 420 Bq/kg of C in 1964, due to atmospheric tests of nuclear weapons. It then decreased due to the increase in  $\text{CO}_2$  content of the air linked to the combustion of fossil energy sources (gas and oil) devoid of carbon-14, thus inducing its "dilution". The share of these activities attributable to nuclear tests can be estimated by subtracting the value of 226 Bq/kg of carbon, considered representative of the background of carbon-14 before nuclear testing, from the activities measured.

The specific activities and activity concentrations of  $^{14}\text{C}$  in all foodstuffs can then be obtained from these activities per unit of carbon mass by considering the carbon content of fresh foodstuffs (kg of C/kg fresh) presented in Table X and taken from the IAEA.

Figure 31 shows the estimated evolution of specific activities attributable to nuclear testing for the main categories of foodstuffs.

**Table X: Carbon content of the main food categories (kg of C/kg of fresh food)**

Leafy vegetables	Fruit vegetables and fruit	Root vegetables	Grains	Milk	Beef
0.03	0.06	0.05	0.4	0.065	0.25

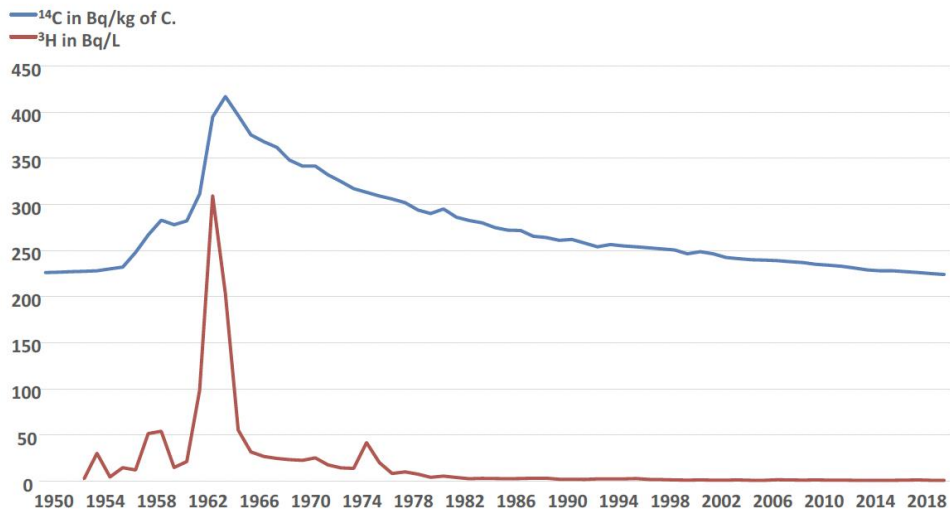


**Figure 30: Evolution of carbon-14 activities per unit of carbon mass measured in plants from different parts of the world and tritium activity concentrations measured in rainwater from Ottawa, Thonon-les-Bains, and Opme**

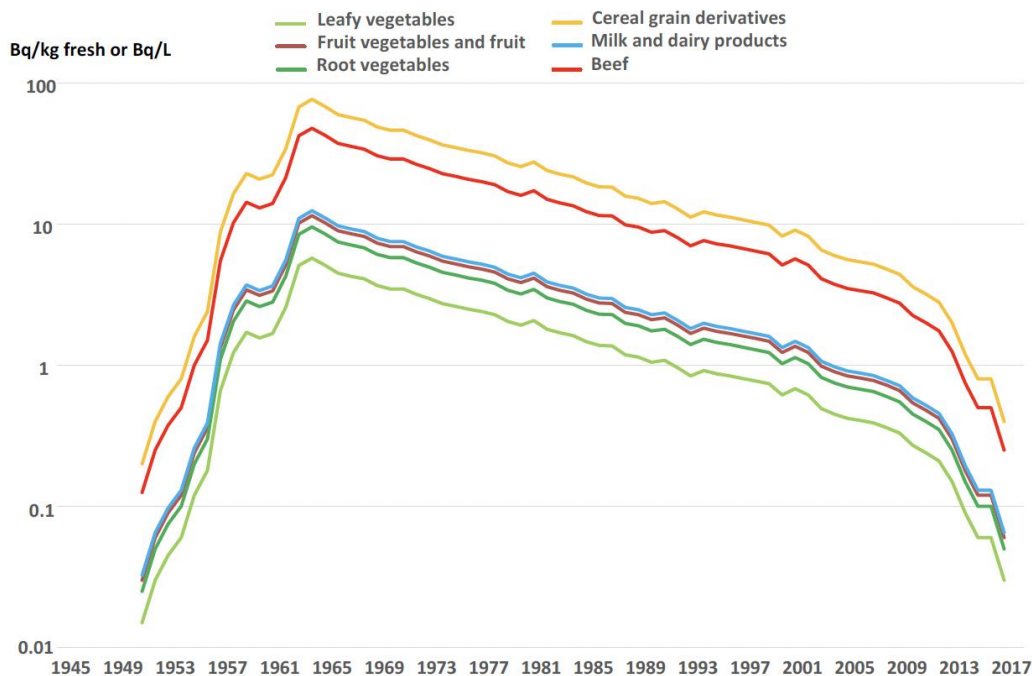


**Figure 31: Evolution of carbon-14 specific activities in various food categories (Bq/kg fresh or Bq/L)**

Like carbon-14, tritium in plants comes from the air, more specifically from atmospheric water vapour, which it incorporates during photosynthesis. It is then transferred to animals, mainly through ingestion of food, though transcutaneous absorption also occurs. Tritium is present in living organisms in the

form of tritiated water contained in tissues (free tritium, denoted HTO) and in the form of organically bound tritium (OBT). The total tritium activity of a foodstuff is therefore equal to the sum of the activities of free tritium (HTO) and bound tritium (OBT).

When the activity of tritium in the air fluctuates little on the scale of a few weeks or months, which is the case of the activity resulting from the fallout of nuclear tests or of cosmogenic origin, it can be considered that the activity concentrations of HTO and OBT are equal to that of water vapour in the air. The specific activities and activity concentrations of tritium in foodstuffs, expressed in Bq/kg fresh or in Bq/L, can therefore be deduced from the activity concentrations measured in atmospheric water vapour. The activities of free tritium (HTO) are estimated by taking into account the water content of the foodstuff<sup>11</sup>; those of bound tritium (OBT) are estimated by considering the amount of water produced during the combustion of the dry organic matter<sup>12</sup>. In order to estimate the portion that is attributable to nuclear tests, an activity concentration of 0.4 Bq/L,<sup>13</sup> considered to be representative of the tritium activity of cosmogenic origin that prevailed before the nuclear tests, was deduced from the activities measured in rainwater.

Figure 32 shows the evolution of specific activities and activity concentrations of tritium due to nuclear testing in the main categories of foodstuffs since 1953. These activities have been added to the activities of natural cosmogenic tritium. The percent of HTO activity in the total activity is indicated for each category; the complement is the activity bound to organic matter. These contributions are directly influenced by the water content of the foodstuffs: the higher the water content, the higher the proportion of HTO activity in the foodstuff. Unlike most other radionuclides, tritium is found in water in dissolved form; it is therefore not stopped by the treatment of drinking water. Water is therefore an important foodstuff to consider for this radionuclide. For this study, it is assumed that the activity concentration of drinking water is equal to that of rainwater. This is true when the origin of drinking water is a river; in the case of groundwater, this assumption is conservative. The specific activities and activity concentrations of tritium in the various foodstuffs are very similar; the lowest activity, that of cereal grains, is only 30% lower than the highest activity, which is that of drinking water.

The specific activities of tritium in foodstuffs were likely between 0.1 and 0.6 Bq/kg fresh prior to 1945. Already above 1 Bq/kg fresh in 1953, they continued to increase rapidly, reaching around 300 Bq/kg fresh in 1963. They have steadily decreased since, due to radioactive decay and the overall loss of tritium in terrestrial environments by dilution in ocean waters.

---

<sup>11</sup> Water content varies greatly from one food to another: from 0.9 L/kg fresh for a leafy vegetable to 0.12 L/kg fresh for a grain of wheat. The water contents used in this study are those recommended by the IAEA, supplemented by data from measurements carried out by IRSN.

<sup>12</sup> The amount of water recovered during the combustion of dry organic matter is fairly constant regardless of the foodstuff in question; it is close to 0.6 L/kg of incinerated dry matter.

<sup>13</sup> The tritium activity prior to nuclear tests was between 0.2 and 0.6 Bq/L; an intermediate value of 0.4 Bq/L was selected in this study.

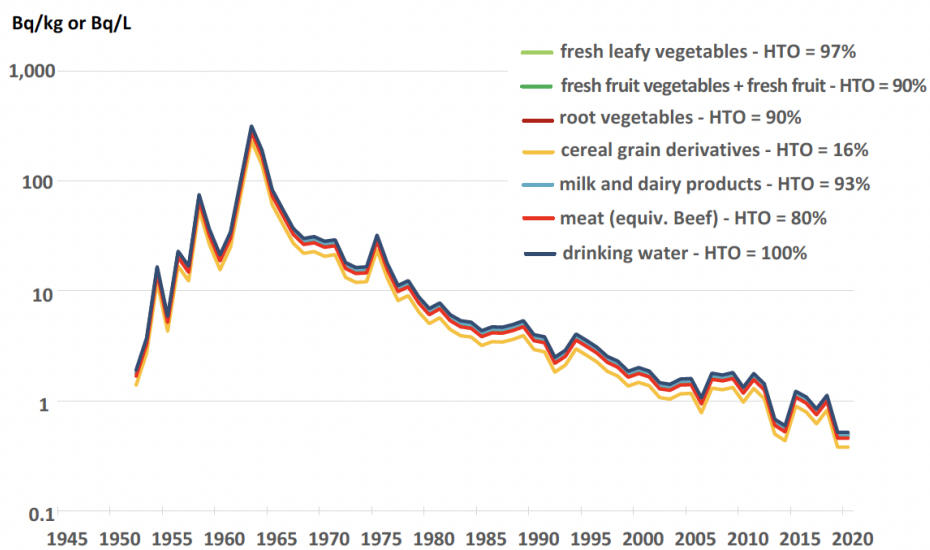


**Figure 32: Specific activities and activity concentrations of <sup>3</sup>H in foodstuffs (Bq/L or Bq/kg fresh) added to cosmogenic activities by nuclear testing and contribution of HTO to these total activities of <sup>3</sup>H**

## 6.8. Overall assessment of food contamination

The numerous results of radiological measurements carried out by the SCPRI and the CEA/DPS provide satisfactory knowledge of the specific activities and activity concentrations for the radionuclides of interest from the fallout of atmospheric testing of nuclear weapons, for the main categories of foodstuffs comprising human food intake.

The activities measured could, for the most part, be explained by the radioactive deposits from which they originate, as well as by the knowledge we have of radionuclide transfer in the food chain. The available measurement results were used to adjust the parameter values of a model specific to the Paris region, likely suitable for any region receiving an average annual rainfall of around 700 mm/year. This adjustment is satisfactory, on the one hand, because it provides a very good concordance between the measured results and those calculated ("calculated/measured" ratio usually close to 1), and, on the other hand, because the parameter values thus determined are very close, and sometimes even equal, to the values recommended in the bibliography. The main exception concerns root vegetables for which the activities measured are significantly higher than expected; the explanation put forward would be pollution by soil particles and samples of roots and tubers insufficiently cleaned during processing.

The model, adjusted to the available data, therefore reliably completes the records of the specific activities and activity concentrations of radionuclides measured in foodstuffs.

The bibliographical knowledge on radionuclides and their transfer to the environment also explains why the activities of certain radionuclides were too low to be measured (case of most radionuclides in milk and meat). It also makes it possible to verify that the radionuclides with measurement results available for adjusting the model are indeed those with the highest specific activities or activity concentrations.

The records of the specific activities of radionuclides not measured but present in the fallout from nuclear tests were reconstructed by modelling using the values adjusted to available measurements for parameters not dependent on radionuclides, and using the values recommended in the CONDOR model for radionuclide-dependent parameters.

With regard to meat, the measurement results relate only to beef, but poultry and pork (including deli meats) are also significant components of the human meat diet. Modelling shows that these two types of meat were most likely less contaminated than beef, due to the feeding of these animals using grains and protein oil crop, whose specific activities were significantly lower than those of fodder given to cattle, which mainly comprised grass.

Finally, the measurement results in certain foodstuffs showed that soil characteristics, farming and animal feeding practices may have introduced additional spatial variability, sometimes greater than that resulting from radioactive deposits. Although it is always possible to adjust the model to a particular sampling site once sufficient measurement results are available, the conditions for applying such specific models to the entire territory are not accessible in the context of this study.

## 7. Reconstruction of inhaled doses

### 7.1. Methodology for calculating inhaled doses for the period of June 1961 to July 1978

The estimation of doses by inhalation is based on the records of the average monthly activity concentrations in air ( $\text{Bq}/\text{m}^3$ ) reconstructed above (see chapter 4). Given the continuous nature of atmospheric contamination, activity concentrations inside homes are assumed to be equal to those measured in air outdoors.

The application of respiratory flow rates ( $\text{m}^3/\text{h}$ ) for different occupations (sleep, light or intense physical activities) and specific to each age group, provides estimates of the activity of radionuclides incorporated by inhalation each month ( $\text{Bq}/\text{month}$ ). Table XI provides the parameter values used in this study; they are derived from the time budgets and respiratory flow rates by type of occupation proposed in ICRP publication 66. The average daily respiratory flow rates calculated for each age group (right-hand column) are the same as those used by UNSCEAR for its assessments of inhaled doses, with the exception of adults, for whom UNSCEAR considers a single respiratory flow rate of  $22.2 \text{ m}^3/\text{d}$ , falling between the rates used for this study and very close to that used for adolescents aged 13-17 years old.

**Table XI: Parameter values for inhalation exposure**

	Sleep		Rest		Light exercise		Intense exercise		Daily average
	$\text{m}^3/\text{h}$	h	$\text{m}^3/\text{h}$	h	$\text{m}^3/\text{h}$	h	$\text{m}^3/\text{h}$	h	$\text{m}^3/\text{d}$
Infant	0.1	24.0	-	-	-	-	-	-	2.2
1-2 years	0.2	14.0	0.2	3.3	0.4	6.7	-	-	5.2
3-7 years	0.2	12.0	0.3	4.0	0.6	8.0	2.0	-	8.7
8-12 years	0.3	10.0	0.4	4.7	1.1	9.3	2.7	-	15.3
13-17 years	0.4	10.0	0.5	4.0	1.3	8.0	3.0	2.0	22.4
Outside worker	0.4	8.5	0.5	3.2	1.4	6.3	2.9	6.0	30.6
Sedentary worker	0.4	8.5	0.5	5.2	1.4	10.3	-	-	19.9

Finally, a dose per unit intake factor (DPUI in  $\text{Bq}/\text{Sv}$  inhaled) makes it possible to estimate the dose received using the activities incorporated by inhalation. The DPUIs used in this study to calculate the effective and committed equivalent doses to the thyroid, brain, colon, lungs, breasts, and prostate, for the different age groups, are taken from the decree of 1 September 2003 published in the Official Journal of the French Republic (JO 2003) and publication 72 of the ICRP. As indicated in chapter 4, and in agreement with the ICRP, it is considered that 50% of the iodine was in gaseous form and 50% in particulate form. In the case of carbon-14, the form considered is carbon dioxide ( $^{14}\text{CO}_2$ )

## 7.2. Estimated effective doses by inhalation for an adult, 1961-1978; comparison with UNSCEAR estimates

Figure 33 shows the evolution of the monthly effective doses for an adult estimated using the previous methodology. This evolution and the respective contributions of the various radionuclides are directly linked to activities in the air and to the different levels of inhalation radiotoxicity specific to each radionuclide (DPUI see section 7.1). This figure clearly shows the seven radionuclides that contribute (with their chaining) to the bulk of the effective doses received by inhalation, in order of significance:  $^{144}\text{Ce}+$ ,  $^{106}\text{Ru}+$ ,  $^{239+240}\text{Pu}$ ,  $^{91}\text{Y}$ ,  $^{241}\text{Pu}$ , and  $^{95}\text{Zr}+$ .

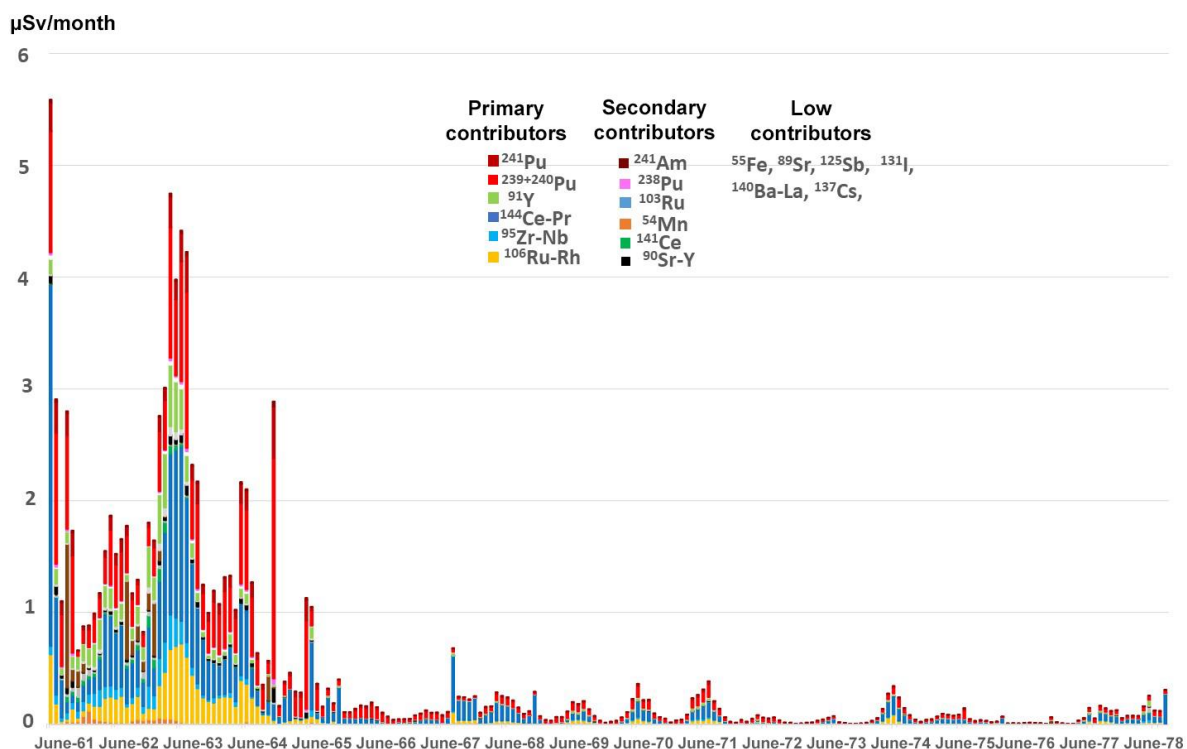


**Figure 33: Monthly effective doses calculated for an adult from June 1961 to July 1978 with contribution of the various radionuclides**

Similar estimates were made for the different age groups. The annual dose records obtained by summing these monthly doses will be discussed in section 7.4.

In its 2000 report, UNSCEAR provides global average estimates of annual effective doses by inhalation for an adult from 1945 to 1985 (UNSCEAR, 2000). These estimates can be compared to the annual averages estimated in this study for the period 1962-1977 (the years 1961 and 1978 were not complete). This comparison is made for a sedentary adult whose average daily respiratory flow rate,  $19.9 \text{ m}^3/\text{d}$ , is close to the rate used by UNSCEAR:  $22.2 \text{ m}^3/\text{d}$ . The graphs in Figure 34 confirm that  $^{144}\text{Ce}+$ ,  $^{106}\text{Ru}+$  (in green and red on the top right graph) and actinides ( $^{239+240}\text{Pu}$ ,  $^{238}\text{Pu}$ ,  $^{241}\text{Pu}$ , and  $^{241}\text{Am}$ , in red on the top left graph), induce the highest effective doses by inhalation for an adult. The actinides were grouped together to allow comparison with UNSCEAR, which does not detail the doses for each actinide in its report.

This comparison shows there is a good level of concordance between the global average estimates of UNSCEAR and those made for mainland France as part of this study. This is the case for the main contributors to the effective doses by inhalation, for which the average ratio of the two estimates (UNSCEAR/IRSN) is close to 1: 1.2 for  $^{144}\text{Ce}$ , 1.1 for  $^{106}\text{Ru}$  and for actinides, 0.9 for  $^{91}\text{Y}$  and  $^{95}\text{Zr}$  (see Table XII). In general, these UNSCEAR/IRSN ratios remain between 0.5 (for  $^{140}\text{Ba}$ ) and 1.9 (for  $^{89}\text{Sr}$ ), except for the case of  $^{90}\text{Sr}$ , which will be discussed in the following paragraph. The fact that the two sets of estimates were very close for most radionuclides was not necessarily expected because, as indicated above, the radioactive fallout over the range of latitudes to which France belongs was greater than anywhere else in the world. It is likely that the weighting applied by UNSCEAR, according to population density, led to the global doses coming closer to those estimated for France.

The case of  $^{90}\text{Sr}$  is significantly different from that of other radionuclides. Indeed, the inhalation dose estimated by UNSCEAR for this radionuclide was, on average over the period, five times higher than that estimated in this study (see Table XII). A review of the results presented in the UNSCEAR report reveals an inconsistency that could explain this deviation. The ratio of the activity concentrations of  $^{90}\text{Sr}$  to  $^{137}\text{Cs}$  ( $^{90}\text{Sr}/^{137}\text{Cs}$ ) observed in the air, in rainwater, and in the deposited surface activities is 0.7 for both UNSCEAR and IRSN (see Table IV). In addition, the ratio of DPUIs for these two radionuclides ( $\text{DPUI } ^{90}\text{Sr}/\text{DPUI } ^{137}\text{Cs}$ ) was 7.8. As a result, the ratio of the doses by inhalation should be around  $7.8 \times 0.7 = 5.5$  (as the values of the other scenario parameters involved in the calculations are identical). However, while the ratio is close to this value in the present study (5.8), it is much higher for the UNSCEAR estimates, with a value of 28. The difference of a factor of 5 ( $28/5.5$ ) corresponds very exactly to that observed between the inhalation doses estimated by UNSCEAR and IRSN. This could have resulted from the choice of lung absorption type. There is indeed a difference of nearly a factor of five between the DPUI corresponding to the S (slow) forms of absorption and M (medium) forms selected for this study and recommended by the ICRP.

Radiological consequences of fallout from atmospheric tests of nuclear weapons in mainland France - Environmental contamination and exposure of the population  
 IRSN Report no. 2024-00559

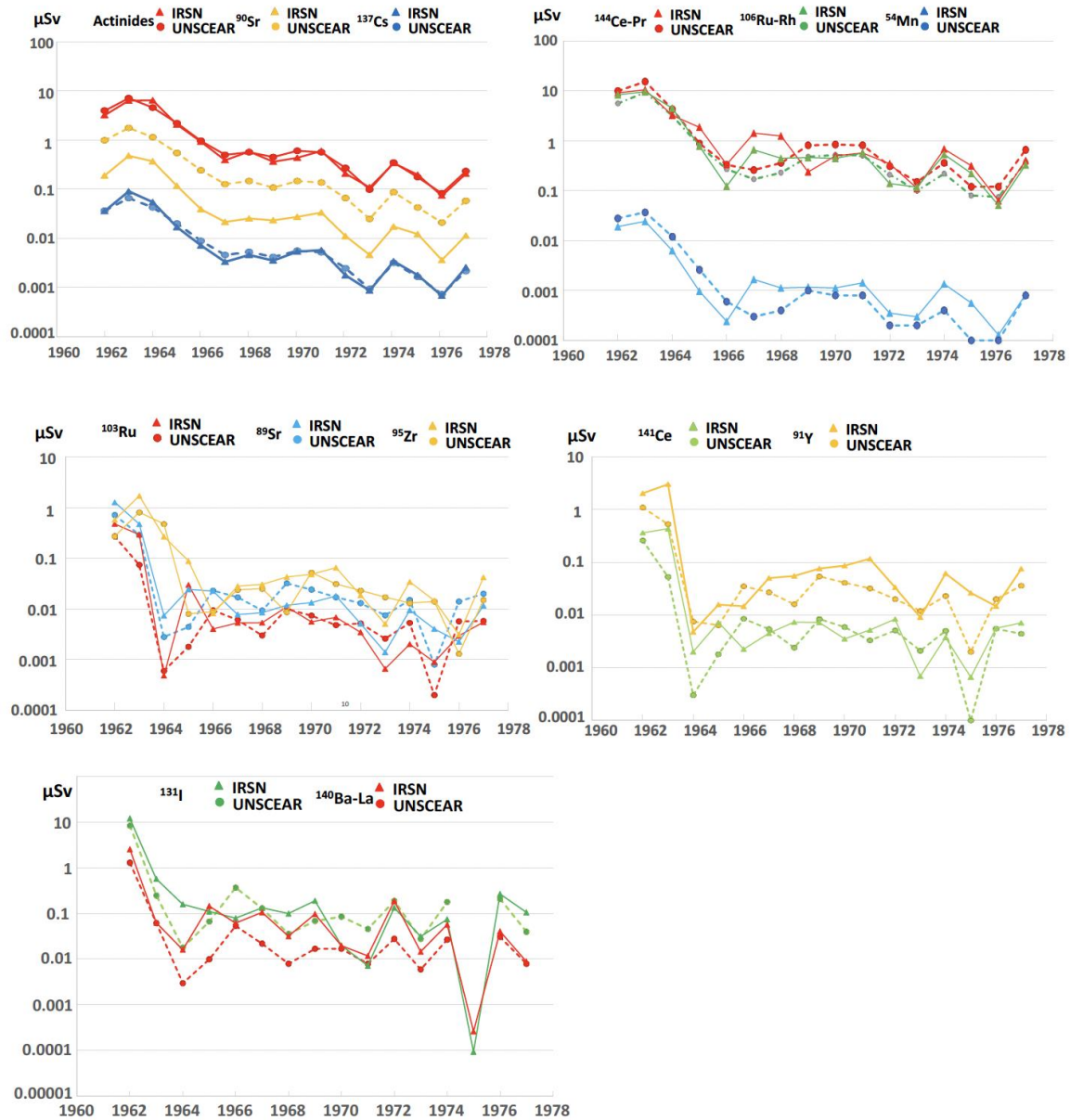


Figure 34: Comparisons between the annual effective doses for adults estimated by UNSCEAR and those estimated using French data for the 1962-1977 period

### 7.3. Methodology for reconstructing records of effective doses by inhalation and doses to organs by age group, 1945-2020

The first objective in this section is to expand the period for estimating effective doses by inhalation to the periods before and after those studied using French data. This expansion is achieved by using the doses estimated by UNSCEAR and by correcting them with the relative deviations observed with the IRSN estimates for the periods 1962-1977 and 1978-1999 (final year of the UNSCEAR estimate) for radionuclides with short to intermediate half-lives. Table XII shows, for each radionuclide, the corrective factors applied to the UNSCEAR dosimetric estimates. For example, the effective dose by inhalation of  $^{144}\text{Ce}+$  for an adult in France is obtained by dividing by 1.2 the corresponding dose provided by UNSCEAR.

**Table XII: Ratio of effective inhaled dose estimates for adults provided by UNSCEAR to those estimated in this study.**

$^{131}\text{I}$	$^{140}\text{Ba}+$	$^{141}\text{Ce}$	$^{103}\text{Ru}+$	$^{89}\text{Sr}$	$^{91}\text{Y}$	$^{95}\text{Zr}+$
1.7	0.5	1.1	1.3	1.9	0.9	0.9
$^{144}\text{Ce}+$	$^{106}\text{Ru}+$	$^{125}\text{Sb}+$	$^{55}\text{Fe}$	$^{90}\text{Sr}+$	$^{137}\text{Cs}+$	<b>Actinides</b>
1.2	1.0	1.2	0.5	5.2	1.1	1.1

Only nine sufficiently long-lived radionuclides induced significant doses received by inhalation beyond 1999. These are  $^3\text{H}$ ,  $^{14}\text{C}$ ,  $^{90}\text{Sr}$ ,  $^{137}\text{Cs}$ , and the actinides whose average annual activity concentrations in air have been reconstructed in section 4.3.5. From these activity concentrations, the effective doses over the period 1978-2020 were calculated according to the methodology described in section 7.2.

In the case of tritium, the estimated doses for inhalation were multiplied by 2 so as to account for the transcutaneous absorption of this radionuclide.

For the periods 1945-1961 and 1978-1985, the effective doses by inhalation for the different age groups can be calculated by applying to the UNSCEAR estimates for adults, the ratio of the effective doses for each age group to the dose calculated for an adult over the period 1962-1977, based on French data (it should be noted that the effective doses by inhalation differ according to the average daily respiratory rates and the DPUIs, and thus according to the age of the people). Table XIII shows these "child/adult" ratios for the different age groups. Although the DPUIs are most often higher for children than for an adult, the increase in respiratory flow rates with age means that these ratios are less than one, and approach one when the age increases, with the exception of  $^{131}\text{I}$  for which the DPUI increases very significantly as age decreases.

Since the effective doses are known per radionuclide and per age group (and per scenario in the case of the distinction of adults working outdoors and sedentary adults), the doses to the organs only differ by the DPUI value.

**Table XIII: Ratios of effective doses for each age group to doses for adults, calculated over the 1962-1977 period**

	<sup>103</sup> Ru	<sup>106</sup> Ru	<sup>95</sup> Zr	<sup>54</sup> Mn	<sup>144</sup> Ce	<sup>141</sup> Ce	<sup>140</sup> Ba	<sup>137</sup> Cs	<sup>90</sup> Sr
<b>0-1 year/adult</b>	0.32	0.35	0.30	0.43	0.37	0.31	0.41	0.14	0.31
<b>1-2 years/adult</b>	0.60	0.67	0.57	0.82	0.85	0.59	0.72	0.20	0.54
<b>3-7 years/adult</b>	0.59	0.65	0.58	0.74	0.70	0.56	0.65	0.22	0.53
<b>8-12 years/adult</b>	0.73	0.73	0.71	0.88	0.76	0.72	0.77	0.40	0.72
<b>13-17 years/adult</b>	0.92	0.81	0.91	0.86	0.84	0.94	0.89	0.70	1.02
	<sup>131</sup> I	<sup>89</sup> Sr	<sup>91</sup> Y	<sup>55</sup> Fe	<sup>125</sup> Sb	<sup>238</sup> Pu	<sup>239+240</sup> Pu	<sup>241</sup> Pu	<sup>241</sup> Am
<b>0-1 year/adult</b>	0.88	0.38	0.39	0.35	0.30	0.12	0.11	0.07	0.12
<b>1-2 years/adult</b>	1.99	0.67	0.72	0.63	0.56	0.27	0.26	0.18	0.28
<b>3-7 years/adult</b>	1.96	0.61	0.64	0.74	0.58	0.35	0.34	0.29	0.35
<b>8-12 years/adult</b>	1.75	0.75	0.77	0.82	0.71	0.48	0.48	0.46	0.48
<b>13-17 years/adult</b>	1.66	0.88	0.87	0.85	0.90	0.69	0.69	0.70	0.70

## 7.4. Estimated effective doses by inhalation, 1945-2020

The annual effective doses received by inhalation for a sedentary adult, estimated according to the methodology presented above, change greatly over time (see Figure 35). In the 1940s, they fluctuated from 0.003 to 0.09 µSv/year, then increased from 0.6 µSv in 1951 to 11 µSv in 1958. Following the moratorium on nuclear testing, they fell to 1.6 µSv in 1959. The resumption of Soviet tests in 1961, and then of American tests in 1962 led to a sudden increase, reaching a maximum value of 34 µSv in 1963. As a result of the cessation of US and Soviet nuclear tests in October 1963, these doses received by inhalation decreased rapidly to 5 µSv in 1965. The fallout from the Chinese tests induced fluctuations throughout the 1970s, between 0.3 and 2 µSv/year depending on the year. After the cessation of Chinese tests in 1980, and due to the purification of the atmospheric compartment that followed, levels decreased during the 1980s to less than 0.008 µSv in 1988. Since the 2000s, resuspension phenomena (wind turbines and combustion of organic matter) have maintained doses at around 0.005 µSv/year.

The respective contributions of the different radionuclides also change over time and two major periods can be distinguished (Figures 35 and 36). Until the early 1980s, the main radionuclides contributing to doses by inhalation were, as indicated above: <sup>144</sup>Ce+, <sup>106</sup>Ru+, <sup>139+240</sup>Pu, <sup>241</sup>Pu, and <sup>95</sup>Zr+. The graph on the left in Figure 35 for the year 1963 illustrates the situation during this period. Starting from 1985, the main radionuclides contributing to the very low doses received by inhalation are <sup>3</sup>H, <sup>14</sup>C, <sup>239+240</sup>Pu, and <sup>241</sup>Am. The graph on the right in Figure 35 for 1990 illustrates these relative contributions.

Figure 37 shows the effective doses by inhalation, all radionuclides combined, for the different age groups and scenarios. It shows that the estimated doses for adults working outdoors are the highest, 50% higher than those estimated for sedentary adults, due to a higher average daily respiratory rate. The estimated doses for children from 1 to 17 years old are lower than those for sedentary adults, but remain very close: the increase in respiratory flow rates with age is compensated by the decrease in DPUIs with age. On the other hand, doses to newborns aged 0 to 1 year are three times lower than those of sedentary adults and five times lower than those of outdoor workers due to the very low respiratory rate of infants.

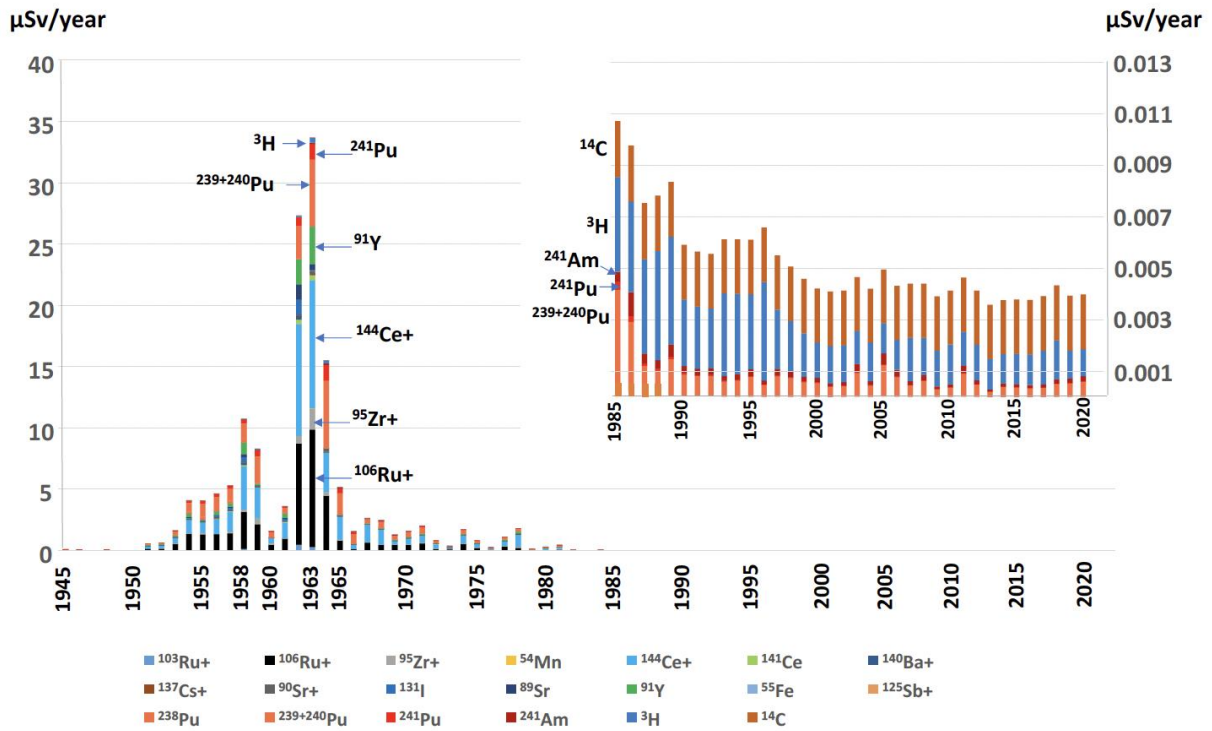


**Figure 35: Estimated annual effective doses by inhalation for a sedentary adult between 1945 and 2020 (μSv) and contribution of the various radionuclides**

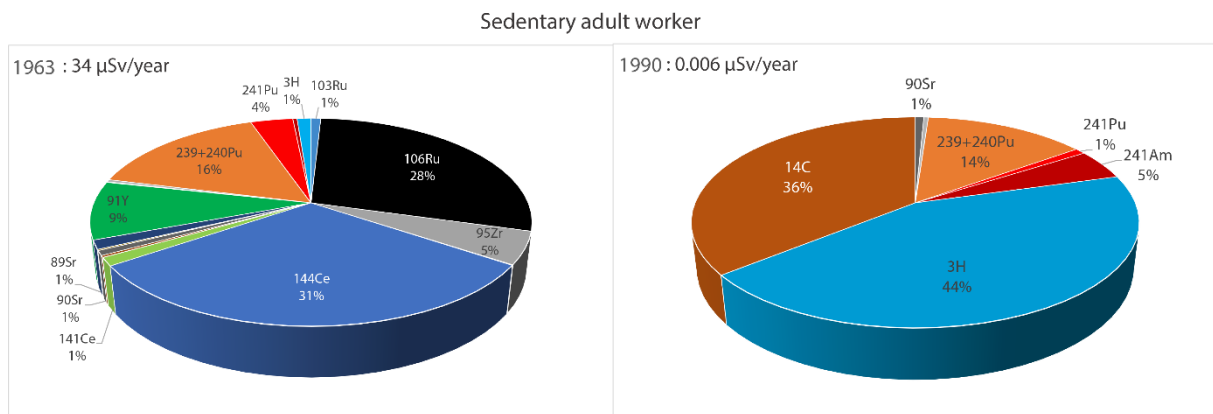


**Figure 36: Contributions of radionuclides to estimated annual effective doses by inhalation for a sedentary adult in 1963 and 1990 (μSv)**

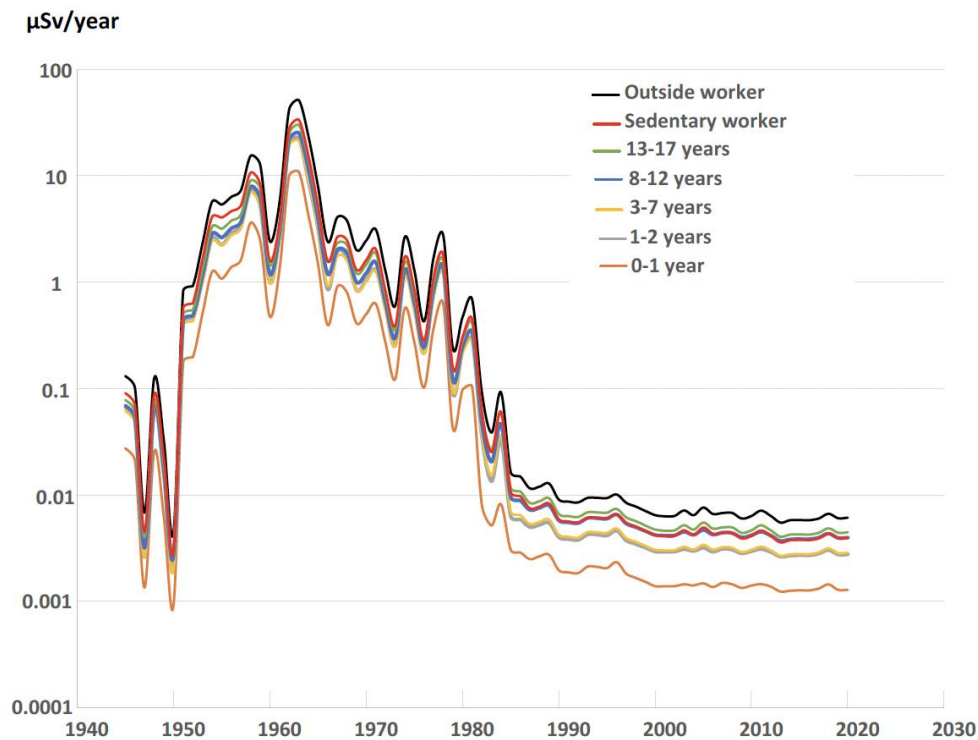


**Figure 37: Annual effective doses for the two adult exposure scenarios and for the different age groups from 1945 to 2020**

The doses to the thyroid are of the same order of magnitude as the effective doses. After adults working outdoors, they are highest for children 1-2 years old (Figure 38): 11  $\mu\text{Sv}/\text{year}$  in 1958, 36  $\mu\text{Sv}/\text{year}$  in 1962 and between 0.002 and 0.003  $\mu\text{Sv}/\text{year}$  since the 1990s. However, the radionuclides that contribute to thyroid doses are very different from those that participate in effective doses. Since there has been iodine-131 present in the air, this radionuclide contributes to most doses to the thyroid. This is the case for years when tropospheric fallout is predominant. Therefore, in the 1940s, then in 1951, 1952, 1958, 1961, 1962, 1976, and 1980,  $^{131}\text{I}$  represented more than 90% of doses to the thyroid (see the example of 1962 in Figure 37). As a result, the doses to the thyroid fluctuate from one year to the next to a greater extent than the effective doses. During the years when stratospheric fallout is predominant (example of the year 1975 in Figure 38), the radionuclides that contribute to thyroid doses are the same as those contributing to effective doses ( $^{144}\text{Ce}$ ,  $^{106}\text{Ru}$ , and  $^{239+240}\text{Pu}$ ) to which  $^3\text{H}$  is added. Since the fallout from nuclear tests has ended,  $^3\text{H}$  and  $^{14}\text{C}$  represent around 99% of doses to the thyroid.

Doses to the brain, breasts, and prostate are around 10 to 20 times lower than the effective doses. They were highest in 1963 for adults, although those of children were very close: for a sedentary adult (add 50% for an adult working outdoors), they were 2.4  $\mu\text{Sv}$  for the brain, 2.9  $\mu\text{Sv}$  for the breasts, and 2.6  $\mu\text{Sv}$  for the prostate (compared to 34  $\mu\text{Sv}$  for the effective dose). The radionuclides that contribute to these doses are the same as those that participate in effective doses to which  $^3\text{H}$  is added as a major contributor and  $^{137}\text{Cs}$  as a secondary contributor.

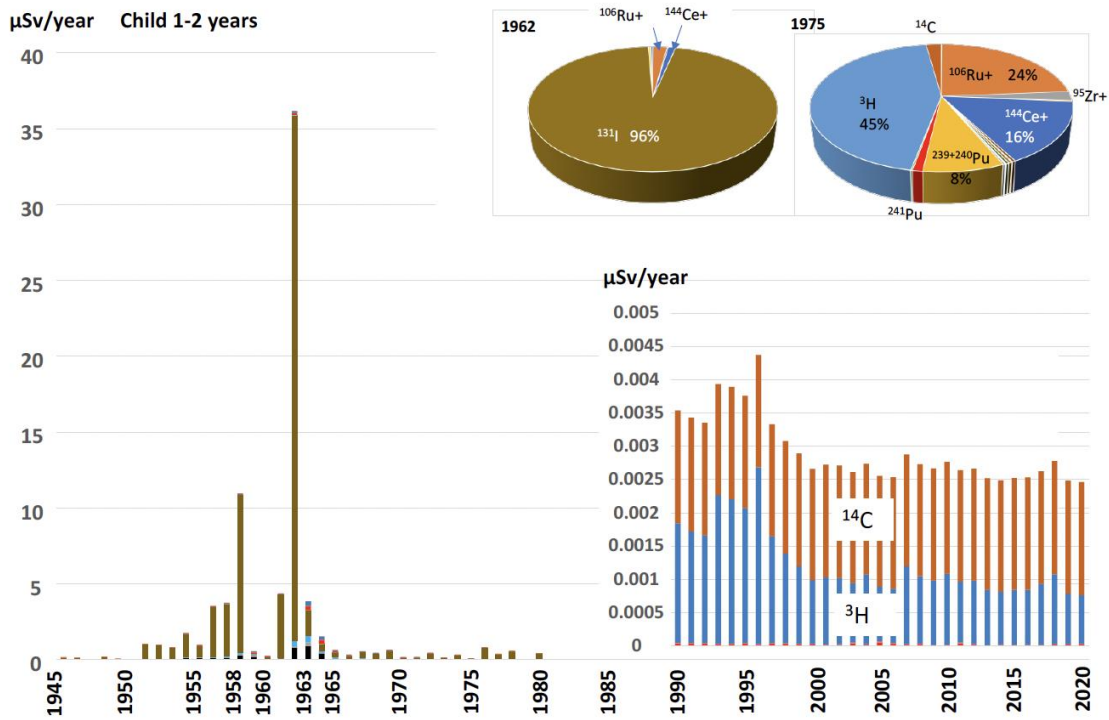


Figure 38: Evolution of doses to the thyroid in children aged 1 to 2 years from 1945 to 2020, and contribution of radionuclides (µSv/year)

## 8. Reconstruction of doses from external exposure to deposits

### 8.1. Methodology for calculating doses from external exposure to deposits for the period of June 1961 to July 1978

#### 8.1.1. General

Radionuclides deposited on the surface of the soil penetrate rather quickly to a few millimetres due to rain. The deeper migration is then slower and practically only concerns radionuclides with a half-life longer than one year. In addition, ploughing an agricultural area leads to the penetration and homogenisation of the activity of a radionuclide in 10 to 20 centimetres of soil, depending on the type of crop.

The deposited radionuclides emit radiation that induces a dose equivalent rate in the air. As soon as the radionuclide penetrates the soil, part of its radiation is absorbed by the thickness of the soil above it. As a result, the radionuclides likely to generate significant external exposure to people are gamma emitters with sufficient energy to cross a thickness of soil, including:  $^{95}\text{Zr-Nb}$ ,  $^{106}\text{Ru-}^m\text{Rh}$ ,  $^{103}\text{Ru-Rh}$ ,  $^{54}\text{Mn}$ ,  $^{144}\text{Ce-}^m\text{Pr}$ ,  $^{125}\text{Sb-}^m\text{Te}$ , and  $^{137}\text{Cs-}^m\text{Ba}$ . For the same deposited surface activity, the radiation in the air above the ground, and therefore the dose rate, decreases when the depth reached by the radionuclide increases; this varies according to the type and energy of the radiation and the density of the soil.

Some of the radionuclides deposited on artificial surfaces are temporarily fixed by adsorption, while the rest run off and end up in urban sewer systems. Wear related to rain, the passage of pedestrians and vehicles, as well as the cleaning of roadways, remobilise the radionuclides initially deposited on the surface of the materials; they are then carried away by runoff.

The kinetics of migration to the depths of the soil or of fixation/remobilisation of radionuclides on artificial surfaces are extremely variable. They depend on the characteristics of the soil or materials, the radionuclide, as well as many other parameters including the characteristics of precipitation, the use and maintenance of surfaces, etc. Moreover, except for  $^{137}\text{Cs+}$ , for which there have been some experimental data and observations following the Chernobyl and Fukushima accidents, all the phenomena mentioned above are poorly understood.

So, unlike exposures related to inhalation and ingestion of radionuclides, external exposure can give rise to a very wide variety of exposure situations and conditions to which, in the current state of knowledge, it is virtually impossible to assign parameters.

Finally, the dose rate inside buildings is lower than it is outdoors. This is mainly due to the fact that the indoor spaces are less contaminated than the outdoors, in particular because of regular cleaning, the fact that the external radiation source is further away, and, to a lesser extent, the fact that building materials shield radiation that comes from outside.

This reduction in the dose rate indoors compared to outdoors is defined by a protection factor as well as by daily time spent inside buildings, assigned for two categories of adults and three age groups of children.

For this study, the choice was made to consider a limited number of exposure scenarios, and their suitability with respect to the main foreseeable exposure situations will be discussed.

### 8.1.2. Case of an adult working outdoors

This scenario is that of a farmer who works 8 hours a day outdoors. He is exposed, on the one hand, to the integrated monthly deposits of the last 12 months (sum of the last 12 monthly deposits, accounting for radioactive decay) assumed to have penetrated to a depth of 0.3 cm, and on the other hand the integrated deposits prior to the last 12 months, assumed to have been homogenised by a single annual ploughing operation to a depth of 15 centimetres. For 16 hours/day, he is inside a single-storey dwelling which provides him with 40% protection against the estimated outdoor dose rate as indicated above (the value of this protection factor is discussed later in section 8.1.4). The dose rate factors per unit of surface activity used (Sv/h per Bq/m<sup>2</sup>) for the two depths considered (0.3 cm and 15 cm) are from ICRP, 2020 and EPA, 2019, respectively.

This scenario of the outdoor worker is a compromise.

For a farmer or any other person working outdoors in a rural area, it allows us to consider the fact that they may be exposed on soil surfaces that have not yet been reworked (around homes, paths, areas that have not yet been ploughed, etc.). In these exposure situations, the penetration at depth (beyond the initial 3 mm) of radionuclides for one year is ignored given the migration rates which are around 1 mm per year. This scenario is well-suited for radionuclides with the shortest radioactive half-lives (up to <sup>95</sup>Zr+ with 2-month half-life). On the other hand, for longer-lived radionuclides, the fact that ploughing occurs after one year means this exposure to unworked soil cannot be taken into consideration beyond this period (only exposure to the ploughed soil remains). For long-lived radionuclides, including <sup>106</sup>Ru+, <sup>125</sup>Sb+, and <sup>137</sup>Cs+ which are potentially the largest contributors to external exposure, dose factors for a depth of 0.3 cm are about 3.5 times those provided for a depth of 15 cm. This deviation is a maximum, first because it would have to be corrected by the proportion of time actually spent on unworked soils compared to that spent on ploughed soils, and also because the radionuclides do penetrate deeply in unworked soils, although more slowly, reducing the difference<sup>14</sup> in dose rate.

This scenario presents both over- and under-estimation biases when applied to an urban outdoor worker. The overestimation bias comes from the fact that all deposits are assumed to remain fixed on surfaces (roads, in particular) for one year, while it is likely that a significant portion of wet deposits is immediately evacuated to the sewers. On the other hand, this scenario is subject to underestimation bias because in urban areas, deposits cannot usually penetrate 0.3 cm into artificial surfaces/coatings; the underestimation which results from the difference between dose factors at the surface and at 0.3 cm is however very moderate. For the radionuclides which potentially contribute the most to external exposure (<sup>95</sup>Zr+, <sup>106</sup>Ru+, <sup>103</sup>Ru+, <sup>125</sup>Sb+, and <sup>137</sup>Cs+), the surface dose factors are only 50% higher than those at 0.3 cm of depth. Finally, it should be noted that the scenario adopted (ploughing after 1 year) induces a 3.5-fold decrease in the dose rate linked to deposits prior to the current year (see the previous paragraph); this decrease limits overestimation linked to the fact that the scenario does not consider the decrease over the years in the urban area dose rate due to the elimination of contamination by rain, cleaning operations, and the wear and tear of urban surfaces linked to passage of people and vehicles, or even the covering/replacement of certain surfaces by new ones. This

---

<sup>14</sup> For example, the dose factors at 5 cm are twice as high as those at 15 cm.

decrease, which mainly concerns  $^{137}\text{Cs}$ , reached 90% (a factor of 10) five years after the deposits that followed the Fukushima accident (Saitoa K. et al, 2019).

### 8.1.3. Case of sedentary adults and children

The scenarios used for children and for sedentary adults are derived from that used for adults working outdoors. The correction relates to the time spent outdoors and indoors, according to the values presented in Table XIV.

**Table XIV: Daily time spent outside and inside buildings**

	Inside	Outside	Inside	Outside
	h/d	h/d Daily fraction	Daily fraction	Daily fraction
Infant	24	0	1.000	0.000
1-2 years	23	1	0.958	0.042
3-7 years	21	3	0.875	0.125
8-12 years	21	3	0.875	0.125
13-17 years	21	3	0.875	0.125
Outside worker	16	8	0.667	0.333
Sedentary worker	21	3	0.875	0.125

The limits of these scenarios for sedentary adults and children are the same as those discussed previously for the scenario of adults working outdoors.

### 8.1.4. Reduction of dose rate inside buildings

The dose rate inside buildings is lower than it is outdoors. This is mainly due to the fact that the indoor spaces are less contaminated than the outdoors, in particular because of regular cleaning, the fact that the external radiation source is further away, and the fact that building materials shield radiation that comes from outside.

This reduction in the dose rate indoors compared to outdoors is defined by a protection factor, which is the ratio of the dose rate inside to the dose rate outside, as well as by daily periods of time spent inside buildings, assigned for two categories of adults and three age groups of children.

The protection factor was well documented after the Fukushima accident. It varies greatly depending on the type of dwelling, from 0.4 (the indoor dose rate represents 40% of the outdoor dose rate) for a single-storey wooden house, to less than 0.01 on the upper storeys of a concrete building (Yoshida-Ohuchi et al. 2019).

The value of the protection factor selected for this study is 0.28 (the indoor dose rate represents 28% of the outdoor dose rate). It comes from a 2016 bibliographical study by the Lawrence Livermore National Laboratory which took into account the many data points acquired after the Fukushima accident and corresponds to a brick family house on one level. This value of 0.28 is lower than 0.4, from the same study, which corresponds to a single-storey house built of light materials such as wood. But it is higher than the value of 0.2 recommended by the IAEA (IAEA, 1979 and IAEA, 2000) on the basis of previous data. It is very conservative with regard to the values mentioned in this same study for residential buildings in urban areas: 0.025 for the lower floors and 0.01 for the upper floors.

For information purposes, Table XV presents the ratio of external doses calculated with protection factors of 0.28 to those calculated with other protection factors, taking into account the various periods of time spent indoors as presented in Table XI. For adults working outdoors, the ratios are low, regardless of the type of dwelling. The same is true for ratios of single-storey dwellings, regardless of age group. On the other hand, ratios are significant between single-storey dwellings and multi-family apartment buildings, like those found in urban areas, especially for young children.

**Table XV: Corrective factors of external doses for an indoor protection factor of 0.28**

	Adult working outdoors	Baby	1-2 years	Other age groups and sedentary adult
0.28/0.4	0.9	0.7	0.7	0.8
0.28/0.2	1.1	1.4	1.3	1.2
0.28/0.025	1.5	16	6.5	3.2
0.28/0.01	1.5	40	6.0	2.8

## 8.2. Estimated external effective doses for an outdoor worker and comparison with UNSCEAR estimates

Figure 39 shows the monthly external doses for an outdoor worker calculated according to the scenario set out above. The doses are higher than those related to inhalation (see Figure 32): six times higher, for example, in 1963, at the height of fallout from atmospheric tests of nuclear weapons. This figure also confirms that only a limited number of radionuclides contribute to the external dose. These are high-energy gamma emitters, which are abundant in deposits or whose radioactive half-life is long enough to have caused accumulation in the soil:  $^{95}\text{Zr}+$  and  $^{106}\text{Ru}+$  over the entire period but more particularly until 1963,  $^{103}\text{Ru}+$  until 1963 and  $^{137}\text{Cs}+$  starting in 1964.  $^{54}\text{Mn}$ ,  $^{144}\text{Ce}+$ , and  $^{125}\text{Sb}+$  are secondary contributors. The other radionuclides are not represented in this figure because their contribution to the external dose is negligible.

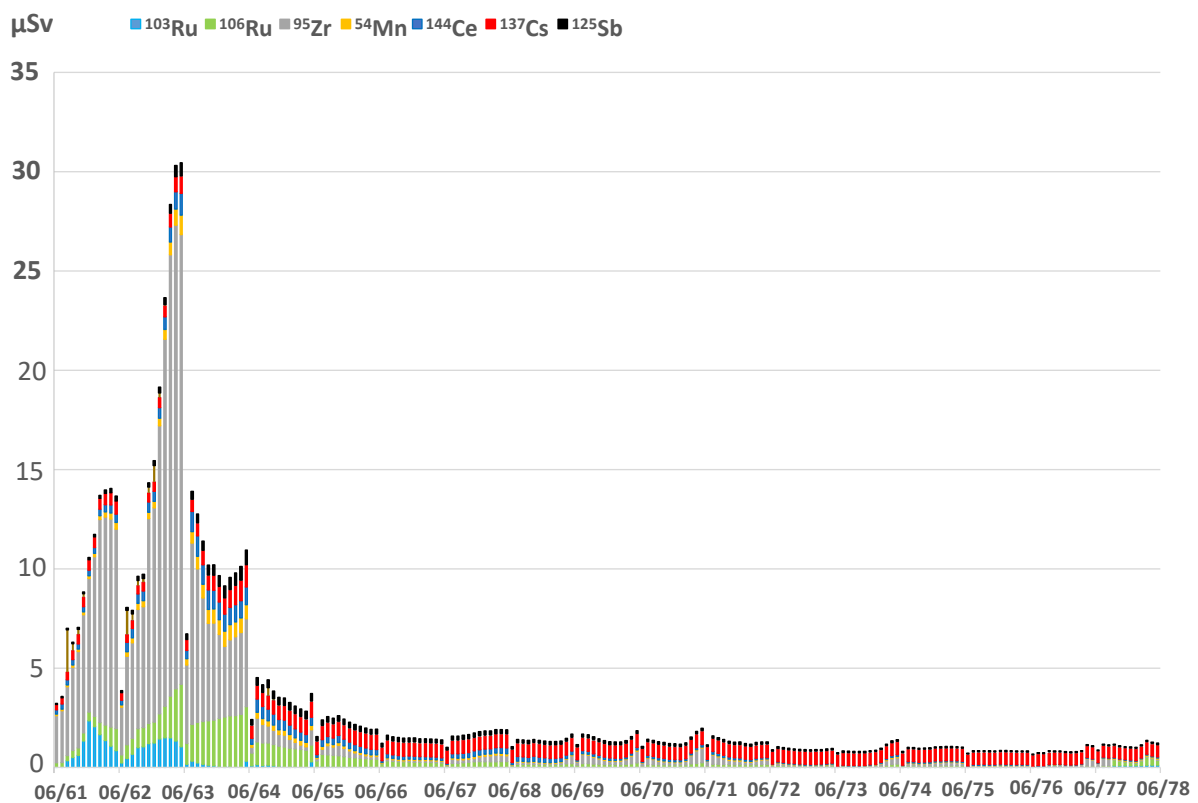


**Figure 39: Estimated monthly external doses for an adult working outdoors with contribution of the main radionuclides**

In its 2000 report, UNSCEAR provided global average annual external doses, estimated for an adult, due to the 10 main contributing radionuclides. As with inhalation, it can be assumed that weighting by population density brings these global estimates close to those of an adult residing in the same latitudinal band as France. Figure 40 compares these estimates with those made for this study using French data. The two estimates are totally in agreement with respect to annual changes and the relative contributions of the different radionuclides. However, the estimated doses for France are systematically higher and, on average, twice as high as those estimated by UNSCEAR, except in the case of  $^{144}\text{Ce}+$  (Table XVI). For the different radionuclides (still with the exception of  $^{144}\text{Ce}+$ ), the ratios of the two "IRSN/UNSCEAR" estimates are between 1.6 ( $^{137}\text{Cs}+$ ) and 3 ( $^{95}\text{Zr}+$ ). These ratios can be explained by the ratios of radioactive deposits at the origin of the external exposure. The "IRSN/UNSCEAR" external dose ratios are indeed consistent with those of the radioactive deposits indicated in Table VII of section 5.2, between 1.6 ( $^{137}\text{Cs}+$ ) and 3.6 ( $^{95}\text{Zr}+$ ). This consistency can be explained by the fact that, while different, the scenario and dose factors used by UNSCEAR<sup>15</sup> are similar to those used for this study. On the other hand, there is no obvious explanation for the fact that the estimated annual external doses in this study for  $^{144}\text{Ce}+$  are nearly 10 times higher than those estimated by UNSCEAR, especially since the dose factor used by UNSCEAR is, conversely, twice as high as that used for this study.

<sup>15</sup> UNSCEAR considers a depth of 0.1 cm for short-lived radionuclides (up to  $^{95}\text{Zr}+$ ) and a depth of 3 cm for other radionuclides. The dose factors provided by UNSCEAR in its report also integrate an overall reduction factor of 0.4 to account for the time spent inside buildings.

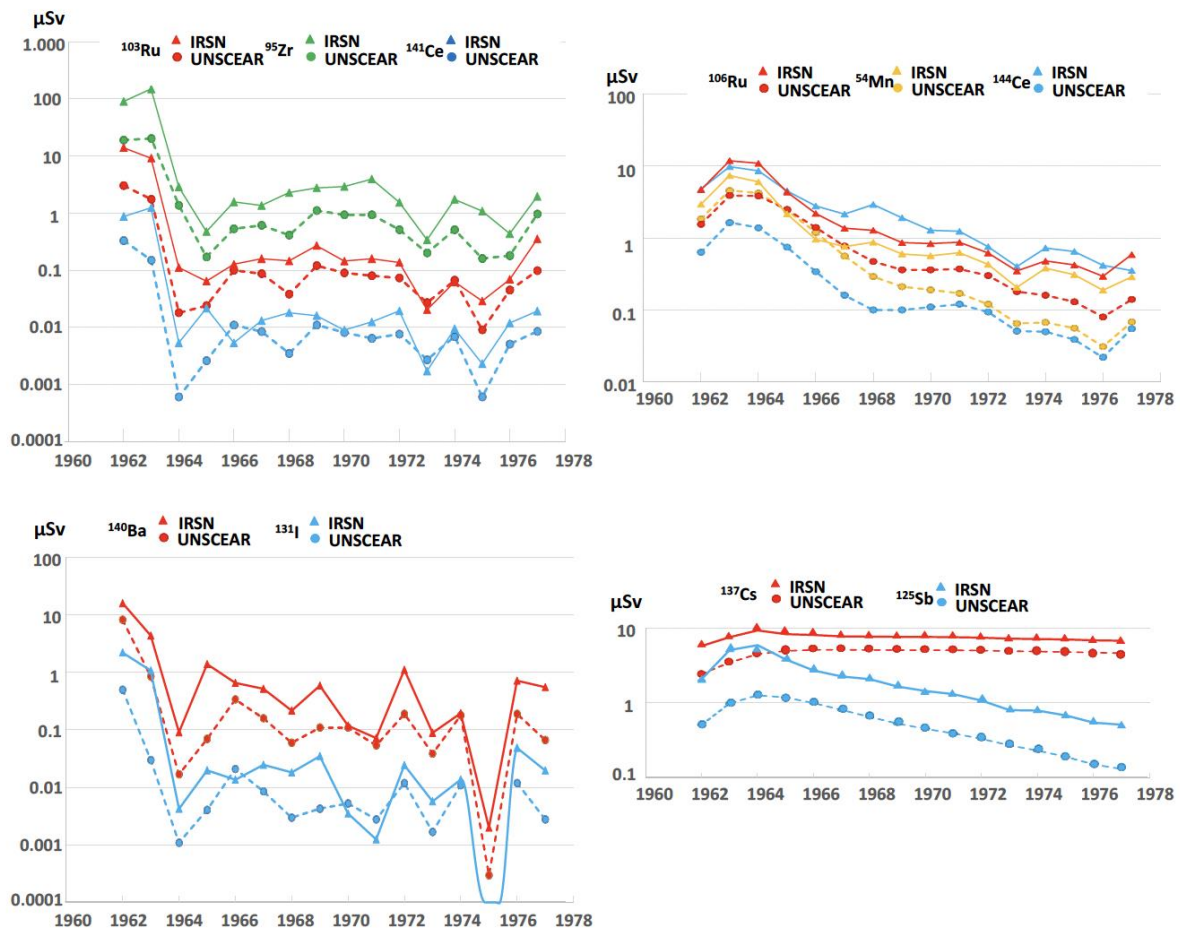


Figure 40: Comparison of the annual external effective doses for an adult estimated by UNSCEAR to those estimated in this study

Table XVI: Ratio of effective external dose estimates for adults provided by UNSCEAR to those estimated in this study (IRSN/UNSCEAR).

<sup>131</sup> I	<sup>140</sup> Ba+	<sup>141</sup> Ce	<sup>103</sup> Ru	<sup>95</sup> Zr+	<sup>144</sup> Ce+	<sup>54</sup> Mn	<sup>106</sup> Ru+	<sup>125</sup> Sb+	<sup>137</sup> Cs+
1.8	2.7	1.7	1.9	3.0	9.5	2.1	2.4	3.4	1.6

### 8.3. Methodology for reconstructing complete records of effective external doses, 1945-1985

The aim here is to expand the period for estimating external doses to the periods before and after those studied using French data, i.e. from 1945 to 1961 and from 1977 to 1999, as the UNSCEAR estimates stop in 1999. Starting from the mid-1980s, external doses resulting from the fallout of atmospheric tests of nuclear weapons were mainly due to <sup>137</sup>Cs+, the activities of other radionuclides having already decreased significantly due to radioactive decay. From May 1986 until today, over most

of mainland France, external exposure to artificial radionuclides present in soils mainly results from deposits following the Chernobyl accident, in particular  $^{137}\text{Cs}$  (IRSN, 2023 forthcoming).

To reconstruct the external doses from 1945 to 1961 and from 1977 to 1985, the doses estimated by UNSCEAR over these two periods are corrected by the deviations observed with the IRSN estimates for the 1962-1977 period. The corrective factors applied to the UNSCEAR estimates for this exposure pathway are therefore the "IRSN/UNSCEAR" ratios shown in Table XVI.

Also, the doses for three radionuclides not considered by UNSCEAR ( $^{89}\text{Sr}$ ,  $^{91}\text{Y}$ , and  $^{90}\text{Sr}$ - $^{90}\text{Y}$ ), probably because they were considered to induce negligible doses, were reconstructed for 1962 to 1977 and have been added for the previous and subsequent periods. The doses due to  $^{89}\text{Sr}$  and  $^{91}\text{Y}$  are deduced from those of  $^{95}\text{Zr}$  over the period 1962 to 1977; the doses due to  $^{90}\text{Sr}$ - $^{90}\text{Y}$  are deduced from those of  $^{137}\text{Cs}$ . Although the external dose due to  $^{90}\text{Sr}$  was negligible until the early 1960s, this was no longer the case in the 1970s and 1980s due to its long radioactive half-life, and therefore its accumulation in the soil. On the other hand, the contributions of  $^{55}\text{Fe}$  and actinides to external doses, which are also not considered by UNSCEAR, are indeed quite negligible.

Finally, since UNSCEAR only provides estimates of doses to adults, the doses to children for the periods 1945-1961 and 1978-1995 must be deduced from this using the "child/adult" dose ratios calculated for the 1962-1977 period, shown in Table XVII. The external doses to children differ from those in the scenario of adults working outdoors, by the value of the dose factor, which depends on the radionuclide, and by the time spent indoors. Table XVII shows that the "child/adult" ratios are equal to or close to one for children aged 0 to 12: the fact that the dose factor increases as the age of the child decreases is almost exactly compensated by the fact that the child spends more time indoors (see Table XIV section 8.1.3). The external doses calculated for children aged 13 to 17 are most often 20% lower (ratio of 0.8) than those of outdoor workers: the dose factors of children in this age group are very similar to those of adults, while children spend more time indoors than the outdoor worker. Finally, Table XVII also provides the ratio of the two adult scenarios: "sedentary adult/adult outdoor worker". In this case, the dose factors are identical and the fact that the sedentary adult only spends 3 hours/day outdoors compared to 8 hours/day for the external worker, results in an external dose that is 20% lower.

**Table XVII: Ratios of "child/adult" external doses calculated from the estimated doses for the 1962-1977 period.**

	$^{103}\text{Ru}$	$^{106}\text{Ru}$	$^{95}\text{Zr}$	$^{54}\text{Mn}$	$^{144}\text{Ce}$	$^{141}\text{Ce}$	$^{140}\text{Ba}$	$^{137}\text{Cs}$	$^{90}\text{Sr}$	$^{131}\text{I}$	$^{89}\text{Sr}$	$^{91}\text{Y}$	$^{125}\text{Sb}$
0-1 year	1.0	1.2	1.0	0.9	0.9	1.0	1.0	0.9	0.8	1.0	1.2	1.1	0.9
1-2 years	0.9	1.2	0.9	0.9	0.9	1.0	0.9	0.9	0.8	0.9	1.1	1.0	0.9
3-7 years	1.0	1.2	1.0	0.8	1.0	1.0	0.9	0.9	0.9	1.0	1.1	1.0	0.9
8-12 years	0.9	1.1	0.9	0.8	0.9	0.9	0.9	0.8	0.8	0.9	0.6	0.9	0.8
13-17 years	0.8	1.1	0.8	0.8	0.8	0.8	0.8	0.8	0.8	0.8	0.9	0.8	0.8
Sed. Adult	0.8	0.8	0.8	0.8	0.8	0.8	0.8	0.8	0.8	0.8	0.8	0.8	0.8

## 8.4. Discussion of external dose results

### 8.4.1. Effective external doses for adults working outdoors

Figure 41 presents the record of the annual external effective doses for outdoor workers with the contributions of the various radionuclides.

This figure shows the evolution of the relative contributions for the various radionuclides. During the fallout from the US and Soviet tests from 1945 to 1963,  $^{95}\text{Zr}+$  was by far the most significant contributor to external effective doses; in 1963, its contribution represented 72% of the total external effective dose, with the other main contributing radionuclides each accounting for less than 6%. Starting in 1964, the accumulation of  $^{137}\text{Cs}+$  in soils made this long-lived radionuclide the main contributor to the external effective dose, with a contribution of 46% in 1971. The deposits resulting from the Chinese tests have  $^{95}\text{Zr}+$  as the second contributor, at 24% of the total dose for the same year. For the same reason as  $^{137}\text{Cs}+$ , and although very weakly irradiating from a distance (pure beta emitter),  $^{90}\text{Sr}+$  appears to be a significant contributor to the external dose. From the early 1980s, long-lived radionuclides accumulated in soils accounted for 97% of the external dose (85% for  $^{137}\text{Cs}+$  and 12% for  $^{90}\text{Sr}+$ ).

#### 8.4.2. Effective external doses for children and sedentary adults

As mentioned in section 8.3, the external effective doses for outdoor workers and children aged 0-1 year are virtually the same (see Figure 42). In 1963, for example, they were 208 and 206  $\mu\text{Sv}$ , respectively. They were followed by doses to children aged 3-7 years (201  $\mu\text{Sv}$  in 1963), 1-2 years (194  $\mu\text{Sv}$  in 1963) and 8-12 years (187  $\mu\text{Sv}$  in 1963). The effective external doses for sedentary adults and for adolescents aged 13-17 years are the lowest and are very similar (167 and 160  $\mu\text{Sv}$ , respectively in 1963). Despite annual fluctuations related to the relative contributions of the various radionuclides, this hierarchy is maintained throughout the period.

#### 8.4.3. Effect of the place of residence (of the building protection factor)

The effective external doses for sedentary adults and children aged 0-1 year living (or working) on the upper storeys of large buildings are also shown in Figure 42. It appears that the influence of this scenario element is largely dominant over all the other causes of variation in external doses (time spent outdoors, age, fate of radioactive deposits, etc.). Improving the personalisation of external doses would first require having this information on the floor of residence/work. A questionnaire to be sent to the members of the "Constances" cohort included in CORALE will include this question.

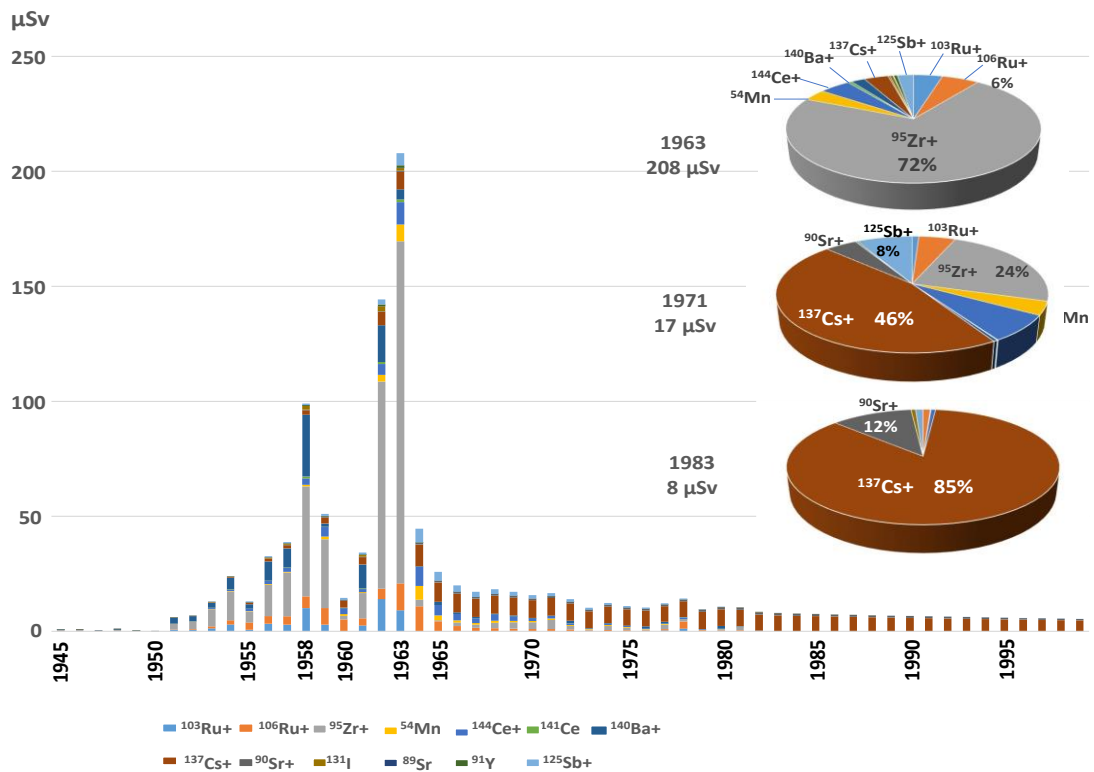


Figure 41: Evolution of effective external doses for adults working outdoors from 1945 to 1999 ( $\mu\text{Sv}/\text{year}$ ) and contributions of radionuclides

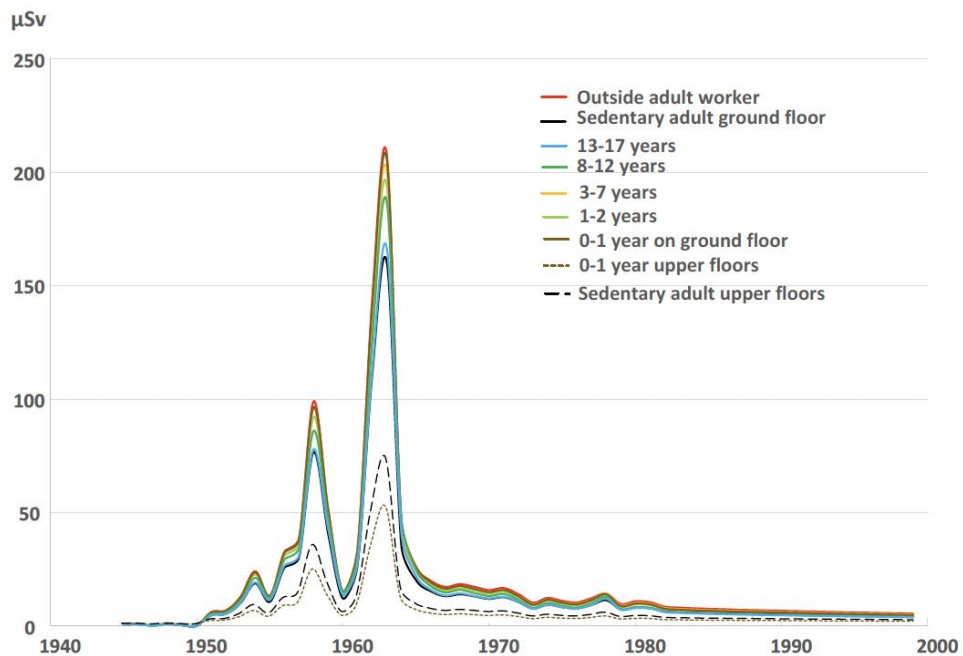


Figure 42: Comparison of external effective doses according to age, time spent outdoors for adults and the building storey of residence/work ( $\mu\text{Sv}/\text{year}$ )

#### 8.4.4. Organ-equivalent external doses

Table XVIII shows that the differences between the effective and organ-equivalent dose factors are negligible for external exposure to deposits: the maximum coefficient of variation around the effective dose factor is between 5% and 10%, depending on the radionuclide. The external dose differences likely to be induced are therefore negligible with regard to the variability of the scenario parameters. In this study, effective external dose estimates were assigned to organ-equivalent external doses.

**Table XVIII: Effective and organ-equivalent dose factors for external exposure to deposits at a depth of 0.3 mm of soil for an adult (Sv/h per Bq/m<sup>2</sup>)**

Sv/h per Bq/m <sup>2</sup>	<sup>103</sup> Ru+	<sup>106</sup> Ru+	<sup>131</sup> I	<sup>137</sup> Cs+	<sup>95</sup> Zr+	<sup>90</sup> Sr+
Effective	1.10E-12	4.73E-13	8.23E-13	1.33E-12	3.35E-12	1.05E-14
Colon	1.06E-12	4.66E-13	8.01E-13	1.29E-12	3.27E-12	1.04E-14
Lungs	1.02E-12	4.50E-13	7.69E-13	1.25E-12	3.15E-12	9.70E-15
Breasts	1.19E-12	5.14E-13	9.05E-13	1.42E-12	3.55E-12	1.17E-14
Thyroid	1.13E-12	4.98E-13	8.58E-13	1.38E-12	3.48E-12	1.15E-14
Brain	1.14E-12	4.96E-13	8.54E-13	1.38E-12	3.49E-12	1.02E-14
Prostate	1.07E-12	4.65E-13	8.00E-13	1.29E-12	3.25E-12	9.43E-15

## 9. Reconstruction of ingested doses

### 9.1. Methodology for calculating ingested doses for the period of June 1961 to July 1978

The reconstruction of doses received by ingestion of foodstuffs is based on the records of specific activities and activity concentrations in foodstuffs (Bq/kg fresh and Bq/L) established in chapter 6.

The application of food intake (kg/month) specific to each age group, with time limits between food production and consumption to account for radioactive decay, provides an estimate of the activities of radionuclides incorporated by ingestion each month (Bq/month).

Finally, a dose per unit intake coefficient (DPUI in Sv/Bq ingested) is used to estimate the doses received by ingestion from the activities incorporated. The DPUIs used in this study to calculate the effective and equivalent doses to the thyroid, brain, colon, lungs, breasts, and prostate, for the different age groups, are taken from the decree of 1 September 2003 (JO 2003) and the series of publications from the ICRP following recommendations of publication 60.

The main issue here is therefore to determine food intake.

The results of 20 food surveys carried out in France between 1977 and 2020 were used to determine the intake to be used for this study. These included four national surveys (INSEE 1991, INCA1 2000, INCA2 2008 and INCA3 2015) and sixteen local food surveys around French nuclear sites conducted, for the most recent, by IRSN (Tricastin 2004, Chinon 2008, Marcoule 2010, Gravelines 2011, Blayais 2012, Bure 2013 and Saint-Alban 2020) and by the CEA (Cadarache 2018), as well as by various organisations for the oldest surveys (Gravelines 1977, Penly 1977, Creys-Malville 1977, Saint-Alban 1977, Flamanville 1978, Marcoule 1979, Civaux 1993 and Nord-Cotentin 1999) (Calmon 2017). All these surveys are referenced in the document (Calmon, 2017), with the exception of the most recent ones conducted around Cadarache (Cohenny, 2019) and Saint-Alban (IRSN, 2022b).

The results of these surveys or their application have limitations, disadvantages, and biases, the most evident of which are presented below. The number of people surveyed is greater for national surveys (a few thousand) than for local surveys (a few hundred). But national surveys were not conducted to meet the needs of dosimetric assessments. In particular, their results most often mention quantities of processed agri-food products, or even prepared meals, that do not correspond to the categories of raw or only slightly processed agricultural products corresponding to radioecological knowledge (leafy vegetables, fruit vegetables, cereals, etc.) and the specific activity and activity concentration data available for this study. To exploit these results, it was therefore necessary to "break down" agri-food products into their basic foods; a pizza is broken down into quantities of cereals (the dough), fruit vegetables (tomatoes), dairy products (cheese), etc. The most recent local surveys conducted by IRSN and the CEA were conducted specifically for dosimetric assessments following the same protocol. However, they concern a very rural population with a voluntary bias to focus on people who are most likely to consume locally-produced foods (they have a vegetable garden, for example); this results in greater consumption of vegetables and fruits. Finally, the protocols of the older local surveys varied from one survey to another and their results do not always make it possible to compare the results for each of the food categories.

Figure 43 shows the quantities from these surveys for the different categories of food consumed annually by an adult. It shows a great variability of results within the same category, with quantities

consumed that can range from single to double or even triple the amount (case of vegetables consumed at the rate of 120 kg/year according to the INCA1 survey and 320 kg/year according to the Saint-Alban 2020 survey). The results of some surveys allow us to differentiate the three categories of vegetables usually distinguished in radioecology.

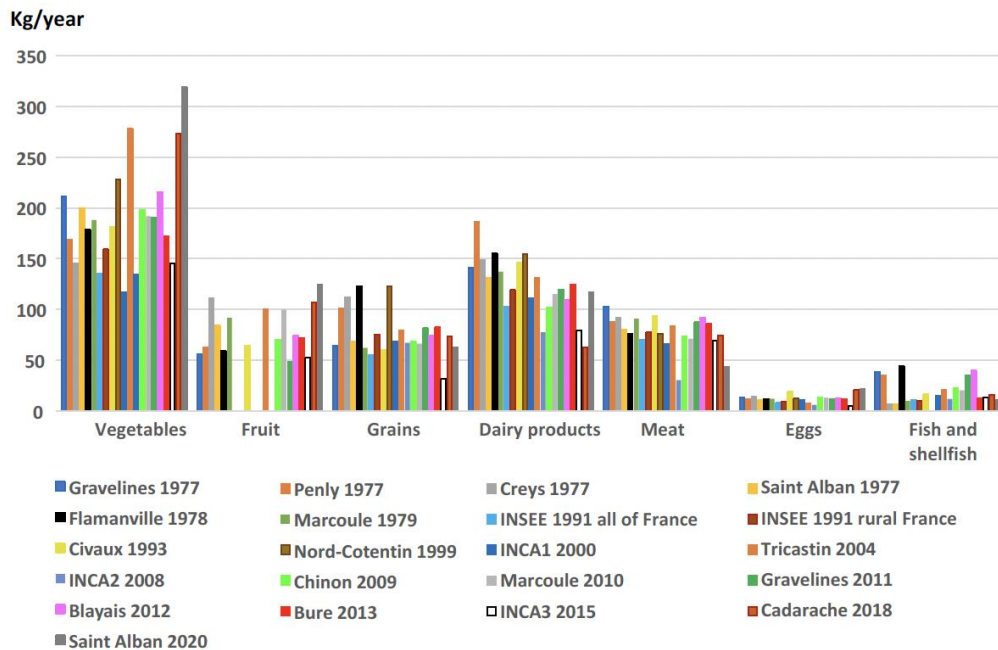


**Figure 43: Comparison of quantities for various categories of food consumed annually by an adult according to the various food surveys conducted in France (kg/year)**

This is the purpose of Figure 44 which shows that despite this distinction, the differences in quantities consumed within these sub-categories remain significant: 20 to 60 kg/year for leafy vegetables, 40 to 130 kg/year for root vegetables and 60 to 170 kg/year for fruit vegetables.

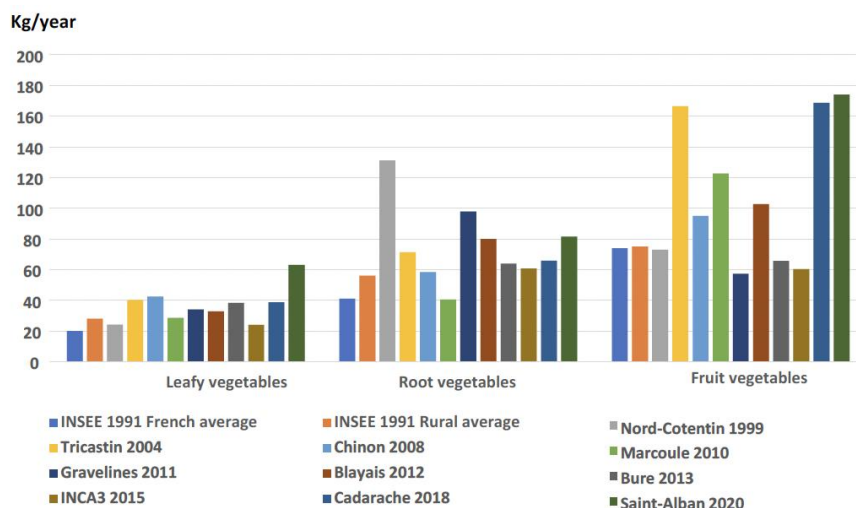


**Figure 44: Comparison of quantities for the three categories of vegetables consumed annually by an adult according to the various food surveys conducted in France (kg/year)**

More generally, we note that the consumed quantities from national surveys are lower than those from local surveys. This remains visible in terms of total quantities of food consumed annually (Figure

45) with an average of 370 kg/year (in a range from 320 to 450 kg/year) for national surveys (red bars on the graph) and 600 kg/year (in a range from 550 to 700 kg/year) for local surveys (blue bars on the graph). The 1991 INSEE survey also confirms that there is a difference in total quantities consumed between the whole of France (380 kg/year) and rural France (450 kg/year), which is more particularly represented in local surveys around nuclear sites.

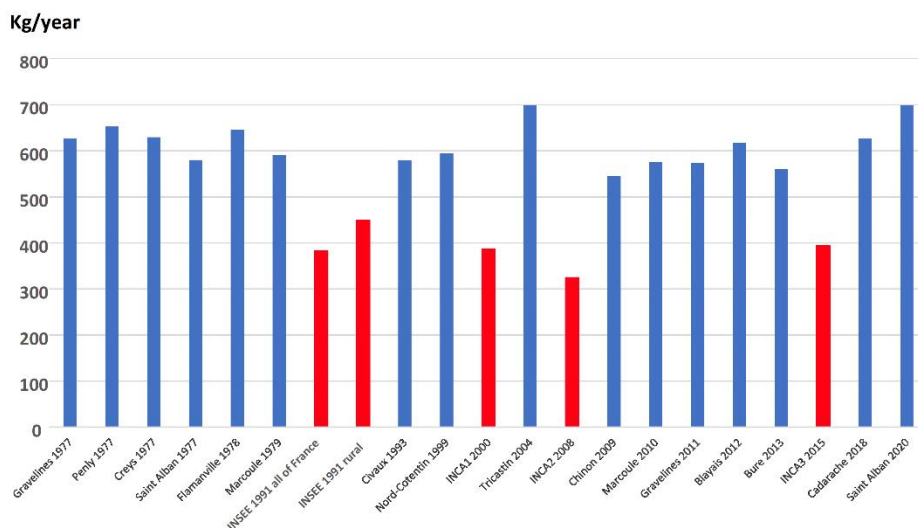


**Figure 45: Total quantities of solid food consumed annually by an adult according to the various food surveys conducted in France (kg/year); the national surveys are shown in red, the local surveys in blue.**

No argument emerges to select the food intake from one survey rather than another, and in order to improve the representativeness of the intake used it seems relevant to employ an average value by food category from the results of several food surveys.

Since the study covering the 1960s and 1970s and Figure 43 may suggest a change over time in the quantities consumed, in particular a decrease for dairy products, we may question whether to use general averages from all surveys combined or averages from the oldest surveys. Figure 46 confirms a decline for dairy products whose consumption (linear relationship) drops from 160 kg/year in 1977 to 100 kg/year. This decrease is also accompanied by an increase in the consumption of vegetables, the quantities consumed increasing from 160 kg/year to 250 kg/year. We can also note a slight increase in fruit consumption and a decrease in meat consumption. Despite these trends, the differences from one decade to the next remain moderate (see Table XIX) and the averages from the results of all surveys combined from 1977 to 2020, presented in Table XX, have been selected for this study.

**Table XIX: Comparison of averages of quantities consumed by category of food according to the period during which the food surveys were conducted (kg/year)**

kg/year	Vegetables	Fruit	Grains	Dairy products	Meat	Eggs
Average for 1970s	182	77	88	150	88	12
Average 1977–2020	192	80	76	122	77	12
Average for 2010s	215	82	67	104	75	14

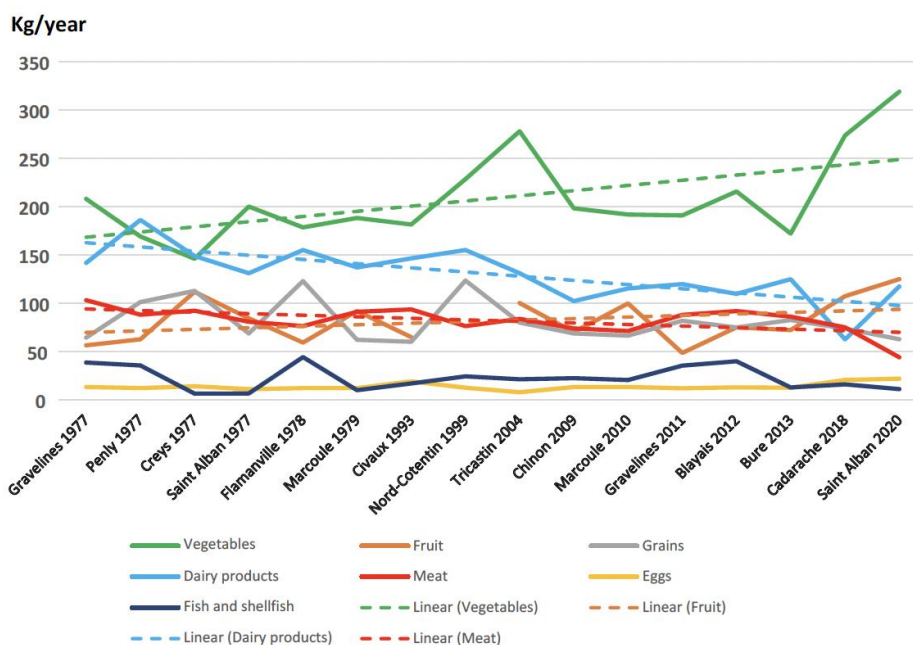


**Figure 46: Evolution over time of the quantities of various types of food consumed annually by an adult (kg/year)**

**Table XX: quantities of food consumed annually by category of food selected for this study.**

	Leafy vegetables	Fruit vegetables and fruit	Root vegetables	Grains	Milk and dairy products	Meat
kg/year	35	183	71	76	122	77
g/d	96	501	194	208	335	211

Most surveys only focus on adults. The few surveys involving children provide disparate and difficult to compare results because the age groups considered vary and are different from those proposed by ICRP for DPUIs. For this study, the quantities consumed by children in the various age groups are determined by applying the ratios of quantities consumed by adults that are recommended by the IAEA. These "child/adult" ratios are provided in Table XXI. Finally, in the case of children aged 0-1 year, milk consumption of 800 g/d alone was used (Vidal and Renaud 2000). Additional information on children's food intake is provided in (Vidal and Renaud 2000 and CEA 2019).

**Table XXI: “Child/adult” ratios of quantities consumed as recommended by the IAEA (IAEA, 1999)**

	1-2 years	3-7 years	8-12 years	13-17 years
Leafy vegetables	0.62	0.79	0.84	1
Fruit vegetables and fruit	0.34	0.68	0.83	1
Root vegetables	0.64	0.73	0.88	1
Grains	0.33	0.49	0.68	1
Dairy products	1.3	0.46	0.64	1
Meat	0.22	0.40	0.63	1

## 9.2. Estimated effective doses by ingestion for an adult, 1961-1978; comparison with UNSCEAR estimates

Figure 47 shows the evolution of the monthly effective ingested doses for an adult, estimated using the previously described methodology. This evolution and the respective contributions of the various radionuclides are directly linked to activities in foodstuffs and to the different levels of ingestion radiotoxicity specific to each radionuclide (DPUI see section 9.1). This figure clearly shows the five radionuclides that, excluding tritium and carbon-14, contribute (with their chaining) to the bulk of the effective doses by ingestion:  $^{131}\text{I}$ ,  $^{137}\text{Cs}+$ ,  $^{90}\text{Sr}+$ ,  $^{144}\text{Ce}+$ , and  $^{106}\text{Ru}+$ . The secondary contributors are  $^{91}\text{Y}$  and  $^{89}\text{Sr}$ ; the other 11 radionuclides considered in this study make negligible contributions to the doses received by ingestion.

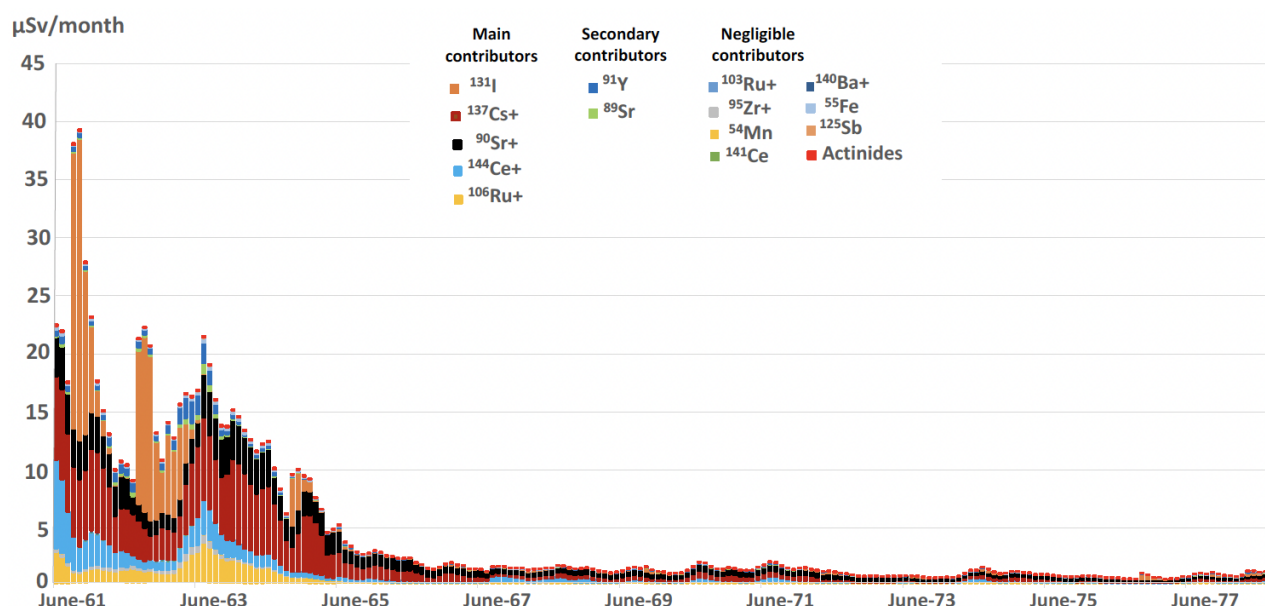


**Figure 47: Estimated monthly effective doses by ingestion for an adult between June 1961 and July 1978 ( $\mu\text{Sv}/\text{month}$ ).**

Similar estimates were made for the different age groups. The annual dose records obtained by summing these monthly doses will be discussed in section 9.4.

In its 2000 report, UNSCEAR provides global average estimates of annual effective doses received by ingestion for an adult from 1945 to 1985 and for five radionuclides:  $^{131}\text{I}$ ,  $^{137}\text{Cs}+$ ,  $^{90}\text{Sr}+$ ,  $^{140}\text{Ba}+$ , and  $^{89}\text{Sr}$ .

For the 1962-1977 period (years 1961 and 1978 were not complete), these estimates can be compared to the annual averages estimated in this study.

The graphs in Figure 48 confirm that  $^{131}\text{I}$ ,  $^{137}\text{Cs}+$  and  $^{90}\text{Sr}+$  (in blue, red, and black) are among the radionuclides that induce the highest effective doses by ingestion for an adult. Doses due to  $^{89}\text{Sr}$  and  $^{140}\text{Ba}+$  are significantly lower.

This comparison shows that, except for the case of  $^{55}\text{Fe}$ , the estimates made for mainland France as part of this study are, on average, twice as high as those from UNSCEAR for the northern hemisphere, while showing similar development over time. The average ratio of the two estimates (UNSCEAR/IRSN) is 0.6 for  $^{137}\text{Cs}+$ , 0.5 for  $^{90}\text{Sr}+$ , 0.3 for  $^{140}\text{Ba}+$  and  $^{89}\text{Sr}$ , and 0.7 for  $^{131}\text{I}$ . This ratio can largely be explained by the fact that radioactive deposits estimated by IRSN in mainland France are twice as high as those estimated by UNSCEAR for the northern hemisphere (see section 5.2). In the case of  $^{55}\text{Fe}$ , no explanation is given for the fact that UNSCEAR's estimates are twice as high as those of IRSN. It should be noted, however, that the evolution of doses estimated by UNSCEAR for this radionuclide shows a surprisingly linear decrease since 1965.

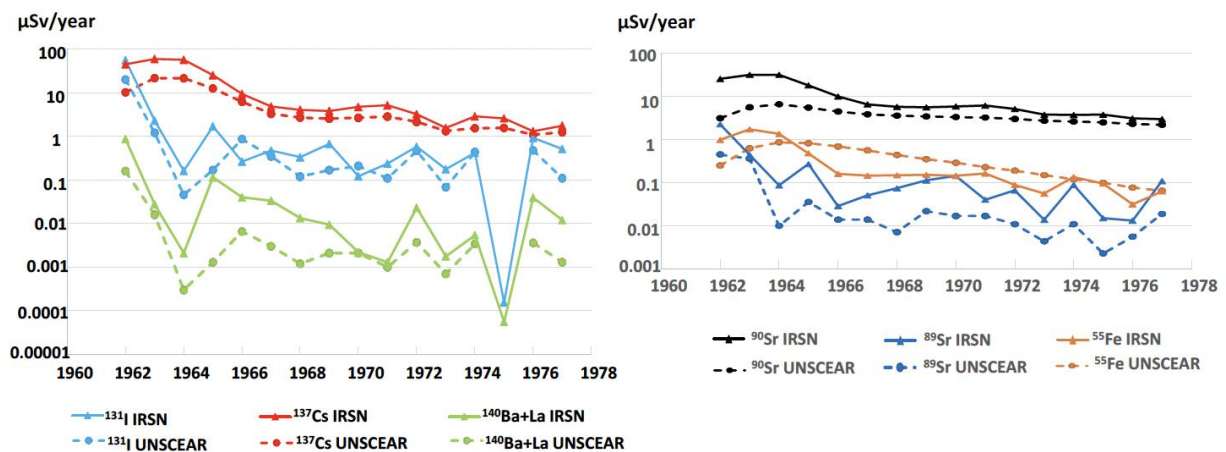


**Figure 48: Comparisons between the annual effective ingested doses for adults estimated by UNSCEAR and those estimated using French data for the 1962-1977 period**

### 9.3. Methodology for reconstructing records of effective doses by ingestion and doses to organs by age group, 1945-2020

The first objective is to expand the period for estimating doses by ingestion to the periods before and after those studied using French data, i.e. from 1945 to 1961 and from 1977 to 2020. For the six radionuclides where the UNSCEAR 2000 report provides dosimetric evaluations from 1945 to 1999, this expansion is achieved by correcting these doses using the deviations observed compared to the IRSN estimates for the 1962-1977 period. Table XXII shows, for each radionuclide, the corrective factors applied to the UNSCEAR dosimetric estimates. For example, the effective dose by ingestion of  $^{90}\text{Sr}+$  for an adult in France is obtained by dividing by 0.5 the corresponding dose provided by UNSCEAR.

**Table XXII: Ratio of effective ingested dose estimates for adults provided by UNSCEAR to those estimated in this study (UNSCEAR/IRSN).**

<sup>131</sup> I	<sup>140</sup> Ba+	<sup>89</sup> Sr	<sup>90</sup> Sr+	<sup>137</sup> Cs+	<sup>55</sup> Fe
0.7	0.3	0.3	0.5	0.6	1.9

For the other radionuclides, the complete dosimetric records from 1945-1999 were reconstructed using the ratio of the estimated doses for the radionuclide in question to those due to <sup>137</sup>Cs: in 1962 for the 1945-1961 period, and average from 1976-1977 for the 1978-1999 period (see Table XXIII). The use of two distinct values for the two periods is justified by the fact that the ratio changes significantly between 1962 and 1977 for short-lived radionuclides (<sup>103</sup>Ru+, <sup>95</sup>Zr+, <sup>141</sup>Ce, and <sup>91</sup>Y).

**Table XXIII: Isotopic ratios of ingested doses estimated for the period 1962-1977 for different radionuclides compared to that of <sup>137</sup>Cs+**

<sup>103</sup> Ru+	<sup>106</sup> Ru+	<sup>95</sup> Zr+	<sup>54</sup> Mn	<sup>144</sup> Ce+	<sup>141</sup> Ce	<sup>91</sup> Y	<sup>125</sup> Sb	<sup>238</sup> Pu	<sup>239+240</sup> Pu	<sup>241</sup> Pu	<sup>241</sup> Am
Cs/Rni ratio 1962											
35	4	19	55	3	75	6	66	4500	120	490	5600
Cs/Rni average ratios in 1976-1977											
149	5	68	65	4	140	17	75	5500	150	640	5800

Only nine sufficiently long-lived radionuclides induced significant doses by ingestion beyond 1999: <sup>3</sup>H, <sup>14</sup>C, <sup>90</sup>Sr+, <sup>137</sup>Cs+, and the actinides.

The doses due to the ingestion of actinides are negligible, around one thousandth of the total ingested doses of all radionuclides combined over the 1961-1978 period. This results from the very low deposits of these radionuclides, their very low level of root uptake, and a virtually non-existent transfer to foods of animal origin. Despite a very limited number of measurement results (the specific activities of actinides in foodstuffs are often too low to be measured), the annual dose by ingestion of actinides was estimated at less than 50 nSv/year over the 2008-2018 period (IRSN 2022a).

Ingested doses due to <sup>137</sup>Cs+ from the fallout of nuclear tests are only estimated in this study until 1985. Starting from 1986, these doses were mainly due to the fallout of the Chernobyl accident over most of the country. This is why the exposure of the population linked to ingestion of this radionuclide since 1985 is estimated in the context of the fallout from the accident.

The ingested doses of <sup>90</sup>Sr+ for 1978-2020 were estimated by linear interpolation between that of 1978 and those estimated on the basis of measurement results acquired over the 2008-2020 period (IRSN, 2022). There was a good level of concordance between these estimates and those of UNSCEAR for the 1978-1999 period.

Ingested doses of <sup>14</sup>C and <sup>3</sup>H from 1953-2020 were estimated using the specific and surface activities of foodstuffs established in section 6.7.

For children of different age groups, the effective doses by ingestion over the periods 1945-1961 and 1978-1999 were calculated by applying to the UNSCEAR estimates for adults, the ratio of the effective doses for each age group to that calculated for an adult over the 1962-1977 period using French data. Table XXIV shows these "child/adult" ratios for the different age groups. These ratios result from the

antagonistic effects of DPUIs, higher for children than for adults and quantities of food consumed, lower for children than for adults. In the case of adolescents aged 13-17 years, food intake identical to those of adults and DPUIs very similar to those of adults, result in ratios close to 1.

Since the effective doses are known per radionuclides and per age group, the doses to the organs only differ by the DPUI value.

**Table XXIV: Ratios of effective doses for each age group to doses for adults, calculated over the period 1962-1977**

	<sup>103</sup> Ru	<sup>106</sup> Ru	<sup>95</sup> Zr	<sup>54</sup> Mn	<sup>144</sup> Ce	<sup>141</sup> Ce	<sup>140</sup> Ba	<sup>137</sup> Cs	<sup>90</sup> Sr	<sup>14</sup> C
0-1 year/adult	0.64	0.98	0.01	0.14	0.21	0.14	1.70	0.52	2.23	0.45
1-2 years/adult	3.01	2.91	2.75	1.46	2.92	3.25	3.99	0.41	1.47	1.88
3-7 years/adult	2.12	2.07	2.16	1.38	2.15	2.39	2.36	0.37	1.03	0.75
8-12 years/adult	1.59	1.58	1.57	1.29	1.57	1.65	1.74	0.53	1.55	1.10
13-17 years/adult	0.97	0.91	1.01	0.86	0.93	0.97	1.08	0.69	1.96	1.02
	<sup>131</sup> I	<sup>89</sup> Sr	<sup>91</sup> Y	<sup>55</sup> Fe	<sup>125</sup> Sb	<sup>238</sup> Pu	<sup>239+240</sup> Pu	<sup>241</sup> Pu	<sup>241</sup> Am	<sup>3</sup> H
0-1 year/adult	0.89	5.22	0.18	0.52	1.01	1.49	1.44	1.00	0.03	2.68
1-2 years/adult	4.96	4.18	3.24	2.24	2.54	0.79	0.77	0.54	0.79	2.14
3-7 years/adult	3.01	2.06	2.30	2.75	1.91	0.81	0.80	0.69	0.83	1.40
8-12 years/adult	1.92	1.67	1.66	2.40	1.47	0.78	0.80	0.79	0.83	1.10
13-17 years/adult	1.26	1.15	0.92	1.68	0.92	0.71	0.71	0.74	0.75	1.00

## 9.4. Estimated effective doses by ingestion, 1945-2020

The annual effective doses received by ingestion by adults change greatly over time (see Figure 49). In the 1940s, they fluctuated from 0.03 to 0.4 µSv/year, then increased to 2.8 µSv in 1951 and 48 µSv in 1958. Following the moratorium on nuclear testing in 1959, they fell slightly before rising sharply to 186 µSv in 1962 and 211 µSv in 1963, with the resumption of Soviet and then American testing. As a result of the cessation of US and Soviet nuclear tests in June 1963, these doses by ingestion decreased rapidly to around 20 µSv in the late 1960s. The fallout from the Chinese tests induced fluctuations throughout the 1970s, between 8 and 20 µSv/year depending on the year. After the cessation of Chinese tests in 1980, they decreased very regularly from 7 to 2 µSv/year in 2020.

The respective contributions of the different radionuclides also change over time and two major periods can be distinguished. Until 1963, and especially during the years of intense fallout (1958, 1961, and 1962), <sup>131</sup>I was the major contributor to ingested doses. It was followed by <sup>144</sup>Ce+ and <sup>106</sup>Ru+. From 1964, the fallout from Chinese tests was lower; <sup>137</sup>Cs+ and <sup>90</sup>Sr+ that accumulated in the soil were transferred to plants by root uptake and then to the entire food chain. Figure 49 shows the dose due to <sup>137</sup>Cs+ in 1985: 0.75 µSv/year. This dose, already low compared to those due to <sup>90</sup>Sr+ and <sup>14</sup>C, has certainly decreased approaching 2020, but we cannot use values after 1985 because, from 1986, <sup>137</sup>Cs+ present in the French environment mainly comes from the fallout of the Chernobyl accident in most of the country. It is not possible to differentiate it from the <sup>137</sup>Cs+ due to nuclear testing. This is why, by design, the doses received by ingestion of this radionuclide from 1986 onwards are estimated in the context of consequences of this accident and not in the context of this study. Since the late 1980s, ingested doses related to persistence in the environment of the fallout of nuclear tests have been due to <sup>90</sup>Sr+ and <sup>14</sup>C. Those of <sup>14</sup>C are constantly decreasing and the same is true of the <sup>90</sup>Sr+ doses. The fact

that the annual doses due to ingestion of  $^{90}\text{Sr}+$  are presented as constant from 2008 to 2018 (1.3  $\mu\text{Sv}/\text{year}$ ) results from the fact that this dose was estimated using all available data over this decade. It would take several years of analysis to make a new estimate.

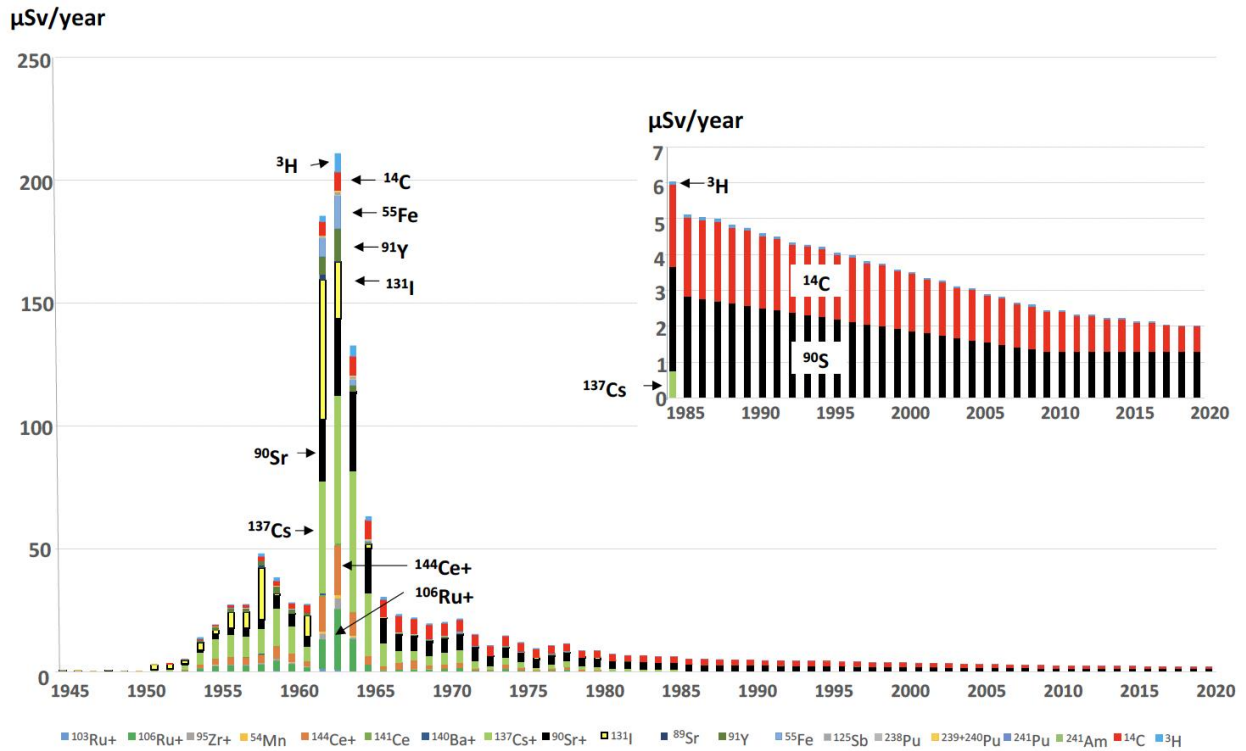


Figure 49: Estimated annual effective doses received by ingestion of foodstuffs for an adult between 1945 and 2020 ( $\mu\text{Sv}$ ) and contribution of the various radionuclides

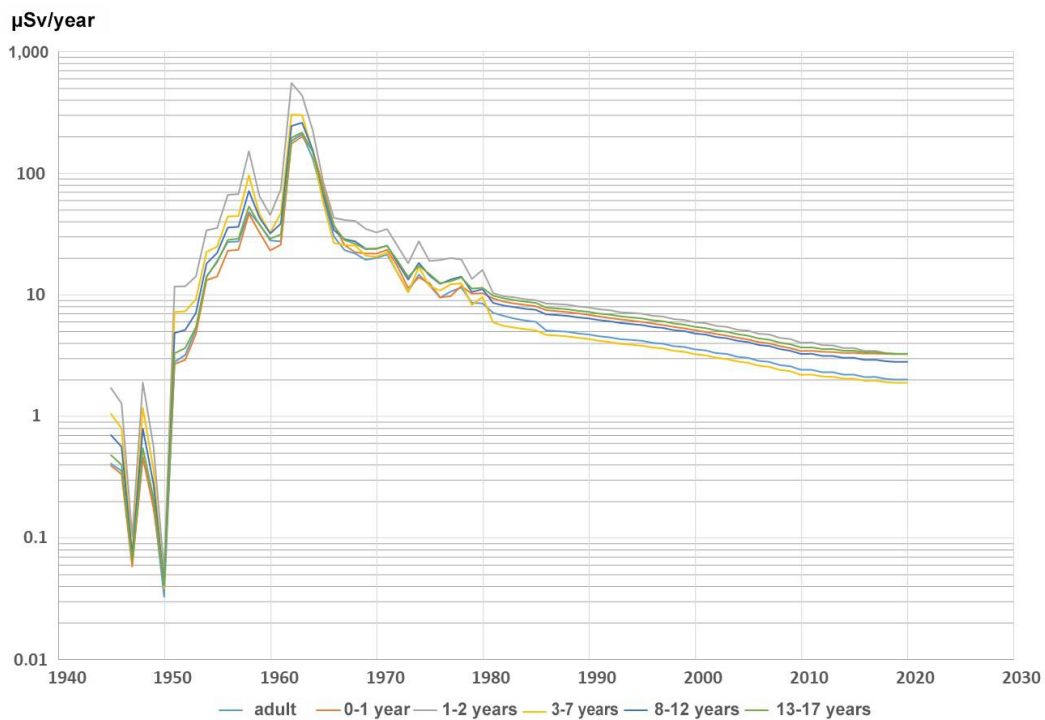
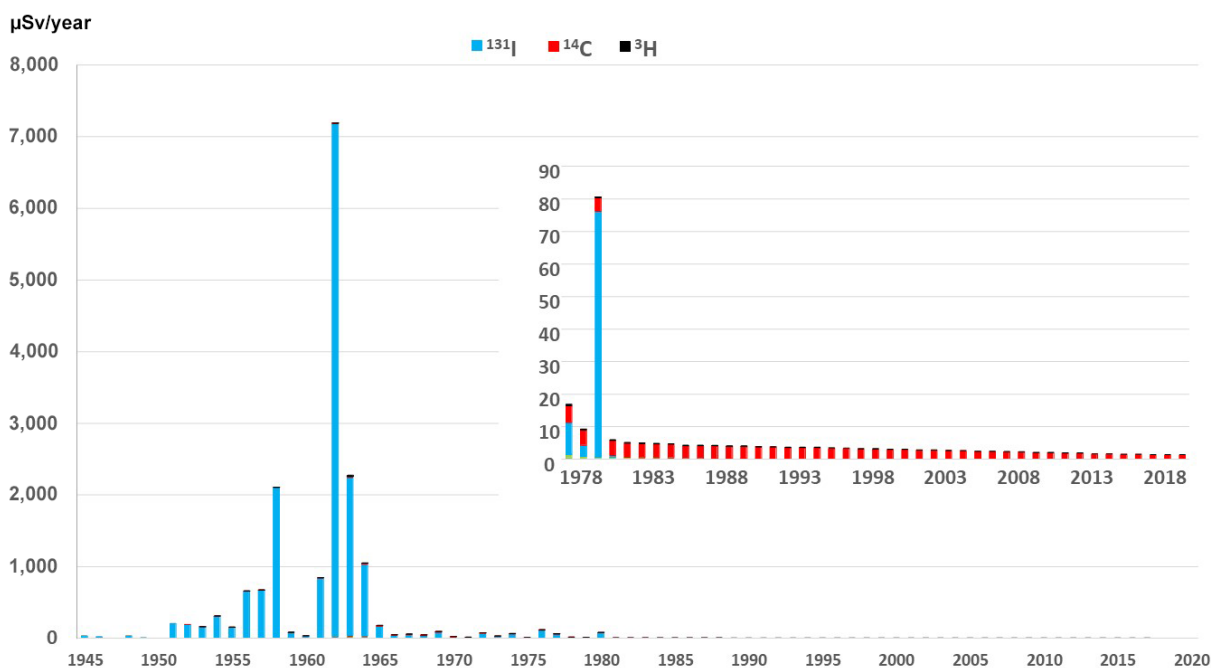


Figure 50: Comparison of estimated doses received by ingestion for various ages ( $\mu\text{Sv}/\text{year}$ )

Figure 50 compares the estimated doses by ingestion for the different age groups. As expected, the estimated doses for children 1-2 years old are the highest over the entire 1945-2020 period. They reached 550  $\mu\text{Sv}$  in 1963, 2.6 times higher than those of adults. This results from higher DPUs that are not completely compensated for by the smaller amounts of food consumed by children. Doses by ingestion for infants are the lowest due to consumption limited to 800 g/d of milk. The largest differences between these two populations and, in general, between the different age groups, are related to the contribution of  $^{131}\text{I}$  in the doses by ingestion. The greater the contribution of  $^{131}\text{I}$ , the greater the inter-age differences. Until the mid-1980s, the estimated doses for adolescents (13-17 years old) were very close to those estimated for adults. From the 1980s onward, doses to adolescents were twice as high as those to adults because of the difference in DPUs of  $^{90}\text{Sr}+$  between these two age groups, due to the development of the skeleton in adolescents.

The highest doses to the thyroid are also those estimated for children 1 to 2 years old; they reached 7200  $\mu\text{Sv}/\text{year}$  in 1962 for this age group (see Figure 51). Those estimated for children 3 to 7 years old are 1.6 to 2 times lower, and those for children 4 to 8 years old are 1.7 to 3 times lower. The doses to the thyroid of infants are the lowest: five to seven times lower than those estimated for children from 1 to 2 years old. As with doses received by inhalation, the doses to the thyroid resulting from ingestion were due mainly to  $^{131}\text{I}$  up to 1963, or almost exclusively due to  $^{131}\text{I}$  during years of intense fallout. During Chinese testing (1964-1980), the contribution of  $^{131}\text{I}$  remained most often predominant, ahead of  $^{14}\text{C}$ ,  $^3\text{H}$ , and  $^{137}\text{Cs}$ . After the fallout from nuclear tests ended, doses to the thyroid by ingestion of foodstuffs have mainly been due to  $^{14}\text{C}$  with a small contribution of  $^3\text{H}$ .



**Figure 51: Estimated doses to the thyroid by ingestion of foodstuffs for children 1 to 2 years old ( $\mu\text{Sv}/\text{year}$ )**

Doses to the brain and prostate are significantly lower than the effective doses. The highest, those of adults, reached a maximum in 1963 of 80  $\mu\text{Sv}$  and 65  $\mu\text{Sv}$  respectively, or around three times lower than the effective doses. After 1963, the highest doses to the brain and breasts were those of children aged 1 to 2 years. Until 1965 the main contributor was  $^{137}\text{Cs}+$  followed by  $^{14}\text{C}$ ,  $^3\text{H}$ ,  $^{55}\text{Fe}$ , and  $^{106}\text{Ru}+$ . From 1966, the contribution of  $^{14}\text{C}$  became predominant and increased to 94% in 2020.

Effective doses to the prostate have many similarities with those to the breasts and brain. The highest were those of adults until 1963, with a maximum of 130  $\mu\text{Sv}$  that year. From 1964, the highest were those of children aged 1 to 2 years. The main contributing radionuclides are the same, with however a contribution of  $^{55}\text{Fe}$  close to that of  $^{137}\text{Cs}+$ , especially for adults (40% and 42% respectively in 1963). After the end of the Chinese tests,  $^{14}\text{C}$  also became the main contributor to the doses to the prostate resulting from the ingestion of foodstuffs. There are also many similarities between doses to the lungs and those to the prostate. However, in the case of doses to the lungs, the highest until 1963 were those of children aged 0 to 1 year, which reached 130  $\mu\text{Sv}$  that year, and the contribution of  $^{55}\text{Fe}$  was much less significant.

Doses to the colon received by ingestion are clearly different from those previous (see Figure 52). They are twice as high (for children from 0 to 1 year old) to eight times higher (for children from 1 to 2 years old) than the effective doses, and reach 1,730  $\mu\text{Sv}$  in 1963 for the latter age group. During the fallout from nuclear tests, from 1945 to 1980, the main contributing radionuclides were  $^{144}\text{Ce}+$ ;  $^{91}\text{Y}$ ,  $^{106}\text{Ru}+$ ,  $^{90}\text{Sr}+$ , and  $^{89}\text{Sr}$  with differing relative significance according to age. The contribution of  $^{90}\text{Sr}+$  increased gradually over the years, as did that of  $^{14}\text{C}$ . From 1980, doses to the colon received by ingestion were mainly due to these two radionuclides, with majority contribution from  $^{90}\text{Sr}+$ .

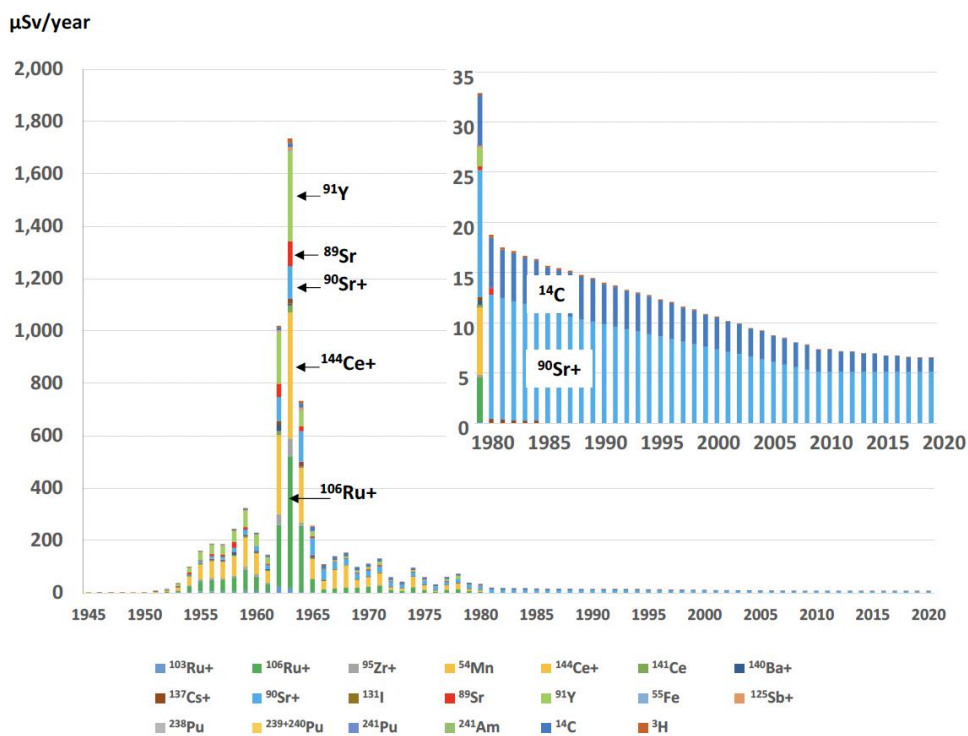
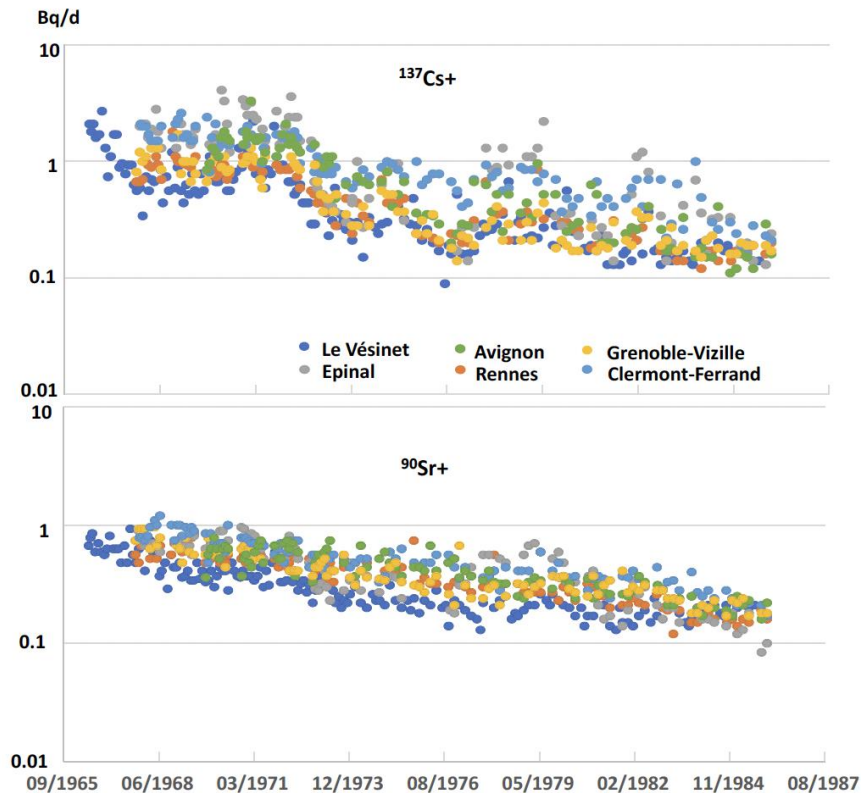


Figure 52: Estimated doses to the colon by ingestion of foodstuffs for children 1 to 2 years old ( $\mu\text{Sv/year}$ )

## 9.5. School lunch measurement results; element of validation for ingested doses and geographical variability

From 1966 to 1985, analyses of  $^{137}\text{Cs}+$  and  $^{90}\text{Sr}+$  were carried out on the contents of lunch trays taken from schools with adolescent students from seven cities in France: Le Vésinet, Epinal, Rennes, Grenoble, Clermont-Ferrand, Bordeaux, and Avignon. The measured activities expressed in Bq/tray

were multiplied by 2.5 to take into account the evening meal and small meals (breakfast and snack) and to obtain daily incorporated activities (Bq/d). These results are shown in Figure 53. This figure shows that the activities of  $^{137}\text{Cs}+$  incorporated daily by adolescents were more fluctuating than those of  $^{90}\text{Sr}+$ . This can be explained by the fact that the activities of  $^{137}\text{Cs}+$  in foodstuffs are mainly the result of foliar uptake and are therefore highly influenced by the variability of monthly deposits, while those of  $^{90}\text{Sr}+$  are largely the result of root uptake. As a result, the activities of  $^{90}\text{Sr}+$  are much less dispersed than those of  $^{137}\text{Cs}+$ .



**Figure 53: Activities of  $^{137}\text{Cs}+$  and  $^{90}\text{Sr}+$  incorporated daily by adolescents, estimated from analyses of the contents of lunch trays taken from schools**

It is noted that for the two radionuclides, the daily activities incorporated differ depending on the location. Some of these inter-location differences can be explained by the variability of the deposits related to that of the average annual precipitation (see chapters 5.3 and 6). The lowest activities concern Le Vésinet (dark blue circles; average annual precipitation around 660 mm), while the highest activities concern Epinal (grey circles; average annual precipitation around 1,100 mm). As indicated in chapter 6, the influences of farming and animal husbandry practices (in particular related to extensive and intensive livestock farming), as well as soil characteristics must be considered as well.

These incorporated activities, directly derived from measurement results, can be compared to those calculated from the selected food intake and estimated specific activities and activity concentrations in foodstuffs. This is the purpose of Figure 54 which compares the activities of  $^{137}\text{Cs}+$  and  $^{90}\text{Sr}+$  incorporated daily from the school lunch measurements with those used for the estimates of doses by ingestion for Le Vésinet and Epinal. The results of the model for Epinal are deduced from those estimated for Le Vésinet by applying the ratio of the average annual precipitation between these two locations (1,100 mm/660 mm = 1.7) as recommended in chapter 5.3.

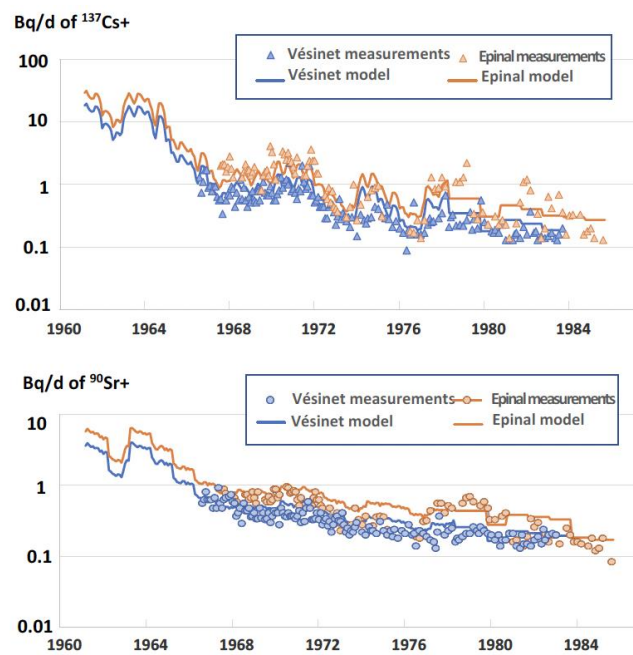


**Figure 54: Comparison of the daily incorporated activities of  $^{137}\text{Cs}+$  and  $^{90}\text{Sr}+$  deduced from the measurements on the contents of school lunches and those corresponding to the ingested doses estimated in this study (Bq/d)**

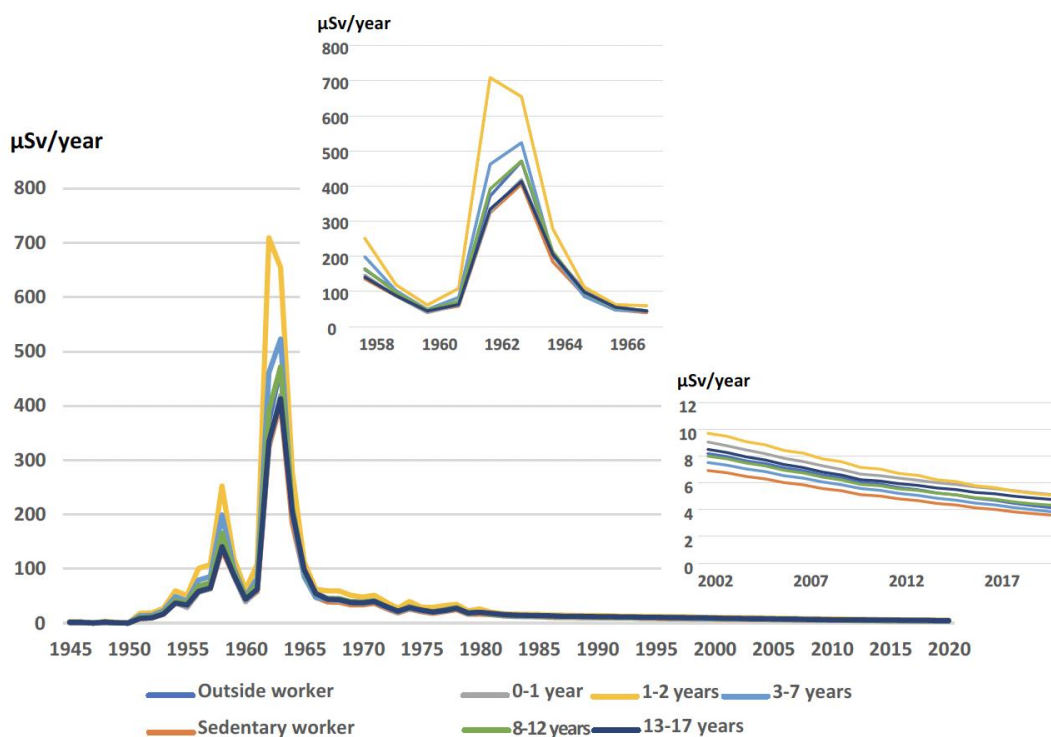
The graphs show that the two estimates are consistent for Le Vésinet and for Epinal, for both  $^{137}\text{Cs}+$  and  $^{90}\text{Sr}+$ . In the case of Le Vésinet, the results of the model are 30% higher than those from the school lunch measurements (35% for  $^{137}\text{Cs}+$  and 28% for  $^{90}\text{Sr}+$ ). In the case of Epinal, the overestimation of the model is also 30% for  $^{90}\text{Sr}+$  while it is only 6% for  $^{137}\text{Cs}+$ .

These deviations are small compared to the assumptions and sources of variability (and therefore uncertainties), inherent in both approaches. The measurements carried out on the contents of school lunches constitute an element of validation of the doses by ingestion for the two radionuclides concerned ( $^{137}\text{Cs}+$  and  $^{90}\text{Sr}+$ ), and more generally for the total doses received by ingestion. As a reminder, apart from years of intense fallout (for which  $^{131}\text{I}$  is the predominant contributor to effective ingested doses), these two radionuclides contribute predominantly, or even very predominantly (up to nearly 70%), to the total doses received by ingestion, all radionuclides combined. Finally, these school lunch analyses also validate the selected food intake, and therefore partially the calculations of doses by ingestion relating to the other radionuclides.

## 10. Total doses, all exposure pathways combined

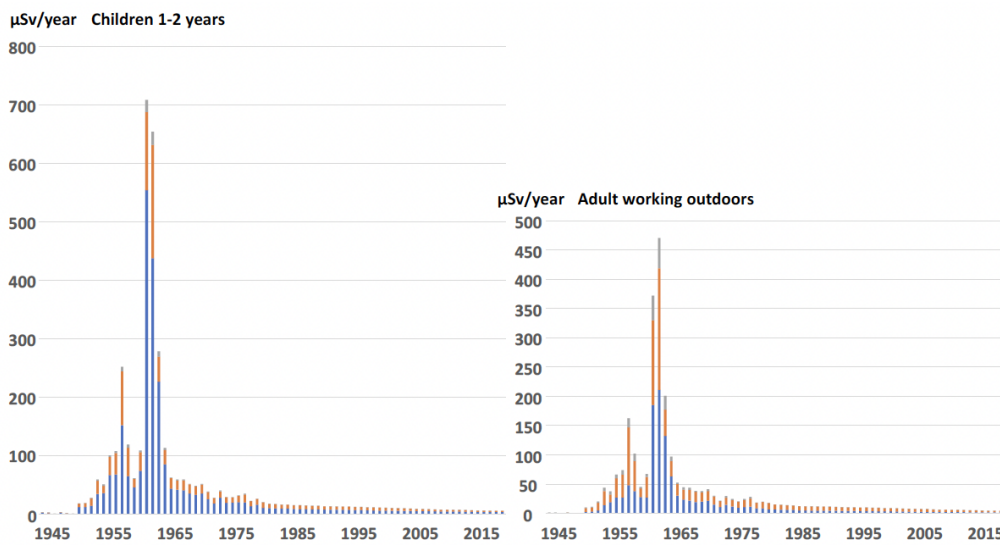
### 10.1. Variability by age and contribution of exposure pathways

Figure 55 shows the total annual effective doses, all exposure pathways combined, from 1945 to 2020 for the Le Vésinet site. Whatever the period considered, children from 1 to 2 years old are always those for whom the estimated doses are the highest, followed by children from other age groups; the estimated doses for adults, especially for sedentary adults, are the lowest. This results from the dominance of doses related to the ingestion of foodstuffs in the total effective doses as shown in Figure 56. While for adults the ingestion of foodstuffs contributes between 30% and 70% of the total effective doses depending on the year, for children 1 to 2 years old, this contribution ranges from 50% to 80% (in 1963).



**Figure 55: Comparison of estimated effective doses for different age groups of people residing in Le Vésinet ( $\mu\text{Sv}/\text{year}$ )**

Depending on age, the effective doses were highest in 1962 or 1963, reaching 710  $\mu\text{Sv}$  for children 1 to 2 years old in 1962 and 470  $\mu\text{Sv}$  for adults in 1963, in Le Vésinet. In 2020, the effective doses related to the persistence of the fallout from atmospheric tests of nuclear weapons were between 3.5  $\mu\text{Sv}$  for adults and 5  $\mu\text{Sv}$  for young children. For adults, this estimate is consistent with that previously made by IRSN based on measurement results for 2008-2018: 2.4  $\mu\text{Sv}$ , excluding the contribution of  $^{137}\text{Cs}$  considered as mainly due to the fallout of the Chernobyl accident (IRSN, 2022).



**Figure 56: Total effective annual doses with contributions of the different exposure pathways (µSv/year): doses received by ingestion are blue, external doses are orange, and doses received by inhalation are green.**

## 10.2. Spatial variability

Figure 57 illustrates the spatial variability, within mainland France, of effective doses for adults working outdoors and children from 1 to 2 years old, across the communes of Le Vésinet (660 mm of annual precipitation), representative of areas of the territory least affected by the fallout from nuclear tests, and Méaudres (1,400 mm), representative of the municipalities where doses due to these fallouts were among the highest in France. Overall, the spatial variability at the scale of mainland France is around a factor of 2.

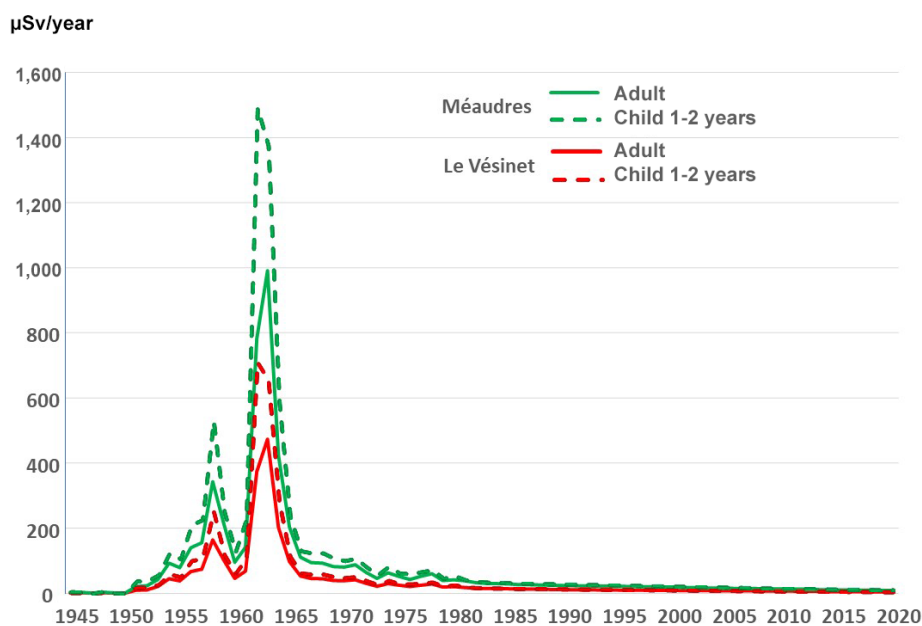


**Figure 57: Illustration of the range of spatial variability, at the scale of mainland France, of estimated effective doses for adults and children aged 1 to 2 years (µSv/year)**

For the children of Méaudre, the effective doses reached 1,500  $\mu\text{Sv}$  in 1962 compared to 700  $\mu\text{Sv}$  in Le Vésinet that same year. For adults working outdoors, effective doses were estimated at 1,000  $\mu\text{Sv}$  in Méaudre in 1963 as opposed to 470  $\mu\text{Sv}$  in Le Vésinet.

### 10.3. Discussion of organ doses

Figure 58 shows the estimated effective and organ-equivalent doses for adults (left-hand graph) and children 1 to 2 years old (right-hand graph). The thyroid-equivalent doses are highest over the entire duration of atmospheric fallout (1945-1980) due to the presence of  $^{131}\text{I}$  in the environment, ahead of the doses to the colon. After 1980, doses to the colon were the highest. Doses to the lungs, breasts, brain, and prostate are significantly lower than the effective doses. The doses relating to these last three organs are very similar and are the lowest.

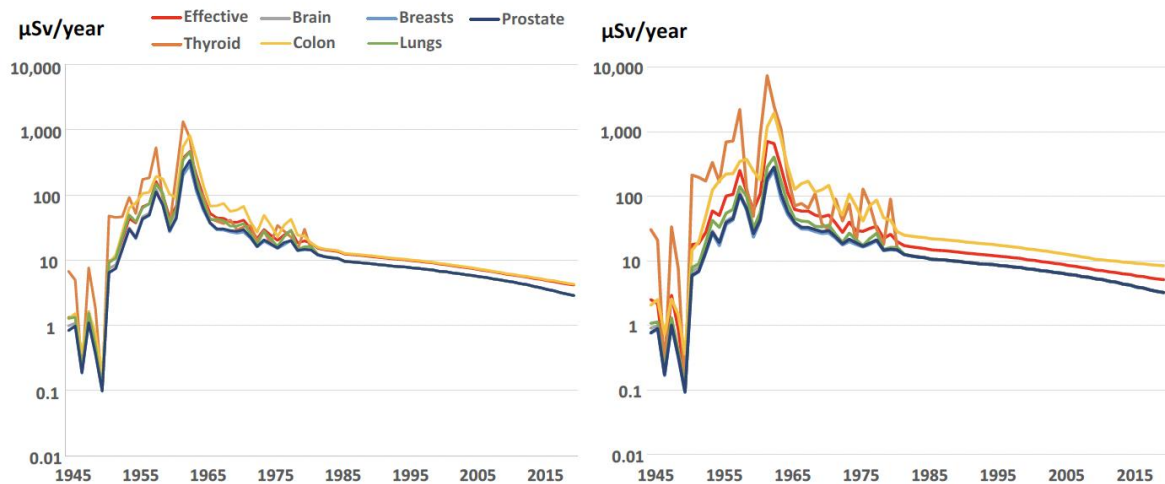


**Figure 58: Comparison of the various types of estimated annual doses for adults (left-hand graph) and children 1 to 2 years old (right-hand graph)**

Regardless of age, doses to the brain, breasts, and prostate are predominantly, or even mainly, the result of external exposure, especially for adults working outdoors, but also for very young children. The second contribution for these organs is that of ingestion, the contribution of inhalation being very small, or even negligible.

The contribution of external exposure remains predominant in doses to the lungs. During atmospheric fallout, it is followed by inhalation, which is predominant for sedentary adults, with the contribution of ingestion to doses to the lungs being lower. From 1980, after fallout ended, the contribution of inhalation ceased and doses to the lungs predominantly resulted from external exposure. The contribution of ingestion became minor, then negligible from the 2000s.

During atmospheric fallout, nearly two-thirds of the doses to the colon resulted from ingestion for adults. For children, this proportion is around 80% during the fallout period (1950-1980) and reaches 90% in some years of intense fallout.

Finally, during atmospheric fallout, doses to the thyroid mainly result from the ingestion of foodstuffs in connection with the presence of  $^{131}\text{I}$  in the environment. This is notably the case for children, for whom other exposure pathways are negligible. Starting from the 1980s, doses to the thyroid were much lower and resulted, in almost equal parts, from ingestion and external exposure.

## 11. Conclusion

The processing of nearly 50,000 measurement results acquired in mainland France, mainly between June 1961 and July 1978, allowed us to reconstruct the records of activities in the air, deposited on the ground, and in the main types of foodstuffs, of about 20 radionuclides from the fallout of atmospheric tests of nuclear weapons. These measurement records were supplemented by various parametric studies and modelling. From these records, effective monthly and organ doses were estimated for adults and children of different age groups residing in Le Vésinet (Paris region) during this period, for the three types of exposure considered: exposure by inhalation<sup>16</sup> of radionuclides in the air, external exposure to radioactive deposits<sup>17</sup>, and exposure by ingestion of contaminated foodstuffs. The doses resulting from the ingestion of contaminated foodstuffs, which predominated from 1961-1978, could also be partially validated by the results of measurements carried out on school lunches.

Comparison of the annual effective doses estimated by UNSCEAR for adults living in the northern hemisphere and those estimated in this study using French data shows a very good level of concordance of the doses received by inhalation. This concordance results from the doses of activities in air, also shown, and the isotopic activity ratios established in this study compared to those mentioned by UNSCEAR. On the other hand, the doses due to external exposure to deposition and ingestion of foodstuffs, estimated by this study for Le Vésinet, are twice as high as those estimated by UNSCEAR. This is a consequence of deposited activities that were twice as high. This difference is most likely due to annual rainfall in France, which, under oceanic influence, is higher than the average for the northern hemisphere.

This dependence of the deposited activities, as well as the resulting external and ingested doses, on the average annual precipitation levels for the territory, has also been shown using different approaches, which have given consistent results. This study of the relationship between precipitation, radioactive deposits, and doses therefore made it possible to spatialize these doses at the scale of the territory by providing estimates by municipality and by year.

The ratios of the doses estimated from French data to those estimated by UNSCEAR for each exposure pathway and for different radionuclides over the period 1961-1978, were used to adapt the doses provided by UNSCEAR to the characteristics of fallout in France in order to have an estimate for the periods 1945-1960 and 1979-1985 (period during which there is no data available for France).

The records of measurements for long-lived radionuclides ( $^3\text{H}$ ,  $^{14}\text{C}$ ,  $^{137}\text{Cs}$ ,  $^{90}\text{Sr}$ ,  $^{238}\text{Pu}$ ,  $^{239+240}\text{Pu}$ ,  $^{241}\text{Pu}$ , and  $^{241}\text{Am}$ ) carried out by IRSN (IPSN before 2004), or from the literature (for  $^3\text{H}$  and  $^{14}\text{C}$  in particular), provide the doses received by inhalation up to 2020. The external and ingested doses between 1999

---

<sup>16</sup> And by transcutaneous transfer in the case of  $^3\text{H}$

<sup>17</sup> External exposure to airborne radionuclides is negligible, including from inhalation

(last year of UNSCEAR's estimate) and 2008, were obtained by interpolation between UNSCEAR's and IRSN's estimates based on measurement results acquired from 2008 to 2018 (IRSN, 2022).

This study therefore provides estimates of effective doses and organ doses for the different age groups by municipality and by year, meeting the needs of the CORALE project. These doses were discussed in terms of their evolution over time, contributing radionuclides, differences according to the age of the individuals and places of residence.

## 12. Bibliography

Beninson D. (1972), Migliori de Beninson A. & Menossi C.: Fallout radiactivo debido a las explosiones en el Pacifico Sur en el período 1966-1970. (*Radioactive fallout due to explosions in the South Pacific, 1966-1970*) Comisión Nacional de Energía Atómica, Buenos Aires, report CNEA-321

Bunzl K. & Kracke W. (1988), Cumulative deposition of  $^{137}\text{Cs}$ ,  $^{238}\text{Pu}$ ,  $^{239+240}\text{Pu}$  and  $^{241}\text{Am}$  from global fallout in soils from forest, grassland and arable land in Bavaria (FRG), *Journal of Environmental Radioactivity* 8: p 1-14.

Calmon P (2017): Etude de faisabilité de l'opérationnalisation des enquêtes alimentaires. (*Feasibility study of the operationalization of food surveys.*) Report IRSN-PRP-ENV/SESURE 2017-22.

Cohenny E (2019): Enquête alimentaire autour du centre de Cadarache ; résultats et analyse. (*Food survey around the Cadarache facility; results and analysis.*) Report CEA/DEN/CAD/DTN/SMETA/LMTE/NT/2019-15.

Goldberg M. et al. (2017): CONSTANCES: a general prospective population-based cohort for occupational and environmental epidemiology: cohort profile. *Occupational and environmental medicine* (2017) 74:66-71.

Hölgge Z. & Filgas R. (1995), Inventory of  $^{238}\text{Pu}$  and  $^{239+240}\text{Pu}$  in the soil of Czechoslovakia in 1990, *Journal of Environmental Radioactivity* 27: p 181-189.

IAEA (1979): International Atomic Energy Agency. Planning for Off-site Response to radiation Accidents in Nuclear Facilities (IAEA-TECDOC-225).

IAEA (2000): International Atomic Energy Agency. Generic Procedures for Assessment and Response during a Radiological Emergency (IAEA-TECDOC-1162).

IAEA (1999): International Atomic Energy Agency. Assessment of dose to the public from ingested radionuclides. Safety reports series No. 14.

ICRP (2020) International Commission on Radiological Protection: Dose coefficients for external exposures to environmental sources. ICRP publication No. 144. 2020.

ICRP (1990) - International Commission on Radiological Protection: Recommendations of the International Commission on Radiological Protection; ICRP publication No. 60. 1990.

ICRP (1994) - International Commission on Radiological Protection: Human Respiratory Tract – Model for Radiological Protection; ICRP Publication No. 66; Volume 24 No. 1-3. 1994

IRSN (2022b) - Institute for radiation protection and nuclear safety Etude radiologique de l'environnement de la centrale de Saint-Alban Saint-Maurice, acquisition d'informations concernant les variables humaines d'exposition ; résultats des enquêtes sur les habitudes alimentaires et sur les déplacements quotidiens des riverains. (*Radiological study of the environment at the Saint-Alban Saint-Maurice power plant, acquisition of information on human exposure variables; results of surveys on eating habits and daily movements of local residents.*) IRSN Report 2022-00145.

IRSN (2021) - Institute for radiation protection and nuclear safety: Bilan de l'état radiologique de l'environnement français de 2018 à 2020. (*Assessment of the radiological state of the French environment from 2018 to 2020.*) IRSN Report 2021-00765.

Radiological consequences of fallout from atmospheric tests of nuclear weapons in mainland France - Environmental contamination and exposure of the population

IRSN Report no. 2024-00559

IRSN (2022a) - Institute for radiation protection and nuclear safety: Le bruit de fond des radionucléides artificiels dans l'environnement français métropolitain. (*Background noise of artificial radionuclides in the environment of mainland France.*) IRSN Report 2022-00131

Lawrence Livermore National laboratory (2016) - Dillon D., Kane J., Nasstrom J., Homann S and Brenda P.: Summary of Building Protection Factor Studies for External Exposure to Ionizing Radiation. LLNL-TR-684121.

Le Roux G., (2009) Duffa C., Vray F., Renaud Ph. Deposition of Artificial Radionuclides from Atmospheric Nuclear Weapon Tests Estimated by Soil Inventories in French Areas Low-Impacted by Chernobyl. *Journal of Environmental Radioactivity* 101: 211–218. 2009.

Mitchell P. I., (1990) Sanchez-Cabeza J. A., Ryan T. P., McGarry A. T., Vidal-Quatras A., Preliminary estimates of cumulative caesium and plutonium deposition in the Irish terrestrial environment, *Journal of Radioanalytical and Nuclear Chemistry*, Articles 138: p 241-256.

Morin M. (2022): Détection des essais nucléaires atmosphériques chinois par les stations aérosols du SCPRI ; Rapport IRSN 2022-00471. (*Detection of Chinese atmospheric nuclear tests by SCPRI aerosol stations; IRSN report 2022-00471.*)

JO (2003): Journal Officiel de la République Française relatif aux modalités de calcul des doses efficaces et des doses équivalentes résultant de l'exposition des personnes aux rayonnements ionisants paru le 13 novembre 2003 et annexé à l'arrêté du 1<sup>er</sup> septembre 2003. (*Official Journal of the French Republic on the methods for calculating effective doses and equivalent doses resulting from the exposure of people to ionizing radiation published on 13 November 2003 and annexed to the decree of 1 September 2003.*)

EPA (2019) -Environmental Protection Agency of the United States: External exposure to radionuclides in air, water and soil; Federal Guidance report No. 15 revised August 2019.

Saitoa K. (2019), Mikamib S., Andohb M., Matsudac M., Kinasec S., Tsudad S., Yoshidae T., Satof T., Sekic A., Yamamotoa H., Sanadag Y., Wainwright-Murakamih H., and Takemiyac H. Summary of temporal changes in air dose rates and radionuclide deposition densities in the 80 km zone over five years after the Fukushima Nuclear Power Plant accident. *Journal of environmental radioactivity*; vol 210; December 2019.

Renaud Ph., Louvat D. and Vray F. (2003): les retombées en France des essais atmosphériques d'armes nucléaires ; production, dispersion atmosphérique et dépôt des produits de fission et d'activation. (*The fallout in France from atmospheric tests of nuclear weapons; production, atmospheric dispersion and deposition of fission and activation products.*) Report IRSN/DEI/SRSURE 2003/03 – 2003.

Renaud Ph. et Louvat D. (2004): Magnitude of fission products deposits from atmospheric nuclear test fallout in France. *Health Physics*, 86(4), 353-358. 2004.

Renaud Ph., Champion D. and Brenot J (2007). Les retombées radioactives de l'accident de Tchernobyl sur le territoire français : conséquences environnementales et exposition des personnes. (*Radioactive fallout of the Chernobyl accident in France: environmental consequences and exposure of the population.*) Book from Editions TEC&DOC Lavoisier, collection Sciences et Techniques. 190 pages. ISBN 978-2-7430-1027-0. 2007.

Renaud Ph. (2019): Les transferts des radionucléides dans les chaînes alimentaires : Eléments de radioécologie opérationnelle. (*Transfer of radionuclides in food chains: Elements of operational radioecology.*) Les Techniques de l'Ingénieur. BN3908. 2019.

Radiological consequences of fallout from atmospheric tests of nuclear weapons in mainland France - Environmental contamination and exposure of the population  
IRSN Report no. 2024-00559

Renaud Ph. (2020): Les transferts des radionucléides dans l'air, les sols et les cours d'eau : Eléments de radioécologie opérationnelle. (*Transfers of radionuclides in air, soil, and waterways: Elements of operational radioecology.*) Les Techniques de l'Ingénieur. BN3907. 2020.

Roussel-Debet S. (2007): Evaluation of carbon-14 dose since the end of the 1950s in mainland France. *Radioprotection* 42(3) pp297-313. 2007.

UNSCEAR (2000): Source and Effects of Ionizing Radiation. Volume I: Sources. pp20-287, United Nations, New York.

Vidal M. and Renaud Ph. (2000): estimation des doses à la thyroïde reçues par les enfants en France en 1986 à la suite de l'accident de Tchernobyl et analyse de sensibilité. (*Estimation of thyroid doses received by children in France in 1986 following the Chernobyl accident and sensitivity analysis.*) Technical Note IPSN-SEGR/SAER/00-67.

Vray F. and Renaud Ph. (2004): contamination de la chaîne alimentaire par les produits de fission et d'activation émis lors des essais aériens d'armes nucléaires. (*Contamination of the food chain by fission and activation products emitted during aerial tests of nuclear weapons.*) Report IRSN/DEI/SRSURE 2004/19. 2004.

Vray F. and Renaud Ph. (2006): Évaluation des conséquences dosimétriques des essais aériens d'armes nucléaires en France métropolitaine ; période 1961-1978. (*Assessment of the dosimetric consequences of aerial tests of nuclear weapons in mainland France; 1961-1978.*) Report IRSN/DEI/SESURE No. 2006/03. 2006.

Wild CP (2005):. Complementing the genome with an "exposome": the outstanding challenge of environmental exposure measurement in molecular epidemiology. *Cancer epidemiology, biomarkers & prevention* (2005) 14:1847-1850.

Yoshida-Ohuchia H., Matsudab N. and Saitob K. (2019) - Review of reduction factors by buildings for gamma radiation from radiocaesium deposited on the ground due to fallout. *Journal of Environmental Radioactivity* 210 (2019) 105810.

### 13. APPENDIX 1: Study of activity ratios of short-lived radionuclides.

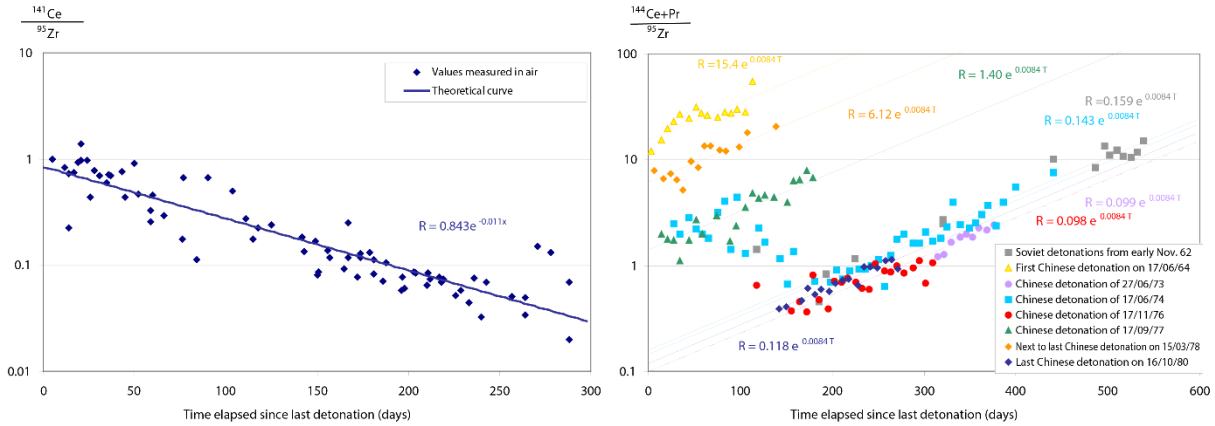


**Figure A1 – Ratio of the activities of cerium and <sup>95</sup>Zr isotopes measured in the air in the Paris region between 1961 and 1978. Evolution according to the age of the contamination**

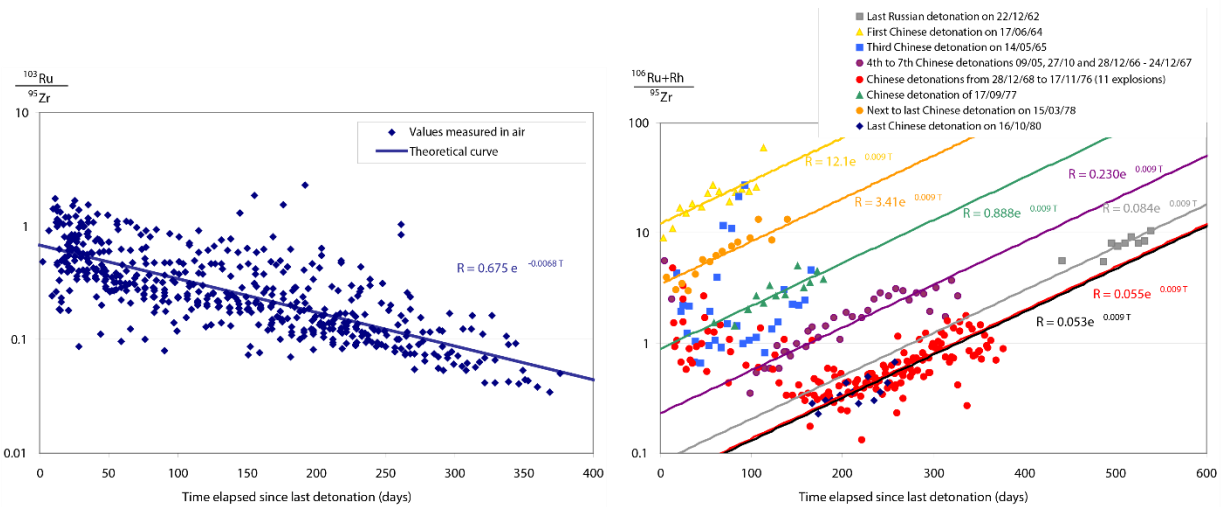


**Figure A2 – Ratio of the activities of ruthenium and <sup>95</sup>Zr isotopes measured in the air in the Paris region between 1961 and 1978. Evolution according to the age of the contamination**

Radiological consequences of fallout from atmospheric tests of nuclear weapons in mainland France -  
 Environmental contamination and exposure of the population  
 IRSN Report no. 2024-00559

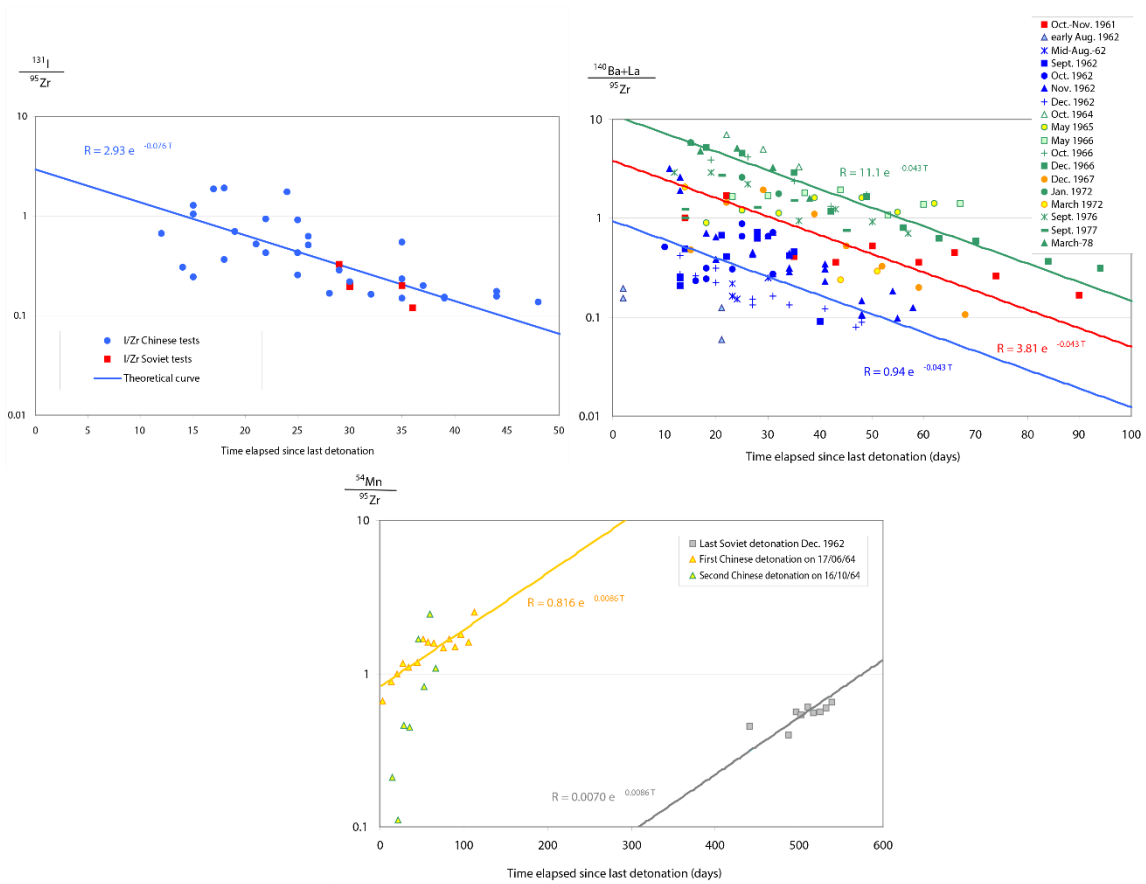


**Figure A3 – Ratio of the activities of  $^{131}\text{I}$ ,  $^{140}\text{Ba}+\text{La}$ , and  $^{54}\text{Mn}$  to  $^{95}\text{Zr}$  measured in the air in the Paris region between 1961 and 1978. Evolution according to the age of the contamination**

## 14. APPENDIX 2: Model of transfer to agricultural plant and animal food products and adjustment of results to the available measurement data

The equations used to model the contamination of products in the food chain are the same for most operational models that calculate the impact of chronic discharges, in particular FOCON (Rommens *et al.*, 1999), but also ABRICOT (Santucci, 1995). For plants, they also correspond to the integration of the expression of contamination following an acute discharge appearing in ASTRAL (Renaud *et al.*, 1999 a and b) or ECOSYS (Müller & Pröhl, 1993).

In the case of an atmospheric intake of radionuclide, considered to be constant over a given time step, the radioactivity of a plant at the end of the time interval  $t$ ,  $C_v(t)$  is expressed in  $\text{Bq kg}^{-1}$  of fresh weight by:

$$C_v(t) = \underbrace{\frac{1}{T_c} \sum_{i=t-T_c}^{i=t} D_i \frac{R_c}{Rdt} f_t \frac{1 - e^{-(\lambda_b + \lambda_p)T_c}}{\lambda_b + \lambda_p}}_{\text{Captation}} + \underbrace{\frac{FT_r}{\mu h} \cdot \sum_{i=0}^{i=t} D_i e^{-(\lambda_s + \lambda_p)(T_t - T_i)}}_{\text{RootUptake}} \quad (3)$$

where:

- $T_c$ : duration of growth of the plant (in days)
- $D_i$ : activity deposited during the time interval  $i$  ( $\text{Bq m}^{-2}$ )
- $R_c$ : capture ratio (dimensionless)
- $Rdt$ : crop yield ( $\text{kg m}^{-2}$  for a crop, weight of fresh plant)
- $f_t$ : translocation factor (dimensionless; its value is 1 in the case of grass or leafy vegetables)
- $\lambda_p$ : physical decay constant of the radionuclide ( $\text{d}^{-1}$ )
- $\lambda_b$ : biomechanical decay constant of the radionuclide for the plant ( $\text{d}^{-1}$ )
- $\lambda_s$ : decay constant of the bioavailable radionuclide in the soil (integrating the phenomena of horizontal and vertical migration as well as the ageing of the radionuclide; in  $\text{d}^{-1}$ )
- $FT_r$ : root uptake factor (in  $\text{kg}$  of dry soil per  $\text{kg}$  of fresh plant);
- $\mu$ : the density of the (dry) soil in place (in  $\text{kg}$  of dry soil per  $\text{m}^3$ ), which was taken equal to  $1,400 \text{ kg m}^{-3}$ , average of 241 measurements archived in the SYLVESTRE database;
- $h$ : the height of the root layer (in  $\text{m}$ );
- $T_i$ : duration in days at the end of the time interval  $i$ .

For vegetables and fruit, crops have been assumed to be continuous over the year, with one vegetable or fruit replacing another. A stoppage of production during the winter was not taken into account as it is too short and the dates vary too widely on the scale of the entire country. Cereal farming, on the other hand, was considered discontinuous, with a single annual harvest.

Transfers to animals (cows) are described by:

$$C_{\text{ani}}(t) = Q_{\text{food}} \times C_{\text{food}}(t) \times FT_{\text{h-ani}} \quad (4)$$

where:

- $C_{\text{ani}}(t)$ : the activity of the animal product in question (milk or meat) in  $\text{Bq kg}^{-1}$  fresh or  $\text{Bq l}^{-1}$
- $Q_{\text{food}}$ : the quantity of food ingested daily ( $\text{kg d}^{-1}$ , fresh weight)
- $C_{\text{food}}(t)$ : the activity of the food during the time interval  $t$  ( $\text{Bq kg}^{-1}$  fresh)
- $FT_{\text{h-ani}}$ : the factor of transfer to the animal product by ingestion of food ( $\text{d kg}^{-1}$  fresh)

In general, the parameter values have been chosen based on the results of available measurements. The suitability of a set of parameter values was tested by studying the ratio of

calculated values to measured values, which must remain close to 1, and by graphical analysis (in order to avoid temporal drifts of the ratio when its average value is close to 1).

In the absence of measurement results or if they are insufficient, the missing parameter values were searched for in the bibliography. Mainly, the default values of the models FOCON (currently CONDOR), ECOSYS, or FARMLAND were used. In all cases, the set of parameters used is reconstructed using these values, considered as references in the literature on the topic.

The values used for the parameters are presented below.

**VALUES USED FOR THE PARAMETERS OF RADIONUCLIDE TRANSFER MODELS IN THE FOOD CHAIN**

	<sup>103</sup> Ru	<sup>106</sup> Ru+Rh	<sup>95</sup> Zr+Nb	<sup>54</sup> Mn	<sup>144</sup> Ce+Pr	<sup>141</sup> Ce	<sup>140</sup> Ba+La	<sup>137</sup> Cs	<sup>90</sup> Sr	<sup>131</sup> I	<sup>89</sup> Sr	<sup>91</sup> Y	<sup>55</sup> Fe	<sup>125</sup> Sb
Physical half-life	39.3 d	372.6 d	64 d	312.2 d	285 d	32.5 d	12.8 d	30 years	28 years	8 d	50.7 d	58.5 d	2.7 years	2.8 years
<b>Leafy vegetables</b>														
Effective soil half-life <sup>(1)</sup>	T.p.	T.p.	T.p.	T.p.	T.p.	T.p.	T.p.	10 years	10 years	T.p.	T.p.	T.p.	T.p.	T.p.
Rc/Rdt (m <sup>2</sup> kg <sup>-1</sup> fresh)	<..... 0.1.....>													
Ft	<..... 1.....>													
Tb (days)	<..... 7.....>													
Tc (days)	<..... 60.....>													
h (cm)	<..... 20.....>													
FTr (kg dry/kg <sup>-1</sup> fresh)	<..... 1E-2.....>		1E-4	4E-2	<..... 1E-3.....>		1E-2	5E-2	9.2E-2	2E-2	9.2E-2	1E-2	2E-4	1E-5
<b>Root vegetables</b>														
Effective soil half-life <sup>(1)</sup>	T.p.	T.p.	T.p.	T.p.	T.p.	T.p.	T.p.	15 years	12 years	T.p.	T.p.	T.p.	T.p.	T.p.
Rc/Rdt (m <sup>2</sup> kg <sup>-1</sup> fresh)	<..... 0.1.....>													
Ft	<..... 0.05.....>		0.2	<..... 0.05.....>		0.2	0.05	0.2	0.05	0.2	<..... 0.05.....>			
Tb (days)	<..... 14.....>													
Tc (days)	<..... 180.....>													
h (cm)	<..... 25.....>													
FTr/μh (m <sup>2</sup> kg <sup>-1</sup> fresh)	<..... 1.5E-2.....>		1E-4	1.5E-2	<..... 1E-3.....>		5E-3	1.5E-2	7E-2	2E-2	7E-2	1E-2	3E-4	5E-5
<b>Fruit Vegetables</b>														
Effective soil half-life <sup>(1)</sup>	T.p.	T.p.	T.p.	T.p.	T.p.	T.p.	T.p.	15 years	12 years	T.p.	T.p.	T.p.	T.p.	T.p.
Rc/Rdt (m <sup>2</sup> kg <sup>-1</sup> fresh)	<..... 0.1.....>													
Ft	<..... 0.05.....>		0.15	<..... 0.05.....>		0.15	0.05	0.15	0.05	0.15	<..... 0.05.....>			
Tb (days)	<..... 14.....>													
Tc (days)	<..... 120.....>													
h (cm)	<..... 25.....>													
FTr (kg dry/kg <sup>-1</sup> fresh)	<..... 7E-3.....>		5E-5	5E-2	<..... 2E-2.....>		3E-2	7E-3	9E-3	2E-2	9E-3	1E-2	3E-2	5E-6
<b>Grains</b>														
Effective soil half-life <sup>(1)</sup>	T.p.	T.p.	T.p.	T.p.	T.p.	T.p.	T.p.	15 years	12 years	T.p.	T.p.	T.p.	T.p.	T.p.
Rc/Rdt (m <sup>2</sup> kg <sup>-1</sup> fresh)	<..... 1.....>													
Ft	<..... 0.01.....>		0.15	<..... 0.01.....>		0.2	0.15	0.15	0.15	0.15	<..... 0.01.....>			
Tb (days)	<..... 14.....>													
Tc (days)	<..... 120.....>													
h (cm)	<..... 25.....>													
FTr (kg dry/kg <sup>-1</sup> fresh)	<..... 4.3E-3.....>		1E-4	2.6E-1	<..... 1E-3.....>		1E-2	2E-2	7.5E-2	2E-2	7.5E-2	1E-2	4E-4	1E-2
<b>Grass</b>														
Effective soil half-life <sup>(1)</sup>	T.p.	T.p.	T.p.	T.p.	T.p.	T.p.	T.p.	8 years	6 years	T.p.	T.p.	T.p.	T.p.	T.p.
Rc/Rdt (m <sup>2</sup> kg <sup>-1</sup> fresh)	<..... 0.35.....>													
Ft	<..... 1.....>													
Tb (days)	<..... 14.....>													
Tc (days)	<..... 90.....>													
h (cm)	<..... 10.....>													
FTr (kg dry/kg <sup>-1</sup> fresh)	<..... 1E-2.....>		1E-4	1.5E-2	<..... 1E-3.....>		5E-3	1E-3	2E-1	2E-2	2E-1	1E-2	3E-4	5E-5
<b>Milk</b>														
FT (d/L)	Fresh grass consumption (50 kg) from April to October – For other periods, see page <b>Erreur ! Signet non défini.</b>													
FT (d/L)	<..... 1E-4.....>		6E-7	1E-4	<..... 2E-5.....>		5E-4	4.5E-3	1E-3	3E-3	1E-3	2E-5	3E-4	1E-4
<b>Meat</b>														
FT (d/kg)	Fresh grass consumption (50 kg) from April to October – For other periods, see page <b>Erreur ! Signet non défini.</b>													
FT (d/kg)	<..... 1E-3.....>		1E-5	5E-3	<..... 1E-3.....>		5E-4	1.5E-2	3E-4	2E-3	3E-4	1E-3	1E-3	1E-3

<sup>(1)</sup> The value is only provided if it is significantly different from the physical half-life of the radionuclide. Otherwise, "T.p" is noted.

<sup>(2)</sup> The density of the soil (μ) was considered as equal to 1,400 kg dry m<sup>-3</sup>

**AVERAGE RATIO OF CALCULATED TO MEASURED VALUES FOR CONTAMINATION  
 IN THE FOOD CHAIN**

Calc./meas. ratio	<sup>103</sup> Ru	<sup>106</sup> Ru+Rh	<sup>95</sup> Zr+Nb	<sup>144</sup> Ce+Pr	<sup>141</sup> Ce	<sup>140</sup> Ba+La	<sup>137</sup> Cs	<sup>90</sup> Sr	<sup>131</sup> I	<sup>89</sup> Sr	Avg.
<b>Leafy vegetables</b>											
average	0.86	2.54	1.52	1.54	1.49		1.27	1.11			1.44
standard deviation	1.23	3.85	3.26	2.67	3.79		2.92	0.52			
number of meas.	87	133	428	228	129		434	267			4178
<b>Root vegetables</b>											
average	0.24	0.43	0.43	0.54	0.12		1.02	1.05			1.02
standard deviation	0.31	0.32	0.63	1.31	0.15		0.94	0.88			
number of meas.	6	9	27	21	9		386	1047			1505
<b>Fruit Vegetables</b>											
average	0.25		1.40	1.44	0.22		1.60	1.12			1.33
standard deviation	0.20		2.12	1.27	0.12		1.55	0.74			
number of meas.	3		19	6	7		267	309			611
<b>Fruit</b>											
average	0.19	2.46	0.83	1.51	0.20		0.80	1.20		0.86	0.91
standard deviation	0.13	2.00	1.47	1.64	0.33		1.13	0.80		0.56	
number of meas.	19	5	34	31	22		160	69		16	356
<b>Grains</b>											
average							1.17	1.01			1.09
standard deviation							0.48	0.33			
number of meas.							79	81			160
<b>Grass</b>											
average	1.56	2.11	1.54	0.65	3.44	0.51	1.05	1.11	0.23	0.91	1.27
standard deviation	1.30	4.52	3.51	0.73	4.94	0.72	0.92	0.53	0.51	0.94	
number of meas.	254	68	538	34	18	84	501	305	75	4	1881
<b>Milk</b>											
average						0.73	1.07	1.06	1.34	1.78	1.35
standard deviation						1.22	0.44	0.38	4.69	6.74	
number of meas.						50	114	214	806	290	1474
<b>Meat</b>											
average							0.96				0.96
standard deviation							0.65				
number of meas.							118				118

The values with a dark grey background are relative to the Paris Region only, those on a light grey background apply to the wider Paris Basin. The values presented on a white background are relative to measurements collected in other regions or for the whole of France.

Radiological consequences of fallout from atmospheric tests of nuclear weapons in mainland France -  
Environmental contamination and exposure of the population  
IRSN Report no. 2024-00559

**IRSN**

Health and Environment Unit  
Environment Division

**Email**

[contact@irsn.fr](mailto:contact@irsn.fr)

**Report No.**

IRSN Report 2024-00559

All rights reserved IRSN

October 2024

Cover photo: Credit: © Galerie Bilderwelt / Bridgeman Images

A mushroom cloud after the explosion of a French nuclear bomb on the French Pacific island of Mururoa, 1971.